



## "Energy efficiency optimization and resource allocation in wireless communication systems"

Wang, Zijian

### Abstract

Nowadays, energy efficiency (EE) for wireless communications is becoming a main economical and societal challenge. This thesis studies resource allocation (RA) in EE optimized wireless communication systems for various system models. The main body of this thesis consists of three parts. In the first part, EE optimization is studied in multiple input multiple output (MIMO)-orthogonal frequency-division multiplexing (OFDM) systems. Two special scenarios are considered respectively in two chapters: rate-dependent circuit power and nonlinear distortion at the high power amplifier (HPA). For the first scenario, the condition of the rate-dependent circuit power such that the global optimal EE is guaranteed to be found is given. The impact of system parameters on EE are analyzed. For the second scenario, the condition of parameters of HPA such that the rate function is concave is given. In the second part, EE maximized subcarrier allocation and precoder design are studied for downlink MIMO ...

Document type : *Thèse (Dissertation)*

### Référence bibliographique

---

Wang, Zijian. *Energy efficiency optimization and resource allocation in wireless communication systems*. Prom. : Vandendorpe, Luc ; Moonen, Marc



**Université catholique de Louvain (UCL)**  
Ecole Polytechnique de Louvain  
ICTEAM Institute  
1348 Louvain-la-Neuve, Belgium

# **Energy Efficiency Optimization and Resource Allocation in Wireless Communication Systems**

Zijian WANG

Thesis presented for the Ph.D degree  
in Engineering Sciences

Jury members:

Luc VANDENDORPE, Supervisor	Université catholique de Louvain, Belgium
Marc MOONEN, Supervisor	Katholieke Universiteit Leuven, Belgium
David BOL, President	Université catholique de Louvain, Belgium
Jérôme LOUVEAUX	Université catholique de Louvain, Belgium
François GLINEUR	Université catholique de Louvain, Belgium
François HORLIN	Université libre de Bruxelles, Belgium

December 2017



# Acknowledgements

First of all, I would like to thank Prof. L. Vandendorpe for bringing me into the topics of energy efficiency and supervising this thesis. His broad and insightful perspectives in this field, as well as constant inspiration and support greatly help me along years to finish this thesis. I would also like to thank Professor M. Moonen, J. Louveaux, F. Glineur, F. Horlin, and D. Bol for their precious effort to examine this thesis.

I would also like to thank Doctor I. Stupia for the sharing of great ideas and the helpful discussions. I would also thank Doctor N. Janatian for the help with the optimization toolbox. I thank the funding of the project IAP BESTCOM under which this thesis has been carried out.

Moreover, I have been deeply indebted to my wife Ge Gao who are always there supporting me unselfishly. Without you, this thesis could have never been completed.

Last but not the least, I would like to thank J. Deschuyter, F. Hubin, Z. Jin, M. E. Soussi, M. M. Cespedes, T. Feuillen, A. I. Akin, T. Ren and all other members in the lab for the help in research and daily life.



# Abstract

Nowadays, energy efficiency (EE) for wireless communications is becoming a main economical and societal challenge. This thesis studies resource allocation (RA) in EE optimized wireless communication systems for various system models. The main body of this thesis consists of three parts.

In the first part, EE optimization is studied in multiple input multiple output (MIMO)-orthogonal frequency-division multiplexing (OFDM) systems. Two special scenarios are considered respectively in two chapters: rate-dependent circuit power and nonlinear distortion at the high power amplifier (HPA). For the first scenario, the condition of the rate-dependent circuit power such that the global optimal EE is guaranteed to be found is given. The impact of system parameters on EE are analyzed. For the second scenario, the condition of parameters of HPA such that the rate function is concave is given.

In the second part, EE maximized subcarrier allocation and precoder design are studied for downlink MIMO - orthogonal frequency-division multiple access (OFDMA) systems. Mathematical proofs to obtain the property of the EE function are provided. A condition on the subcarrier allocation and the precoder at the base station at the optimum EE is obtained and the optimality of the condition for fixed transmit power is shown.

In the third part, EE maximization for relay assisted channel is studied. Two special techniques are considered respectively in two chapters: relay selection in multi-relay networks and subcarrier pairing (SP) for multi-carrier systems. For the first scenario, a relay selection method with low complexity is proposed. In the second scenario, an alternating optimization approach is adopted to solve the problem. In each subproblem, the power allocation is

optimized together with subcarrier allocation and pairing at the relay.

# Contents

<b>Acronyms</b>	<b>ix</b>
<b>Notations</b>	<b>xi</b>
<b>List of Figures</b>	<b>xiii</b>
<b>Algorithms</b>	<b>xv</b>
<b>1 Introduction</b>	<b>1</b>
1.1 Motivations . . . . .	1
1.2 Outline and contributions . . . . .	4
1.3 Related publications . . . . .	6
<b>2 Preliminaries and mathematical background</b>	<b>9</b>
2.1 Convex sets . . . . .	9
2.2 Convex and concave functions . . . . .	10
2.3 Convex optimization . . . . .	11
2.3.1 Properties . . . . .	12
2.3.2 Standard form . . . . .	12
2.3.3 Lagrange multipliers . . . . .	13
2.4 Quasi-convex and quasi-concave functions . . . . .	14
2.5 Bisection method . . . . .	14
2.6 Fractional programming . . . . .	16
2.6.1 Transformation to a concave program . . . . .	16
2.6.2 Dinkelbach's algorithm . . . . .	17

<b>3</b>	<b>MIMO-OFDM systems with rate-dependent circuit power</b>	<b>19</b>
3.1	Related works and chapter review . . . . .	19
3.2	System model . . . . .	20
3.3	Energy efficient precoder design . . . . .	21
3.3.1	Precoder optimization . . . . .	21
3.3.2	Algorithm description . . . . .	26
3.4	Impact of system parameters . . . . .	26
3.5	Numerical results . . . . .	29
3.5.1	Effect of link distance $d$ . . . . .	30
3.5.2	Effect of bandwidth enlargement . . . . .	31
3.5.3	Effect of antenna configuration . . . . .	33
3.6	Conclusion . . . . .	34
<b>4</b>	<b>MIMO-OFDM systems with imperfect amplifier</b>	<b>35</b>
4.1	Related works and chapter review . . . . .	35
4.2	System model . . . . .	36
4.3	Problem formulation . . . . .	38
4.4	Power allocation algorithm . . . . .	39
4.4.1	Optimal precoding strategy . . . . .	40
4.4.2	Concavity condition . . . . .	41
4.4.3	Algorithm . . . . .	46
4.5	Numerical results . . . . .	46
4.6	Conclusion . . . . .	49
<b>5</b>	<b>EE maximization in MIMO-OFDMA downlink systems</b>	<b>51</b>
5.1	Related works and chapter review . . . . .	51
5.2	System model . . . . .	54
5.2.1	Transmission model . . . . .	54
5.2.2	EE model . . . . .	54
5.3	EE maximization problem . . . . .	55
5.3.1	Optimal precoder . . . . .	55
5.3.2	Time-sharing approach . . . . .	57
5.3.3	Remarks . . . . .	60
5.4	Optimal EE solution . . . . .	60
5.5	Numerical results . . . . .	66
5.6	Conclusion . . . . .	69

5.7	Appendix . . . . .	69
5.7.1	Proof of Theorem 5.1 . . . . .	69
5.7.2	Proof of Lemma 5.1 . . . . .	71
5.7.3	Proof of Lemma 5.2 . . . . .	72
5.7.4	Proof of Theorem 5.2 . . . . .	73
5.7.5	Proof of Theorem 5.3 . . . . .	75
5.7.6	Proof of Proposition 1 . . . . .	76
<b>6</b>	<b>Power allocation and relay selection in MIMO relay channels</b>	<b>77</b>
6.1	Related works and chapter review . . . . .	77
6.2	System model . . . . .	78
6.3	EE maximization . . . . .	80
6.3.1	Problem reformulation . . . . .	80
6.3.2	Optimization of $\mathbf{Q}_k$ for given $\Theta_k$ . . . . .	81
6.3.3	Optimization of $\Theta_k$ for given $\mathbf{Q}_k$ . . . . .	86
6.3.4	Algorithm for EE maximization . . . . .	88
6.4	Numerical results . . . . .	88
6.5	Conclusion . . . . .	93
6.6	Appendix . . . . .	95
6.6.1	Proof of Theorem 6.1 . . . . .	95
6.6.2	Proof of Theorem 6.2 . . . . .	97
<b>7</b>	<b>RA and SP in Relay-Assisted OFDMA Downlink Systems</b>	<b>99</b>
7.1	Related works and chapter review . . . . .	99
7.2	System Model and Problem Formulation . . . . .	100
7.2.1	System model . . . . .	100
7.2.2	EE model . . . . .	101
7.2.3	Problem formulation . . . . .	102
7.3	Theoretical Analysis and Algorithm . . . . .	102
7.3.1	Optimize $\mathbf{q}$ , $\{\alpha_{i,j,n}\}$ for given $\mathbf{p}$ . . . . .	103
7.3.2	Optimize $\mathbf{p}$ , $\{\alpha_{i,j,n}\}$ for given $\mathbf{q}$ . . . . .	106
7.3.3	Algorithm . . . . .	107
7.4	Complexity Comparison . . . . .	107
7.5	Numerical results . . . . .	110
7.6	Conclusion . . . . .	112

<b>8</b>	<b>Conclusions and perspectives for future works</b>	<b>115</b>
8.1	Summary of contributions . . . . .	115
8.2	Future work . . . . .	117
<b>9</b>	<b>Bibliography</b>	<b>119</b>

# Acronyms

AF	amplify-and-forward
BER	bit error rate
BNC	Busgang noise cancellation
CSI	channel state information
CSIT	channel state information at the transmitter
DFT	discrete Fourier transform
DPC	dirty paper coding
EE	energy efficiency
EVM	error vector magnitude
HPA	high power amplifier
IBO	input backoff
KKT	Karush-Kuhn-Tucker
LTE	long-term evolution
MIMO	multiple input multiple output
OBO	output backoff
OFDM	orthogonal frequency-division multiplexing

OFDMA	orthogonal frequency-division multiple access
PAPR	peak-average power ratio
RA	resource allocation
RF	radio frequency
RB	resource block
SE	spectrum efficiency
SER	symbol error rate
SISO	single-input-single-output
SNR	signal-to-noise ratio
SP	subcarrier pairing
SUS	semi-orthogonal user selection
SVD	singular value decomposition
ZF	zero forcing

# Notations

$\mathbf{a}$	a vector
$\mathbf{A}$	a matrix
$(\mathbf{A})_{(i,j)}$	the entry at the $i$ th row and $j$ th column of $\mathbf{A}$
$\mathbf{I}_N$	$N \times N$ the identity matrix
$(\mathbf{a})_i$	the $i$ th entry of $\mathbf{a}$
$\nabla_{\mathbf{x}}^2 f(\mathbf{x})$	the Hessian matrix of $f(\mathbf{x})$ with respect to $\mathbf{x}$
$\mathbb{S}$	a set
$(\cdot)^H$	conjugate transpose
$(\cdot)^T$	transpose
$\text{tr}(\mathbf{A})$	trace of a matrix
$ \mathbf{A} $	the determinant of a matrix
$\mathbf{a}(m)$	the $(m)$ -th entry of the vector $\mathbf{a}$
$\{x\}^+$	$\max\{0, x\}$
$\mathbb{E}\{\cdot\}$	the expectation of a variable
$X_{dB}$	$X$ expressed in decibels
<i>diag</i>	Operation that extracts every diagonal entries of the original matrix to form a new matrix

$f'(x)$	the first-order derivative of the function
$\nabla f$	the gradient of $f$
$f''(x)$	the second-order derivative of the function

# List of Figures

2.1	An example of convex function . . . . .	11
2.2	An example of the bisection method . . . . .	15
3.1	Power consumption and EE comparison for different $d$ . . .	30
3.2	Power consumption and EE comparison for different $K$ . . .	31
3.3	EE comparison for different antenna configurations (1) . . .	32
3.4	EE comparison for different antenna configurations (2) . . .	32
3.5	EE comparison for different antenna configurations (3) . . .	33
4.1	Rate as a function of IBO and HPA power . . . . .	47
4.2	Maximum rate as a function of HPA power . . . . .	48
4.3	Rate performance versus HPA power ( $P_{am}$ ) for different IBO. . . . .	48
4.4	Rate performance versus $d$ for different IBO. . . . .	49
5.1	User selection and the transmission power of the MIMO channel . . . . .	62
5.2	The rate, transmit power and EE vs. water level . . . . .	63
5.3	Transmit power, rate, and EE versus water level . . . . .	66
5.4	EE and rate comparison for different $P_C$ . . . . .	67
5.5	EE and rate comparison for different $\phi$ . . . . .	67
5.6	EE and rate comparison for different $K$ . . . . .	68
6.1	EE increases as the number of relays . . . . .	94
6.2	Number of remaining relays at each iteration . . . . .	94
6.3	Percentage of each relay being selected (1) . . . . .	95
6.4	Percentage of each relay being selected (2) . . . . .	96

- 7.1 EE performances versus power constraints.  $d_1 = d_2 = 10\text{m}$ . 110
- 7.2 EE performances versus power constraints.  $d_1 = d_2 = 15\text{m}$ . 111
- 7.3 EE performances versus power constraints.  $d_1 = d_2 = 25\text{m}$ . 112
- 7.4 EE performances versus power constraints.  $d_1 = d_2 = 50\text{m}$ . 112

# List of Algorithms

3.1	MIMO-OFDM: Calculate $\Theta^*$ and $\varepsilon^*$ . . . . .	27
5.1	MIMO-OFDMA: calculate $\text{EE}^*$ . . . . .	65
5.2	MIMO-OFDMA: subcarrier allocation . . . . .	65
6.1	EE maximization with relay selection . . . . .	88
6.2	Relay selection: alternating EE maximization . . . . .	89
6.3	Relay selection: find $\Theta_k$ for given $\mathbf{Q}_k$ . . . . .	89
6.4	Relay selection: find $\mathbf{Q}_k$ for given $\Theta_k$ . . . . .	90
6.5	Relay selection: case 1 and case 2 . . . . .	90
6.6	Relay selection: case 3 . . . . .	91
6.7	Relay selection: case 4 . . . . .	92
6.8	Relay selection: bisection method to find $f(x^*) = 0$ . . . . .	92
7.1	An alternating method for EE maximization . . . . .	108
7.2	Optimize $\mathbf{q}$ for given $\mathbf{p}$ . . . . .	108
7.3	Optimize $\mathbf{p}$ for given $\mathbf{q}$ . . . . .	109



# Chapter 1

## Introduction

This chapter first explains the motivations of this thesis, then states the outline and contributions, and finally lists related publications.

### 1.1 Motivations

Nowadays, energy efficiency (EE) for wireless communications is becoming a main economical and societal challenge [LXX<sup>+</sup>11]. Hence, instead of maximizing the information rate under a certain power constraint, engineers wish to study a better tradeoff between maximizing the information rate and minimizing the consumed power. In this respect, the most investigated criterion is to maximize the transmission rate per consumed energy. This is also referred to as the EE maximization problem. There are two main reasons why EE is defined in this way. The first reason is that this definition has a straightforward physical meaning, making it similar with the performance-cost ratio in economics. The second reason is that it has a tractable mathematical structure, especially when the circuit power of the considered system is modeled as being constant. Hence, in this thesis, we will focus on the maximizing the EE defined in this way. Other formulations concerning tradeoffs between the rate and the power, like multi-objective optimization, will not be considered in this thesis.

Among the early contributions in this area, the authors in [KD10] originally considered the transmission rate per consumed energy to adapt the

transmission mode (i.e. number of streams, space time signaling, MIMO detection, etc.) of a multiple input multiple output (MIMO)-orthogonal frequency-division multiplexing (OFDM) system. Paper [BL11] investigated the optimal precoding strategy for EE maximization in MIMO systems, showing that without considering the power used to feed circuitries, the optimum transmission power will be zero for a Gaussian MIMO channel. This result showed the significance of considering the circuit power and triggered a more proper and reasonable modeling of the circuit power when studying EE maximization. In [ICJF12], the authors used the mathematical tool of convex fractional programming to address the power allocation problem for EE maximization in OFDM systems, showing the optimality of the waterfilling power allocation policy. In MIMO-OFDM systems, when perfect channel state information (CSI) is available at both at the transmitter and the receiver side, the EE optimal precoder for each subcarrier is based on the singular value decomposition (SVD) of the channel matrices associated with the parallel OFDM subchannels in the frequency domain. The power allocation has a global water filling structure [PD10, ED12, WSV15, Tel99]. More recently, the authors of [HHJY13] extended this work to a multi-user and multi-cell scenario.

While there exist already many doubtless conclusions for single-user MIMO-OFDM systems, most works about EE, however, consider the overall circuit power consumption (except the transmit power) to be either zero or a constant value. In this condition, the objective function of EE maximization problem is shown to be quasi-concave, and therefore the mathematical framework proposed in [ICJF12] can be invoked to solve the problem. On the contrary, the authors of [WV13] accounted for the variability of the circuit power consumption for discrete-time base-band signal processing (due to different modulation orders and coding rates) by modelling this power as being dependent on the transmission rate. This consideration has provided a more general model of the circuit power for the feasibility of EE maximization. In addition, it is worth investigating the impact of various system parameters on EE [WV13]. MIMO-OFDM has become the predominant air interface technology for the fourth generation of wideband wireless communication system due to its robustness to frequency selective fading [STT<sup>+</sup>02]. Therefore, in Chapter 3, we study EE for MIMO-OFDM systems with rate dependent circuit power and investigate the impact of various system param-

eters on EE performance. An essential drawback of an OFDM system is the high peak-average power ratio (PAPR) of the multicarrier signals which, in turn, may lead to severe nonlinear distortions at the output of the high power amplifier (HPA). In Chapter 4, we will study EE for MIMO-OFDM with nonlinear distortion at HPA.

With respect to the extension to multi-user systems, several studies on precoder design and resource allocation (RA) for EE maximization in multi-user setup are reported. Zero-forcing (ZF), user selection and antenna selection were jointly implemented in paper [YBC14]. Multi-user MIMO systems were studied in papers [OHI13, XQ13, VTFH16, MB16, LTY15], where suboptimal solutions were investigated by means of asymptotic capacity, block-coordinate ascent algorithm, Lower-bound or upper-bound approximations, ZF assumptions, etc. Concerning multi-user systems operating over frequency-selective channels, papers [XLZ<sup>+</sup>11, XLZ<sup>+</sup>12] studied single antenna orthogonal frequency-division multiple access (OFDMA) systems. Papers [TSA<sup>+</sup>15, SH14, XTL15, XYL<sup>+</sup>13] studied EE maximization for systems based on both MIMO and OFDM, where the multi-user dimension is handled either by means of the multiple antennas or the multiple frequencies. For systems combining OFDM with multi-user MIMO, paper [TSA<sup>+</sup>15] considered dirty paper coding (DPC) for the multi-user symbols of each subcarrier, while ZF precoding was assumed for each subcarrier in paper [SH14]. For MIMO-OFDMA systems, paper [XYL<sup>+</sup>13] considered power minimization for a given capacity by optimizing various system parameters such as the number of subcarriers and number of radio frequency (RF) chains, etc. However, channel state information at the transmitter (CSIT) was assumed to be unavailable and therefore precoding was not considered. For the long-term evolution (LTE) standard, paper [XTL15] maximized EE by optimizing resource block (RB) allocation. The precoders considered in papers [TSA<sup>+</sup>15, SH14, XTL15, XYL<sup>+</sup>13] are selected before and independently of the optimization of other system resources such as subcarrier allocation. To the best of our knowledge, no work has jointly considered the EE-optimized subcarrier allocation and precoder design for a MIMO-OFDMA downlink system. While the precoder optimization for MIMO-OFDM systems is widely known as a quasi-concave problem [PD10, WSV15], the quasi-concavity property for MIMO-OFDMA downlink system is worth substantial theoretical analysis. This paper pro-

vides mathematical proofs to understand the properties of the problem. In Chapter 5, we consider the EE maximization problem in a MIMO-OFDMA downlink, where we jointly optimize the subcarrier allocation and the precoder design.

As future wireless communication systems require ubiquitous radio coverage, coverage extension continues to deserve attention. Among various ways to counteract the large attenuation associated with long distances, relaying between base stations and users plays an important role. In addition, relay-assisted networks can be considered as a simplified scenario of user cooperation. In Chapter 6 and Chapter 7, we study EE maximization considering two key refinement techniques in systems operating over frequency-selective channels and aided with multiple relays (or users): relay selection and subcarrier pairing.

## 1.2 Outline and contributions

The structure of this thesis will be as follows. We first provide some basic preliminaries for EE maximization. Then we study the EE maximization problem for MIMO-OFDM systems. Finally, we study the problem for multi-user systems (MIMO-OFDMA) and for relay channels. Specifically, the outline and contributions of this thesis are listed as follows:

In Chapter 2, some basic preliminaries and mathematical backgrounds are provided.

In Chapter 3, we study the energy efficient design of precoders for point-to-point MIMO OFDM systems. We show that for a total power made of a constant term plus another one that is increasing and convex with the transmission rate, the consumed energy per bit is a quasi-convex function of the total transmission rate. Thanks to that, the problem of minimizing the consumed energy per bit could be reformulated as a convex fractional program and solved by means of a simple bisection algorithm. The effects of various system parameters on the optimal value of the objective function have been analyzed and illustrated by means of computational results.

In Chapter 4, we investigate the optimal design of MIMO precoders for OFDM systems in the presence of nonlinear distortions due to the HPA. In traditional approaches, the designer lets the input backoff (IBO) of the HPA

be large enough to neglect the unavoidable nonlinear effects of the amplifier. However, this hypothesis may severely hinder the efficiency of the HPA and, consequently, the global EE of the link. On the other hand, making full use of the available power gives rise to unbearable nonlinear effects with consequent strong rate degradations. We model the time domain signal by the Bussgang theorem to unveil the impact of the nonlinear distortion noise on the optimal precoding and to derive a power allocation algorithm that achieves the optimal tradeoff between HPA efficiency and rate degradation. We also provide a sufficient condition for the concavity of the information rate objective function in this nonlinear scenario. Finally, numerical results show that the proposed algorithm outperforms conventional fixed-IBO precoding strategies.

In Chapter 5, we study the subcarrier allocation and precoder design problem for downlink MIMO-OFDMA systems. The criterion is to maximize the EE of the system. We adopt the time-sharing concept to allocate each subcarrier to one user, which results in a criterion similar with that of rate maximization. However, this approach does not make it possible to solve the problem for all values of the transmit power. We found that there exist gaps along the direction of total transmit power when the user selection switches for each subcarrier, which leads to a discontinuous EE function, for which quasi-concavity has to be checked. We first show that the sufficient conditions obtained for the subcarrier allocation approach are the optimal ones among all possibilities with the same transmit power. Then we show that the proposed subcarrier allocation results in a discontinuous and quasi-concave EE function. We also give an upper bound of the EE function when the proposed sufficient conditions are not met. Finally, we propose an algorithm to find the maximal EE and its performance is illustrated by means of numerical results.

In Chapter 6, we consider the EE maximization problem for MIMO relay channels with relay selection and individual power constraints for each node. We implement Dinkelbach's method for the whole system to iteratively select the relays. Closed-form expressions of the precoding matrix at the source and the beamforming matrix at the selected relay are obtained thanks to the concavity of the objective function. We also give the mathematical property of monotonicity which guarantees that the values of Lagrangian multipliers can always be found. Finally, we report numerical results illus-

trating the performance gain due to relay selection.

In Chapter 7, we study the EE maximization problem in AF relay-assisted downlink channels with OFDMA. The power allocation is optimized together with subcarrier allocation and pairing at the relay. As the base station and the relay have individual power constraints, an alternating optimization approach is adopted to solve the problem. Numerical results show that the proposed algorithm outperforms other benchmark schemes in terms of EE.

### 1.3 Related publications

The content of Chapter 3 has been published in

- Z. Wang, I. Stupia and L. Vandendorpe, “Energy Efficient Precoder Design for MIMO-OFDM with Rate-dependent Circuit Power,” *IEEE International Conference on Communications (ICC)*, pp. 1897-1902, Jun. 8-12, 2015.

The content of Chapter 4 has been published in

- Z. Wang, I. Stupia and L. Vandendorpe, “Optimal Precoder Design for MIMO-OFDM: Understanding the Role of Power Amplifiers and Nonlinear Distortion Noise,” *IEEE International Conference on Communications (ICC)*, 23-27, May, 2016.

The content of Chapter 5 has been published in

- Z. Wang and L. Vandendorpe, “Energy Efficient Resource Allocation in MIMO-OFDMA Downlink Systems,” *Proc. IEEE SPAWC*, Jul. 3-6, 2016.
- Z. Wang and L. Vandendorpe, “Subcarrier Allocation and Precoder Design for Energy Efficient MIMO-OFDMA Downlink Systems,” *IEEE Trans. Commun.*, vol. 65, no. 1, pp. 136-146, Jan. 2017.

The content of Chapter 6 has been published in

- Z. Wang and L. Vandendorpe, “Energy efficient power allocation and relay selection in MIMO relay channels,” *IEEE International Symposium on Personal, Indoor and Mobile Radio Communications (PIMRC)*, 4-7, Sept, 2016.

The content of Chapter 7 has been published in

- Z. Wang and L. Vandendorpe, “Resource Allocation and Subcarrier Pairing in Energy Efficient Relay-Assisted OFDMA Downlink Systems,” *International Symposium on Wireless Communication Systems (ISWCS)*, 28-31, Aug., 2017.



# Chapter 2

## Preliminaries and mathematical background

In this chapter, some preliminaries and mathematical backgrounds about convex optimization that are necessary for EE maximization will be introduced.

### 2.1 Convex sets

In convex geometry, a convex set is defined as a subset of an affine space that is closed under convex combinations. More specifically, in a Euclidean space, a convex region is a region where, for every pair of points within the region, every point on the straight line segment that joins the pair of points is also within the region. That is, if  $\mathbb{S}$  is a convex set in  $n$ -dimensional space, then for any pair of  $n$ -dimensional vectors  $u_1$  and  $u_2$  in  $\mathbb{S}$ , and for any nonnegative numbers  $\lambda_1, \lambda_2$  such that  $\lambda_1 + \lambda_2 = 1$ , then one has:

$$\lambda_1 u_1 + \lambda_2 u_2 \in \mathbb{S}. \quad (2.1)$$

More generally, if  $\mathbb{S}$  is a convex set in  $n$ -dimensional space, then for any collection of  $K$ ,  $K > 1$ ,  $n$ -dimensional vectors  $u_1, \dots, u_K$  in  $\mathbb{S}$ , and for any nonnegative numbers  $\lambda_1, \dots, \lambda_K$  such that

$$\lambda_1 + \dots + \lambda_K = 1, \quad (2.2)$$

then one has:

$$\sum_{k=1}^K \lambda_k u_k \in \mathbb{S}. \quad (2.3)$$

A vector of this type is known as a convex combination of  $u_1, \dots, u_K$ .

## 2.2 Convex and concave functions

Define  $\mathbb{X}$  as a convex set in a real vector space and let the mapping  $f : \mathbb{X} \rightarrow \mathbb{R}$  be a function. Then function  $f$  is called convex if for  $\forall x_1, x_2 \in \mathbb{X}$  and  $\forall t \in [0, 1]$ , we have

$$f(tx_1 + (1-t)x_2) \leq tf(x_1) + (1-t)f(x_2). \quad (2.4)$$

$f$  is called strictly convex if for  $\forall x_1 \neq x_2 \in \mathbb{X}$  and  $\forall t \in (0, 1)$ , we have

$$f(tx_1 + (1-t)x_2) < tf(x_1) + (1-t)f(x_2). \quad (2.5)$$

Some properties of convex functions are provided below.

- A function  $f$  is (strictly) concave if  $-f$  is (strictly) convex.
- Suppose  $f$  is a function of one real variable defined on an interval, and  $x_1, x_2 \in \mathbb{R}$ . Let

$$R(x_1, x_2) = \frac{f(x_1) - f(x_2)}{x_1 - x_2}, \quad (2.6)$$

which is the slope of the purple line in Fig. 2.2. Then  $f$  is convex if and only if  $R(x_1, x_2)$  is monotonically non-decreasing in  $x_1$ , for any fixed  $x_2$  (or vice versa).

- A differentiable function of one variable is convex on an interval if and only if its derivative is monotonically non-decreasing on that interval. If a function is differentiable and convex then it is also continuously differentiable. For the basic case of a differentiable function from (a subset of) the real numbers to the real numbers, being convex is equivalent to be increasing at an increasing rate.

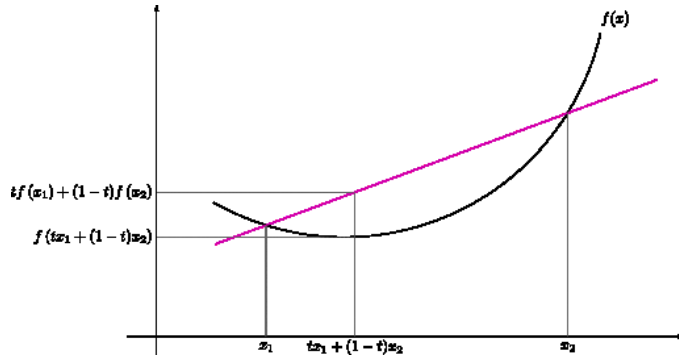


Figure 2.1: An example of convex function. Image from Wikipedia: [https://en.wikipedia.org/wiki/Convex\\_function](https://en.wikipedia.org/wiki/Convex_function)

- A differentiable function of one variable is convex on an interval if and only if the function lies above all of its tangents

$$f(x) \geq f(y) + f'(y)(x - y) \quad (2.7)$$

for all  $x$  and  $y$  in the interval. In particular, if  $f'(c) = 0$ , then  $c$  is a global minimum of  $f(x)$ .

- Any local minimum of a convex function is also a global minimum. A strictly convex function will have at most one global minimum.
- Jensen's inequality applies to every convex function  $f$ . If  $X$  is a random variable taking values in the domain of  $f$ , then  $\mathbb{E}(f(X)) \geq f(\mathbb{E}(X))$ .

## 2.3 Convex optimization

By understanding concepts of convex sets and convex functions, we come to the definition of convex optimization problems.

The general form of an optimization problem, if more specifically a minimization problem, is to find some  $x^* \in \mathbb{X}$  such that

$$f(x^*) = \min\{f(x) : x \in \mathbb{X}\}, \quad (2.8)$$

for some feasible set  $\mathbb{X} \subset \mathbb{R}^n$  and objective function  $f(x) : \mathbb{R}^n \rightarrow \mathbb{R}$ . The optimization problem is called a convex optimization problem if  $\mathbb{X}$  is a convex set and  $f(x)$  is a convex function defined on  $\mathbb{R}^n$ .

An convex optimization problem has a general form as below:

$$\text{minimize} \quad f(x) \quad (2.9)$$

$$\text{subject to} \quad g_i(x) \leq 0, \quad i = 1, \dots, m \quad (2.10)$$

where the functions  $f, g_1 \dots g_m : \mathbb{R}^n \rightarrow \mathbb{R}$  are all convex functions.

### 2.3.1 Properties

Some properties of convex minimization problems are listed as follows:

- if a local minimum exists, then it is a global minimum;
- the set of all minima is convex;
- for each strictly convex function, if the function has a minimum, then the minimum is unique.

### 2.3.2 Standard form

A convex minimization problem can be expressed by standard form, which consists of the following three parts:

- a convex function  $f(x) : \mathbb{R}^n \rightarrow \mathbb{R}$  to be minimized over the variable  $x$ ;
- inequality constraints of the form  $g_i(x) \leq 0$ , where the functions  $g_i$  are convex;
- equality constraints of the form  $h_i(x) = 0$ , where the functions  $h_i$  are affine.

In practice, the terms "linear" and "affine" are often used interchangeably. Such constraints can be expressed in the form  $h_i(x) = a_i^T x + b_i$ , where

$a_i$  is a column-vector and  $b_i$  a real number. A convex minimization problem is thus written as

$$\underset{x}{\text{minimize}} \quad f(x) \quad (2.11)$$

$$\text{subject to} \quad g_i(x) \leq 0, \quad i = 1, \dots, m \quad (2.12)$$

$$h_i(x) = 0, \quad i = 1, \dots, p. \quad (2.13)$$

Note that every equality constraint  $h(x) = 0$  can be equivalently replaced by a pair of inequality constraints  $h(x) \leq 0$  and  $-h(x) \leq 0$ .

Following from this fact, it is easy to understand why  $h_i(x) = 0$  has to be affine as opposed to merely being convex. If  $h_i(x)$  is convex,  $h_i(x) \leq 0$  is convex, but  $-h_i(x) \leq 0$  is concave. Therefore, the only way for  $h_i(x) = 0$  to be convex is for  $h_i(x)$  to be affine. By rewriting the constraint  $h_i(x) = 0$  as  $h_i(x) \leq 0$  and  $-h_i(x) \leq 0$ , the standard form reduces to the general form in (2.9).

### 2.3.3 Lagrange multipliers

Consider a convex minimization problem in standard form with a cost function  $f(x)$  and inequality constraints  $g_i(x) \leq 0$  for  $1 \leq i \leq m$ . Thus the domain  $\mathbb{X}$  is:

$$\mathbb{X} = \{x \in \mathbb{X} | g_1(x), \dots, g_m(x) \leq 0\}. \quad (2.14)$$

The Lagrangian function for the problem is defined as

$$L(x, \lambda_0, \lambda_1, \dots, \lambda_m) = \lambda_0 f(x) + \lambda_1 g_1(x) + \dots + \lambda_m g_m(x). \quad (2.15)$$

For each point  $x \in \mathbb{X}$  that minimizes  $f$  over  $\mathbb{X}$ , there exist Lagrange multipliers  $\lambda_0, \lambda_1, \dots, \lambda_m$ , that satisfy these conditions simultaneously:

- $x$  minimizes  $L(y, \lambda_0, \lambda_1, \dots, \lambda_m)$  over all  $y \in \mathbb{X}$ ,
- $\lambda_0, \lambda_1, \dots, \lambda_m \geq 0$ , with at least one  $\lambda_k > 0$ ,
- $\lambda_1 g_1(x) = \dots = \lambda_m g_m(x) = 0$  (complementary slackness).

Note that if there exists a "strictly feasible point", that is, a point  $z$  satisfying  $g_1(z), \dots, g_m(z) < 0$ , then the statement above can be strengthened to require that  $\lambda_0 = 1$ .

## 2.4 Quasi-convex and quasi-concave functions

The EE function is shown to be quasi-concave in the most common cases. Therefore in this section, we briefly introduce the concept of quasi-convex and quasi-concave functions.

A function  $f : \mathbb{S} \rightarrow \mathbb{R}$  defined on a convex subset  $\mathbb{S}$  of a real vector space is called quasiconvex if for all  $x, y \in \mathbb{S}$  and  $\lambda \in [0, 1]$ , we have

$$f(\lambda x + (1 - \lambda)y) \leq \max\{f(x), f(y)\}. \quad (2.16)$$

If furthermore

$$f(\lambda x + (1 - \lambda)y) < \max\{f(x), f(y)\} \quad (2.17)$$

for all  $x \neq y$  and  $\lambda \in (0, 1)$ , then  $f$  is called strictly quasiconvex.

A function  $f$  is quasi-concave if  $-f$  is quasi-convex.

A function that is both quasi-convex and quasi-concave is called quasi-linear.

## 2.5 Bisection method

In EE maximization problems, the bisection method is very useful and easy to implement if the problem is able to be simplified to a one-dimension search problem.

The bisection method in mathematics is a root-finding method that repeatedly bisects an interval and then selects a subinterval in which a root must lie for further processing. It is a very simple and robust method, but it is also relatively slow. Because of this, it is often used to obtain a rough approximation to a solution which is then used as a starting point for more rapidly converging methods. An example of the bisection method to find a root is illustrated in Fig. 2.2.

The method is applicable for numerically solving the equation  $f(x) = 0$  for the real variable  $x$ , where  $f$  is a continuous function defined on an interval  $[a, b]$  and where  $f(a)$  and  $f(b)$  have opposite signs. In this case  $a$  and  $b$  are said to bracket a root since, by the intermediate value theorem, the continuous function  $f$  must have at least one root in the interval  $(a, b)$ .

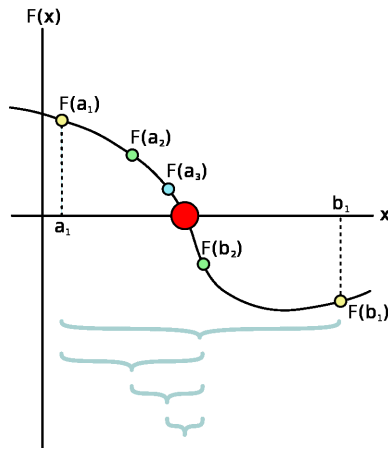


Figure 2.2: A few steps of the bisection method applied over the starting range  $[a_1; b_1]$ . The bigger red dot is the root of the function. Image from Wikipedia: [https://en.wikipedia.org/wiki/Bisection\\_method](https://en.wikipedia.org/wiki/Bisection_method)

As will be seen in the following chapters, the derivative of the obtained EE function is, in general, positive at zero power and negative at a relatively large value of power. Finding the global or local maximum EE is equivalent to finding the power value with a zero derivative. Therefore, the bisection method is of great use in EE maximization.

At each step the method divides the interval in two by computing the midpoint  $c = (a + b)/2$  of the interval and the value of the function  $f(c)$  at that point. Unless  $c$  is itself a root (which is very unlikely, but possible) there are now only two possibilities: either  $f(a)$  and  $f(c)$  have opposite signs and bracket a root, or  $f(c)$  and  $f(b)$  have opposite signs and bracket a root. The method selects the subinterval that is guaranteed to be a bracket as the new interval to be used in the next step. In this way an interval that contains a zero of  $f$  is reduced in width by 50% at each step. The process is continued until the interval is sufficiently small.

Explicitly, if  $f(a)$  and  $f(c)$  have opposite signs, then the method sets  $c$  as the new value for  $b$ , and if  $f(b)$  and  $f(c)$  have opposite signs then the method sets  $c$  as the new  $a$ . (If  $f(c) = 0$  then  $c$  may be taken as the solution and the process stops.) In both cases, the new  $f(a)$  and  $f(b)$  have opposite signs, so the method is applicable to this smaller interval.

## 2.6 Fractional programming

In general, EE maximization is a fractional programming [ICJF12]. In mathematical optimization, fractional programming is a generalization of linear-fractional programming. The objective function in a fractional program is a ratio of two functions that are in general nonlinear. The ratio to be optimized often describes some kind of efficiency of a system.

Let  $f, g, h_j, j = 1, \dots, m$  be real-valued functions defined on a set  $\mathbf{S}_0 \subset \mathbb{R}^n$ . Let  $\mathbf{S} = \{\mathbf{x} \in \mathbf{S}_0 : h_j(\mathbf{x}) \leq 0, j = 1, \dots, m\}$ . The nonlinear program

$$\underset{\mathbf{x} \in \mathbf{S}}{\text{maximize}} \quad \frac{f(\mathbf{x})}{g(\mathbf{x})}, \quad (2.18)$$

where  $g(\mathbf{x}) > 0$  on  $\mathbf{S}$ , is called a fractional program.

A fractional program in which  $f$  is nonnegative and concave,  $g$  is positive and convex, and  $\mathbf{S}$  is a convex set is called a concave fractional program. If  $g$  is affine,  $f$  does not have to be restricted in sign. The linear fractional program is a special case of a concave fractional program where all functions  $f, g, h_j, j = 1, \dots, m$  are affine.

The function  $q(\mathbf{x}) = f(\mathbf{x})/g(\mathbf{x})$  is semistrictly quasiconcave on  $\mathbf{S}$ . If  $f$  and  $g$  are differentiable, then  $q$  is pseudoconcave. In a linear fractional program, the objective function is pseudolinear.

The two most common ways to solve a fractional program are 1) to reformulate it to a concave program and 2) to use the bisection method thanks to the quasi-concavity.

### 2.6.1 Transformation to a concave program

By the transformation  $\mathbf{y} = \frac{\mathbf{x}}{g(\mathbf{x})}; t = \frac{1}{g(\mathbf{x})}$ , any concave fractional program can be transformed to the equivalent parameter-free concave program

$$\underset{\frac{\mathbf{y}}{t} \in \mathbf{S}_0}{\text{maximize}} \quad tf\left(\frac{\mathbf{y}}{t}\right) \quad (2.19)$$

$$\text{subject to} \quad tg\left(\frac{\mathbf{y}}{t}\right) \leq 1, \quad (2.20)$$

$$t \geq 0. \quad (2.21)$$

## 2.6.2 Dinkelbach's algorithm

Another efficient method to solve a fractional program is Dinkelbach's algorithm. The original problem is equivalent to find  $\lambda^*$  such that  $F(\lambda^*) = 0$ , where

$$F(\lambda) = \underset{\mathbf{x} \in \mathbf{S}}{\text{maximize}} \quad f(\mathbf{x}) - \lambda g(\mathbf{x}). \quad (2.22)$$

$F(\lambda)$  is shown to be concave by the following theorem.

**Theorem 2.1.**  $F(\lambda)$  is a concave function w.r.t  $\lambda$ .

*Proof.* Since  $\mathbf{x}$  changes with  $\lambda$ , let us denote  $\mathbf{x}$  as  $\mathbf{x}(\lambda)$ . Because

$$\mathbf{x}(\lambda) = \arg \max_{\mathbf{x} \in \mathbf{S}} \quad f(\mathbf{x}) - \lambda g(\mathbf{x}), \quad (2.23)$$

we have

$$f'(\mathbf{x}(\lambda)) - \lambda g'(\mathbf{x}) = 0, \quad (2.24)$$

where the derivative is w.r.t  $\mathbf{x}(\lambda)$ . Then

$$F'(\lambda) = [f'(\mathbf{x}(\lambda))]^T \mathbf{x}'(\lambda) - [\lambda g'(\mathbf{x})]^T \mathbf{x}'(\lambda) - g(\mathbf{x}) = -g(\mathbf{x}) < 0. \quad (2.25)$$

Thus  $F(\lambda)$  is concave. □

Using Newton's method,  $\lambda$  is updated at each iteration to find  $\lambda^*$ :

$$\lambda_{n+1} = \lambda_n - \frac{F(\lambda_n)}{F'(\lambda_n)} = \lambda_n - \frac{f(x_n) - \lambda_n g(x_n)}{-g(x_n)} = \frac{f(x_n)}{g(x_n)}. \quad (2.26)$$

Observing (2.22), Dinkelbach's algorithm makes a link between EE maximization and rate maximization:  $f(\mathbf{x})$  denotes the rate and  $\lambda g(\mathbf{x})$  is linear with the power consumption. Therefore, by using Dinkelbach's algorithm, the solution of EE maximization has a structure similar to that for rate maximization.



# Chapter 3

## MIMO-OFDM systems with rate-dependent circuit power

### 3.1 Related works and chapter review

As EE is traditionally defined as the transmitted information per consumed energy, an alternative formulation of the original EE maximization problem was proposed by the authors of [IF10] who stated it as the minimization of the consumed energy per bit of information received. This route has also been pursued in [PD10] and [ED12] to investigate the power allocation problem in OFDM systems, confirming the waterfilling nature of the optimal solution. All the papers above, however, consider the overall circuit power consumption (except the transmit power) to be either zero or a constant value. On the contrary, the authors of [WV13] accounted for the variability of the circuit power consumption for discrete-time base-band signal processing (due to different modulation orders and coding rates) by modelling this power as being dependent on the transmission rate.

In this chapter, we consider the EE design of precoders for MIMO-OFDM systems, formulated as the minimization of the consumed energy per bit of information received. As a main result, capitalizing on the quasi-convexity of the EE function, we derive the optimum precoding and power allocation strategy. Eventually, the impact of system parameters is mathematically analyzed and the results are confirmed by means of computational results.

## 3.2 System model

Consider a MIMO-OFDM system with  $M$  transmit antennas,  $N$  receive antennas and  $K$  subcarriers. Assuming perfect synchronization, the observation model at the  $k$ -th subcarrier is given by

$$\mathbf{y}_k = \sqrt{\beta} \mathbf{H}_k \mathbf{x}_k + \mathbf{n}_k. \quad (3.1)$$

$\mathbf{H}_k \in \mathbb{C}^{N \times M}$  is the MIMO channel matrix for the  $k$ -th subcarrier, whose entries are assumed to be independent and identically distributed (i.i.d.) zero-mean circularly-symmetric complex Gaussian random variables with unit variance.  $\beta = (G_1 M_l d^n)^{-1}$  is the path loss budget where  $n$  is the path loss exponent,  $G_1$  is the gain factor at  $d = 1\text{m}$  and  $M_l$  is the link margin accounting for the hardware process variations and other noise and interference [CGB05].  $\mathbf{x}_k$  is an  $M \times 1$  vector which denotes the transmitted symbols with a transmission power  $P_k = \mathbb{E}\{\mathbf{x}_k^H \mathbf{x}_k\}$ .  $\mathbf{n}_k$  is a zero-mean complex additive white Gaussian noise vector with covariance  $\mathbb{E}\{\mathbf{n}_k \mathbf{n}_k^H\} = \sigma^2 \mathbf{I}_N$ , where  $\sigma^2 = BN_0 N_f$ ,  $B$  is the bandwidth per subcarrier,  $N_0$  is the one-sided noise power spectral density, and  $N_f$  is the noise figure defined as in [CGB05].

According to [WV13], the total power consumption of the transceiver can be modeled as

$$P_{\text{total}} = \frac{1}{\omega} \sum_{k=1}^K P_k + P_c + \kappa \phi \left( B \sum_{k=1}^K \theta_k \right) \text{ (Watt)}, \quad (3.2)$$

where  $\omega$  is the efficiency of the power amplifier,  $P_c = \rho_{tc}M + \rho_{rc}N$  accounts for the power needed to feed the radio frequency (RF) chain [CGB05], while  $\kappa \phi \left( B \sum_{k=1}^K \theta_k \right)$  is the rate-dependent term due to the discrete-time baseband signal processing.  $\kappa$  represents a constant coefficient,  $\theta_k$  is the information rate at the  $k$ -th subcarrier, and  $\phi(\cdot)$  is assumed to be monotonically increasing function with  $\phi(0) = 0$ . Traditionally, the EE function is defined as the information rate divided by the total energy consumption:  $\left( B \sum_{k=1}^K \theta_k \right) / P_{\text{total}}$ . In this chapter, we pursue a different route by investigating the consumed energy per bit of information received, i.e.

$$\varepsilon = \frac{\frac{1}{\omega} \sum_{k=1}^K P_k + P_c + \kappa \phi \left( B \sum_{k=1}^K \theta_k \right)}{B \sum_{k=1}^K \theta_k} \text{ (Joule/bit)}. \quad (3.3)$$

In the following, we will see that thanks to this formulation of the performance metric, we can restate the problem as a convex program and derive the optimal solution. Note that in other chapters, we will always stick to the conventional EE definition, i.e., the transmission rate per consumed energy.

### 3.3 Energy efficient precoder design

In this section, we first restate the original fractional program as a convex optimization problem and then we derive the optimal precoding strategy. Finally we propose an algorithm achieving the minimum energy consumption per bit received.

#### 3.3.1 Precoder optimization

Our aim is to minimize the function defined as in (3.3). The problem can therefore be formulated as

$$\min_{\{\mathbf{Q}_k\}} \frac{\frac{1}{\omega} \sum_{k=1}^K P_k(\mathbf{Q}_k) + P_c + \kappa \phi \left( B \sum_{k=1}^K \theta_k(\mathbf{Q}_k) \right)}{B \sum_{k=1}^K \theta_k(\mathbf{Q}_k)} \quad (3.4)$$

where  $\mathbf{Q}_k = \mathbf{x}_k \mathbf{x}_k^H$  is the covariance transmission matrix for the  $k$ -th subcarrier with  $P_k(\mathbf{Q}_k) = \text{tr}(\mathbf{Q}_k) = \mathbb{E}\{\mathbf{x}_k^H \mathbf{x}_k\}$ . Assuming Gaussian codewords, we have

$$\theta_k = \log_2 \left| \mathbf{I}_N + \frac{\beta \mathbf{H}_k \mathbf{Q}_k \mathbf{H}_k^H}{\sigma^2} \right| \quad (\text{bits/channel use}). \quad (3.5)$$

We first show the following lemma.

**Lemma 3.1.** *The optimal structure of  $\mathbf{Q}_k$  is  $\mathbf{Q}_k = \mathbf{V}_k \tilde{\mathbf{Q}}_k \mathbf{V}_k^H$ ,  $k = 1, \dots, K$ , where  $\tilde{\mathbf{Q}}_k$  is a diagonal matrix and  $\mathbf{V}_k$  comes from the singular value decomposition (SVD) of  $\mathbf{H}_k$  that  $\mathbf{H}_k = \mathbf{U}_k \mathbf{\Sigma}_k \mathbf{V}_k^H$ , where  $\mathbf{U}_k \in \mathbb{C}^{N \times N}$ ,  $\mathbf{\Sigma}_k \in \mathbb{C}^{N \times M}$ , and  $\mathbf{V}_k \in \mathbb{C}^{M \times M}$ .*

*Proof.* Assume that  $\mathbf{Q}_k^*$  is the solution of (3.4) and  $\mathbf{V}_k^H \mathbf{Q}_k^* \mathbf{V}_k$  is not diagonal. According to SVD of  $\mathbf{H}_k$ , we have

$$\beta \mathbf{H}_k^H \mathbf{H}_k = \mathbf{V}_k \mathbf{\Lambda}_k \mathbf{V}_k^H, \quad (3.6)$$

where  $\mathbf{V}_k$  is a unitary matrix and  $\mathbf{\Lambda}_k = \beta \mathbf{\Sigma}_k^H \mathbf{\Sigma}_k$  is a diagonal matrix. Define  $\tilde{\mathbf{Q}}_k^* = \mathbf{V}_k^H \mathbf{Q}_k^* \mathbf{V}_k$ , where  $\text{tr}(\tilde{\mathbf{Q}}_k^*) = \text{tr}(\mathbf{Q}_k^*)$ , thanks to Hadamard's inequality, we have

$$\begin{aligned} \log_2 \left| \mathbf{I}_N + \frac{\beta \mathbf{H}_k \mathbf{Q}_k^* \mathbf{H}_k^H}{\sigma^2} \right| &= \log_2 \left| \mathbf{I}_M + \frac{\tilde{\mathbf{Q}}_k^* \mathbf{\Lambda}_k}{\sigma^2} \right| \\ &< \log_2 \prod_{m=1}^M \left( 1 + \frac{(\tilde{\mathbf{Q}}_k^*)_m (\mathbf{\Lambda}_k)_m}{\sigma^2} \right) = \log_2 \prod_{m=1}^M \left( 1 + \frac{(\tilde{\mathbf{Q}}_k^*)_m (\mathbf{\Lambda}_k)_m}{\sigma^2} \right), \end{aligned} \quad (3.7)$$

where the first equality is due to Sylvester's determinant theorem stating that  $\log_2 |\mathbf{I}_p + \mathbf{A}\mathbf{B}| = \log_2 |\mathbf{I}_q + \mathbf{B}\mathbf{A}|$ , where  $\mathbf{A}$  is a  $p \times q$  matrix and  $\mathbf{B}$  is a  $q \times p$  matrix. Therefore there exists a diagonal matrix  $\tilde{\mathbf{Q}}_k'$  such that

$$P'_k = \text{tr}(\tilde{\mathbf{Q}}_k') < \text{tr}(\tilde{\mathbf{Q}}_k^*) = P_k^*, \quad (3.8)$$

and

$$\log_2 \prod_{m=1}^M \left( 1 + \frac{(\tilde{\mathbf{Q}}_k')_m (\mathbf{\Lambda}_k)_m}{\sigma^2} \right) = \log_2 \left| \mathbf{I}_N + \frac{\beta \mathbf{H}_k \mathbf{Q}_k^* \mathbf{H}_k^H}{\sigma^2} \right|. \quad (3.9)$$

Then from (3.3), defining  $\mathbf{Q}'_k = \mathbf{U}_k^H \tilde{\mathbf{Q}}_k' \mathbf{U}_k$ , we have

$$\varepsilon \{ \mathbf{Q}_1^*, \dots, \mathbf{Q}'_k, \dots, \mathbf{Q}_K^* \} < \varepsilon \{ \mathbf{Q}_1^*, \dots, \mathbf{Q}_k^*, \dots, \mathbf{Q}_K^* \}, \quad (3.10)$$

which is contradictory with the fact that  $\mathbf{Q}_k^*$  minimizes the objective function. Therefore, every matrix  $\tilde{\mathbf{Q}}_k^*$ ,  $k = 1, \dots, K$ , should be a diagonal matrix.  $\square$

In the following, we only consider the subset of matrices  $\mathbf{Q}_k$  that have the structure as in Lemma 3.1. Hence, the rate for subcarrier  $k$  can be rewritten as

$$\begin{aligned} \theta_k &= \log_2 \left| \mathbf{I}_N + \frac{\beta \mathbf{H}_k \mathbf{Q}_k \mathbf{H}_k^H}{\sigma^2} \right| \\ &= \sum_{m=1}^M \log_2 \left( 1 + \frac{(\tilde{\mathbf{Q}}_k)_m (\mathbf{\Lambda}_k)_m}{\sigma^2} \right) \triangleq \sum_{m=1}^M \theta_{k,m}, \end{aligned} \quad (3.11)$$

which defines  $\theta_{k,m}$ . As

$$\left(\tilde{\mathbf{Q}}_k\right)_m = \frac{\sigma^2}{(\mathbf{\Lambda}_k)_m} (2^{\theta_{k,m}} - 1), \quad (3.12)$$

and

$$P_k = \sum_{m=1}^M \left(\tilde{\mathbf{Q}}_k\right)_m, \quad (3.13)$$

it appears that there is a one-to-one mapping between the rate and the covariance matrix, and that  $P_k$  can be written as a function of  $\theta_{k,1}, \dots, \theta_{k,M}$ . Therefore, instead of formulating the problem in the variables  $\mathbf{Q}_k$ , we can restate it in the variables  $\theta_{k,m}$ , which is similar to the approach of [IF10]:

$$\begin{aligned} \min_{\{\theta_{k,m}\}, t \in \mathbb{R}_+} \quad & t \left( \frac{1}{\omega} \sum_{k=1}^K P_k + P_c + \kappa \phi \left( B \sum_{k=1}^K \sum_{m=1}^M \theta_{k,m} \right) \right) \\ \text{s.t.} \quad & t \left( B \sum_{k=1}^K \sum_{m=1}^M \theta_{k,m} \right) = 1 \end{aligned} \quad (3.14)$$

where, for a given  $t$ , this problem is convex. The corresponding Lagrangian is:

$$\begin{aligned} & L(\theta_{1,1}, \dots, \theta_{K,M}, v) \\ = & t \left( P_c + \frac{1}{\omega} \sum_{k=1}^K \sum_{m=1}^M \frac{\sigma^2}{(\mathbf{\Lambda}_k)_m} (2^{\theta_{k,m}} - 1) + \kappa \phi \left( \frac{1}{t} \right) \right) \\ & + v \left( 1 - tB \sum_{k=1}^K \sum_{m=1}^M \theta_{k,m} \right). \end{aligned} \quad (3.15)$$

Therefore, the optimal solution must fulfill the following Karush-Kuhn-Tucker (KKT) conditions:

$$\theta_{k,m}^* \geq 0, \quad k = 1, \dots, K \quad (3.16)$$

$$1 - tB \sum_{k=1}^K \sum_{m=1}^M \theta_{k,m}^* = 0 \quad (3.17)$$

$$\frac{t}{\omega} \cdot \frac{\sigma^2 \ln 2}{(\mathbf{\Lambda}_k)_m} 2^{\theta_{k,m}^*} - vtB = 0, \quad k = 1, \dots, K \quad (3.18)$$

which, after some manipulation of (3.18), leads to

$$\theta_{k,m}^* = \left[ \log_2(vB\omega) - 1 \circ \mathfrak{g}_2 \left( \frac{\sigma^2 \ln 2}{(\Lambda_k)_m} \right) \right]_0^+ \quad (3.19)$$

Substituting (3.19) into (3.12), we get

$$(\tilde{\mathbf{Q}}_k)_m^* = \left[ \frac{\omega v B}{\ln 2} - \frac{\sigma^2}{(\Lambda_k)_m} \right]_0^+ \quad (3.20)$$

Defining the water level as being  $\mu = \frac{\omega v B}{\ln 2}$ , the next step is to find its optimal value. This can be obtained by rewriting the total power ( $P = \sum_{k=1}^K P_k$ ) as a function of the total rate ( $\Theta = \sum_{k=1}^K \theta_k$ ), leading to

$$P(\Theta) = \sigma^2 \sum_{l=1}^L \left( \sqrt[L]{\frac{2^\Theta}{\prod \Lambda_l}} - \frac{1}{\Lambda_l} \right), \quad (3.21)$$

because

$$\Theta = \sum_{l=1}^L 1 \circ \mathfrak{g}_2 \left( 1 + \frac{p_l \Lambda_l}{\sigma^2} \right) = \sum_{l=1}^L 1 \circ \mathfrak{g}_2 \left( \frac{\mu \Lambda_l}{\sigma^2} \right), \quad (3.22)$$

where  $L$  is the number of eigenchannels receiving a non-zero power among the  $\min\{M, N\} \times K$  space/frequency subchannels.  $p_l$  denotes the transmission power and  $\Lambda_l$  denotes the channel gain for the  $l$ -th subchannel. The derivative of the transmit power with respect to the total rate is given by

$$\frac{dP}{d\Theta} = \frac{\sigma^2 \ln 2}{\sqrt[L]{\prod_{l'=1}^L \Lambda_{l'}}} \cdot 2^{\frac{\Theta}{L}}, \quad (3.23)$$

from which it can clearly be seen that  $P(\Theta)$  is a strictly increasing and strictly convex function.

Then we have the following lemma:

**Lemma 3.2.** *If  $\frac{P(\Theta)}{\omega} + \kappa\phi(B\Theta)$  is convex, then  $\varepsilon(\Theta)$  is quasi-convex.*

*Proof.* Let us denote  $g(\Theta) = \frac{P(\Theta)}{\omega} + \kappa\phi(B\Theta)$ . We have

$$\varepsilon(\Theta) = \frac{P_c + g(\Theta)}{B\Theta}. \quad (3.24)$$

Assume that  $\Theta_1 < \Theta_2$  and  $0 < \lambda < 1$ . If

$$\varepsilon(\lambda\Theta_1 + (1 - \lambda)\Theta_2) > \varepsilon(\Theta_1), \quad (3.25)$$

we have

$$\frac{P_c + g(\lambda\Theta_1 + (1 - \lambda)\Theta_2)}{B(\lambda\Theta_1 + (1 - \lambda)\Theta_2)} > \frac{P_c + g(\Theta_1)}{B\Theta_1}. \quad (3.26)$$

Noting that, thanks to the convexity of  $g(\Theta)$ ,

$$g(\lambda\Theta_1 + (1 - \lambda)\Theta_2) < \lambda g(\Theta_1) + (1 - \lambda)g(\Theta_2), \quad (3.27)$$

we get

$$\begin{aligned} & P_c B(\lambda\Theta_1 + (1 - \lambda)\Theta_2) + Bg(\Theta_1)(\lambda\Theta_1 + (1 - \lambda)\Theta_2) \\ & < P_c B\Theta_1 + B\Theta_1 g(\lambda\Theta_1 + (1 - \lambda)\Theta_2) \\ & < P_c B\Theta_1 + B\Theta_1 \lambda g(\Theta_1) + B\Theta_1 (1 - \lambda)g(\Theta_2) \end{aligned} \quad (3.28)$$

which after some manipulations, leads to

$$P_c < \frac{\Theta_1 g(\Theta_2) - \Theta_2 g(\Theta_1)}{\Theta_2 - \Theta_1}. \quad (3.29)$$

If instead of (3.25), we assume that

$$\varepsilon(\lambda\Theta_1 + (1 - \lambda)\Theta_2) > \varepsilon(\Theta_2), \quad (3.30)$$

and similarly we get

$$P_c > \frac{\Theta_1 g(\Theta_2) - \Theta_2 g(\Theta_1)}{\Theta_2 - \Theta_1}. \quad (3.31)$$

Equations (3.29) and (3.31) cannot be met simultaneously, which means that

$$\varepsilon(\lambda\Theta_1 + (1 - \lambda)\Theta_2) \leq \max\{\varepsilon(\Theta_1), \varepsilon(\Theta_2)\}, \quad (3.32)$$

which implies that  $\varepsilon(\Theta)$  is a quasi-convex function.  $\square$

Lemma 2 means that  $\frac{P(\Theta)}{\omega} + \kappa\phi(B\Theta)$  should be convex to guarantee that the objective function is quasi-convex.

The optimal transmission rate should fulfill the following condition:

$$\varepsilon'(\Theta) = \frac{1}{B\Theta} \left( P'_{\text{total}}(\Theta) - \frac{P_{\text{total}}(\Theta)}{\Theta} \right) = 0. \quad (3.33)$$

Let us consider a generic convex model for the baseband power consumption, in the form of  $\phi(B\Theta) = (B\Theta)^\alpha$  ( $\alpha \geq 1$ ). Then, we obtain

$$P'_{\text{total}}(\Theta) = \alpha\kappa B^\alpha \Theta^{\alpha-1} + \frac{P'(\Theta)}{\omega} = \alpha\kappa B^\alpha \Theta^{\alpha-1} + \frac{\mu(\Theta)\ln 2}{\omega}, \quad (3.34)$$

where we made explicit the dependence of  $\mu$  with respect to  $\Theta$ . Hence, the value of the total information rate minimizing the consumed energy per bit must be such that

$$\varepsilon'(\Theta) = \frac{\mu(\Theta)\ln 2}{\omega} - \frac{1}{\Theta} \left( \frac{P(\Theta)}{\omega} + P_c \right) + (\alpha - 1) \kappa B^\alpha \Theta^{\alpha-1} = 0. \quad (3.35)$$

### 3.3.2 Algorithm description

In the previous subsection, we showed that the original fractional program can be solved by simply finding an information rate value that satisfies (3.35). Unfortunately, such a value cannot be obtained in a closed form. Hence, we resort to an iterative approach based on a bisection algorithm. The algorithm is provided hereafter. The initial value  $\Theta_u^0$  can be set to any arbitrary strictly positive value. The iteration stops when the search interval becomes smaller than a prescribed threshold  $\delta$ .

## 3.4 Impact of system parameters

In this section, we analyze the impact of some system parameters on the EE link performance metric. We first consider the impact of the distance  $d$  on the minimum consumed energy per received bit when all the other parameters are kept to a given constant value.

---

**Algorithm 3.1:** Calculate  $\Theta^*$  and  $\varepsilon^*$ 


---

```

1: Set  $\Theta_l = 0$ ;  $\Theta_u = \Theta_u^0$ 
2: Calculate  $\mu_u$  and  $P_u$  at the point  $\Theta_u$ . Calculate  $\varepsilon'(\Theta_u)$ .
3: while  $\varepsilon'(\Theta_u) < 0$  do
4:    $\Theta_u = \Theta_u \times 2$ 
5: end while
6: while  $\Theta_u - \Theta_l > \delta$  do
7:    $\Theta_c = 0.5(\Theta_l + \Theta_u)$ 
8:   Calculate  $\Pi(\Theta_c)$ 
9:   if  $\varepsilon'(\Theta_c) = 0$  then
10:    go to line 15
11:  else if  $\Pi(\Theta_c) > 0$  then
12:     $\Theta_u = \Theta_c$ 
13:  else
14:     $\Theta_l = \Theta_c$ 
15:  end if
16: end while

```

---

Assume two different values of the transmitter-receiver separation  $d$ , namely  $d_1$  and  $d_2$ , where  $d_2 > d_1$ . Denote by  $\varepsilon(\Theta; d)$  the consumed energy per bit evaluated for a rate  $\Theta$  at distance  $d$ . Denote by  $P_c(d)$  the power consumption needed to feed the RF chains for distance  $d$  and by  $\Theta^*(d) = \arg \min_{\Theta} \{\varepsilon(\Theta; d)\}$  the value of the rate  $\Theta$  corresponding to the minimum consumed energy per bit at distance  $d$ . Finally, denote by  $P(\Theta; d)$  the total transmit power evaluated at distance  $d$  to achieve the rate  $\Theta$ . Then

we have

$$\begin{aligned}
\varepsilon(\Theta^*(d_2); d_2) &= \frac{\frac{P(\Theta^*(d_2), d_2)}{\omega} + P_c(d_2) + \kappa\phi(B\Theta^*(d_2))}{B\Theta^*(d_2)} \\
&= \frac{\left(\frac{d_2}{d_1}\right)^n \cdot \frac{P(\Theta^*(d_2), d_1)}{\omega} + P_c(d_1) + \kappa\phi(B\Theta^*(d_2))}{B\Theta^*(d_2)} \\
&> \frac{\frac{P(\Theta^*(d_2), d_1)}{\omega} + P_c(d_1) + \kappa\phi(B\Theta^*(d_2))}{B\Theta^*(d_2)} \\
&= \varepsilon(\Theta^*(d_2); d_1) \geq \varepsilon(\Theta^*(d_1); d_1). \tag{3.36}
\end{aligned}$$

The second equality comes from (3.6), (3.21) and (3.22) observing that, when the distance  $d$  increases from  $d_1$  to  $d_2$ , the channel gain of every subchannel ( $\Lambda_l$  in (3.21)) is multiplied by  $(d_2/d_1)^{-n}$ . Hence, according to (3.22), the rate can be kept constant if the water level is multiplied by  $(d_2/d_1)^n$ . Since the rate is a strictly monotonic function of the water level, this is the unique possible choice. Thus according to the waterfilling policy, the number of subchannels with non-zero power is not changed, and the total transmit power is multiplied by  $(d_2/d_1)^n$ .  $P_c$  is independent of the value  $d$ . The last inequality is due to the fact that  $\Theta^*(d_1)$  minimizes the function when  $d = d_1$ . Therefore we have,  $\varepsilon(\Theta^*(d_2); d_2) > \varepsilon(\Theta^*(d_1); d_1)$ , meaning that the minimum number of Joules per received bit increases with the distance.

Let us now analyze the impact of distance  $d$  on the rate value at the optimal point. Let us define  $P_{\text{total}}(\Theta, d)$  as the total power written as a function of  $\Theta$  and  $d$ . With the definitions provided above, we have the following theorem:

**Theorem 3.1.** *If  $\phi(\cdot)$  is linear, then  $\Theta^*(d_2) < \Theta^*(d_1)$  for  $d_2 > d_1$ .*

*Proof.* Since  $\Theta^*(d_1)$  is the optimal point that minimizes the objective function when  $d = d_1$ , according to (3.33),

$$\varepsilon'(\Theta^*(d_1), d_1) = \frac{P'_{\text{total}}(\Theta^*(d_1), d_1) - \frac{P_{\text{total}}(\Theta^*(d_1), d_1)}{\Theta^*(d_1)}}{B\Theta^*(d_1)} = 0. \tag{3.37}$$

If  $\phi(\cdot)$  is linear, after some manipulations, we get

$$\frac{P'(\Theta^*(d_1), d_1)}{\omega} = \frac{\frac{P(\Theta^*(d_1), d_1)}{\omega} + P_c(d_1)}{\Theta^*(d_1)}. \quad (3.38)$$

Then

$$\begin{aligned} \varepsilon'(\Theta^*(d_1), d_2) &= \frac{1}{B\Theta^*(d_1)} \left( \frac{P'(\Theta^*(d_1), d_2)}{\omega} \right. \\ &\quad \left. - \frac{1}{\Theta^*(d_1)} \left( \frac{P(\Theta^*(d_1), d_2)}{\omega} + P_c(d_1) \right) \right) \\ &= \frac{1}{B\Theta^*(d_1)} \left( \left( \frac{d_2}{d_1} \right)^n \cdot \frac{P'(\Theta^*(d_1), d_1)}{\omega} \right. \\ &\quad \left. - \frac{1}{\Theta^*(d_1)} \left( \left( \frac{d_2}{d_1} \right)^n \cdot \frac{P(\Theta^*(d_1), d_1)}{\omega} + P_c(d_1) \right) \right) \\ &= \frac{1}{B\Theta^*(d_1)} \left( \left( \frac{d_2}{d_1} \right)^n \cdot \frac{P_c(d_1)}{\Theta^*(d_1)} - \frac{P_c(d_1)}{\Theta^*(d_1)} \right) > 0. \quad (3.39) \end{aligned}$$

where the derivative of the power in the first line together with equation (3.23) yields the third line. Using the fact that  $\varepsilon(\Theta, d)$  is quasi-convex,  $\varepsilon'(\Theta, d) > 0$  for  $\Theta > \Theta^*(d)$ ,  $\varepsilon'(\Theta, d) < 0$  for  $\Theta < \Theta^*(d)$ , which is proven in detail in Theorem 1 in [WV13]. Therefore we have  $\Theta^*(d_1) > \Theta^*(d_2)$ .  $\square$

A similar analysis can be carried out for parameters  $\sigma^2$ ,  $\rho_{tc}$  and  $\rho_{rc}$ . We however omit it for the sake of concision. It appears that increasing the noise variance  $\sigma^2$  has an impact similar to increasing the distance, meaning that the optimal rate value decreases with increasing noise variance. As far as  $\rho_{tc}$  and  $\rho_{rc}$  are concerned, increasing their value also leads to a decrease of the corresponding optimal value of the rate.

## 3.5 Numerical results

In this section, we illustrate our analytical findings by means of numerical results. The system parameters are set as follows: the bandwidth for each subcarrier is set to  $B = 10\text{KHz}$ ,  $\rho_{tc} = 82.5\text{mW}$ ,  $\rho_{rc} = 105.5\text{mW}$  [CGB05], and we fix  $\kappa = 5 \times 10^{-8}$  as in [WV13]. We also select the following values:

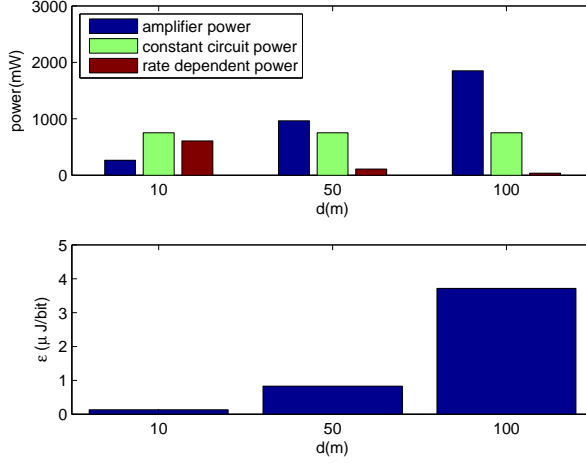


Figure 3.1: Power consumption and EE comparison for different  $d$  with  $M = N = 4$  and  $K = 64$ .

$n = 3.5$ ,  $G_{0dB} = -(G_{1dB} + M_{l_{dB}}) = -70dB$  where  $G_{1dB} = 30dB$  is the gain factor at  $d = 1m$  and  $M_{l_{dB}} = 40dB$  [CGB05]. The noise power spectral density is set to  $N_{0dB} = -170dBm/Hz$ , the noise figure to  $N_{f_{dB}} = 10dB$  as in paper [CGB05] and the amplifier efficiency is chosen to be  $\omega = 0.4$ . Unless otherwise specified, we use a parameter  $\alpha = 1$  for the rate dependent power consumption term. Finally, we set  $\delta = 0.01$  as the tolerance of the bisection algorithm. The results are averaged over 1000 different channel realizations.

### 3.5.1 Effect of link distance $d$

Fig. 3.1 reports both the different power consumption terms and the value of the objective function  $\varepsilon$  at the optimal point, for different values of  $d = 10, 50, 100m$ . The number of antennas and the number of carriers are set to  $M = N = 4$  and  $K = 64$ , respectively. As said before, the value of the objective function  $\varepsilon$  increases with the distance. So does the transmit power. As expected from Theorem 3.1, the optimum rate value decreases with increasing distance which means that the rate dependent power consumption also decreases with increasing distance. In view of these different depen-

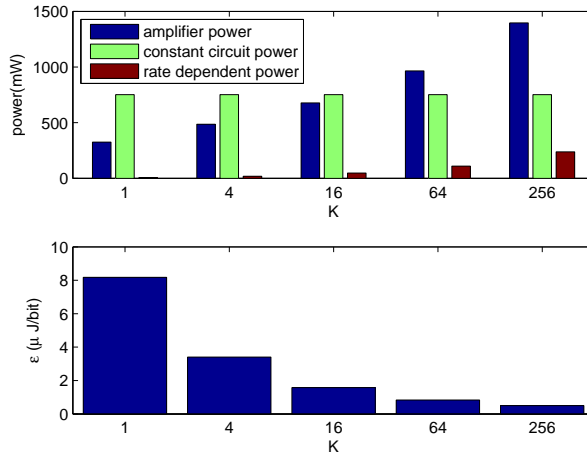


Figure 3.2: Power consumption and EE comparison for different  $K$  with  $M = N = 4$  and  $d=50\text{m}$ .

dencies of power consumption terms with respect to distance it is however difficult to predict the evolution of the total power with the distance.

### 3.5.2 Effect of bandwidth enlargement

Fig. 3.2 reports both the different power consumption terms and the value of the objective function  $\varepsilon$  at the optimal point, for a number of subcarriers  $K$  growing from 1 to 256, meaning different bandwidth sizes  $KB$ . We select  $d = 50\text{m}$  and  $M = N = 4$ . As it is expected, it can be observed that the consumed energy per bit decreases when the number of subcarriers grows. As a matter of fact, when the number of carriers is increased from  $K_1$  to  $K_2$  the solution space for  $K_1$  is contained in the solution space of  $K_2$  and the solution for  $K = K_2$  cannot be worse than the solution for  $K = K_1$ . It is also observed that both the transmit power and the rate dependent power grow with  $K$ , meaning that the rate increases with an increasing value of  $K$ .

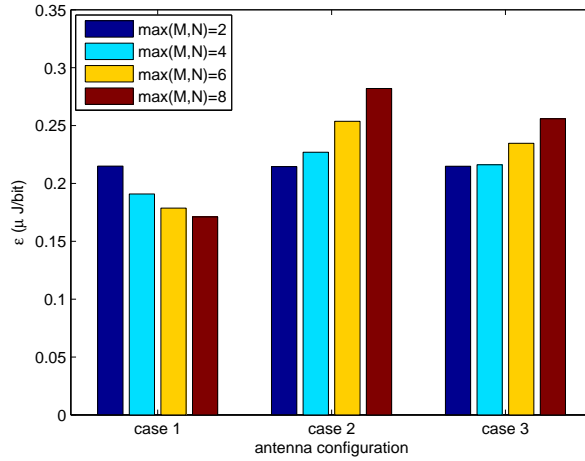


Figure 3.3: Power consumption and EE comparison for different antenna configurations with  $d=10\text{m}$  and  $K=32$ .

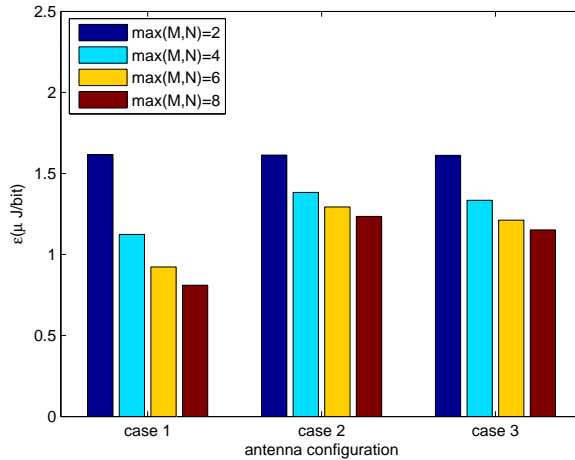


Figure 3.4: Power consumption and EE comparison for different antenna configurations with  $d=50\text{m}$  and  $K=32$ .

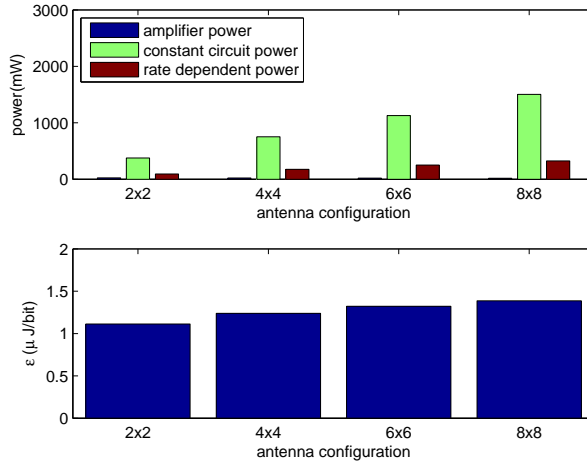


Figure 3.5: Power consumption and EE comparison for different antenna configurations with  $d = 10\text{m}$  and  $K = 32$ .  $\phi(B\Theta) = (B\Theta)^{1.2}$  which is nonlinear.

### 3.5.3 Effect of antenna configuration

Finally, we investigate the impact of antenna configurations on our objective function. Figs. 3.3 and 3.4 report the value of the objective function at the optimum for 3 different sets of configurations. In the first set  $M$  and  $N$  take simultaneously values of  $\{2, 4, 6, 8\}$ , which is beneficial for the spatial dimensions captured. In the second set  $M = 2$  and  $N \in \{2, 4, 6, 8\}$ , which corresponds to receive diversity. The third set corresponds to transmit diversity:  $M \in \{2, 4, 6, 8\}$  and  $N = 2$ . As it appears from figure 3.3, for the system parameters selected here and with  $d = 10\text{m}$  and  $K = 32$ , set 1 is more beneficial when the number of antennas increases. This is mainly due to the pre-log factor associated with the spatial multiplexing gain. On the contrary, it is detrimental to only increase  $M$  (the number of transmit antennas) or  $N$  (the number of receive antennas). This can be explained by the fact that the short distance between transmitter and receiver translates into a small transmit power, which turns out not to be the dominating term in the total power consumption. Otherwise stated, the total power is more impacted by the constant term, meaning that the optimal point corresponds to a

high signal-to-noise ratio (SNR) value [BL11]. Hence, when the number of transmit (receive) antennas increases, the diversity gain cannot compensate the increase of power consumption due to the additional RF chains. Fig. 3.4 compares the three sets of antenna configurations for a larger distance, i.e.  $d = 50\text{m}$ . While the conclusion remains the same for the first set of configurations, increasing the number of antennas turns out to be beneficial for the two other sets, exploiting diversity. As a matter of fact, the transmitted power increases due to distance and becomes dominating in the total power. The optimal operating point corresponds to a lower SNR [BL11] at which diversity gain prevails over the additional power due to the increasing number of RF chains.

Interestingly, our previous conclusions are sensitive to the value of  $\alpha$ . Fig.3.5 reports result for a scenario where the  $\phi(\cdot)$  function is nonlinear with  $\alpha = 1.2$ . The first set of configurations, i.e.  $M = N$ , is considered. It now turns out that increasing  $M = N$  is detrimental, in opposition to what we had for  $\alpha = 1$ . This is due to the rate dependent power consumption that grows with the multiplexing gain faster than the information rate. This shows the crucial role played by the power consumption model in optimally designing the link.

## 3.6 Conclusion

In this chapter, we studied the energy efficient design of precoders for point-to-point MIMO OFDM systems. We showed that for the total power made of a constant term plus another one that is increasing and convex with the transmission rate, the consumed energy per bit is a quasi-convex function of the total transmission rate. Thanks to that, the problem of minimizing the consumed energy per bit could be reformulated as a convex fractional program and solved by means of a simple bisection algorithm. The effects of various system parameters on the optimal value of the objective function have been analyzed and illustrated by means of computational results.

# Chapter 4

## MIMO-OFDM systems with imperfect amplifier

### 4.1 Related works and chapter review

In this chapter, we model the nonlinear distortion of HPA as an additional noise component, also referred to as nonlinear distortion noise. Imperfect HPA has severe impact on transmission rate and also EE. The so-called clipping effect of the HPA in OFDM systems has originally been investigated by means of simulations in [LC98] while an analytical characterization of the nonlinear distortions has been proposed in [DTV00] and [LO15]. In [GDM15], the authors propose three different approaches to deal with the nonlinear distortion. The first approach, which we will follow in this chapter, is to consider it as noise. With this consideration, [SST13] gives an upper bound and a lower bound of the capacity, while [ASG13] studies error vector magnitude (EVM) and symbol error rate (SER) for OFDM systems. The second one is to design a transceiver that aims to eliminate the impact of distortion. In [FMF12, QA12, GDM13], the authors propose optimized designs on MIMO and OFDM systems. The third one is to take advantage of the distortion to improve the performance [GDM15]. On the other hand, in [SA09], the tradeoff between low SNR transmission and high SNR transmission is investigated. An optimum output backoff (OBO) is obtained considering the Bussgang noise cancellation (BNC) algorithm.

In this thesis, we first formalize the optimization problem by taking ad-

vantage of the Bussgang theorem. Then, we derive the optimal precoding strategy by jointly optimizing the signal covariance as well as the input back-off (IBO) of the HPA. We also demonstrate that the optimization problem presents a hidden convexity under certain conditions. Finally, we propose a power allocation algorithm relying on a simple yet effective Dichotomous search as in [Kim97] which is similar with the bisection method. The main difference of our work from the previous is that we derive a new precoding strategy for a MIMO-OFDM system and study the effect of nonlinear distortion on the concavity of the rate function. Numerical results illustrate the advantage of our approach with respect to the conventional fixed-IBO algorithm.

## 4.2 System model

Consider a MIMO-OFDM system with  $M$  transmit antennas,  $N$  receive antennas and  $K$  subcarriers. In this chapter, for the sake of simplicity of notations, we assume  $N \geq M$  and full multiplexing is implemented. The precoded data vector  $\mathbf{x} = [\mathbf{x}_1^T, \dots, \mathbf{x}_M^T]^T$ , with  $\mathbf{x}_m \in \mathbb{C}^K$  and  $m \in \{1, 2, \dots, M\}$ , has Gaussian distribution with covariance  $\mathbb{E}\{\mathbf{x}_m \mathbf{x}_m^H\} = P_m \mathbf{I}_K$ . Denote with  $\mathbf{x}'_m = \mathbf{W}_{\text{DFT}}^H \mathbf{x}_m \in \mathbb{C}^K$  the inverse discrete Fourier transform (DFT) of  $\mathbf{x}_m$ . Without loss of generality, assume that the HPA is a simple clipper with  $A_m$  being the clipping level. According to the Bussgang theorem, [ZF05], the time-domain signal delivered by the HPA serving the  $m$ -th antenna can be modeled as

$$\mathbf{c}_m = \alpha_m(\omega_m) \mathbf{x}'_m + \mathbf{v}'_m \quad (4.1)$$

where  $\omega_m = A_m^2/P_m$  represents the IBO,  $\alpha_m \in (0, 1]$ , and  $\mathbf{v}'_m$  is the Gaussian distributed nonlinear distortion noise whose covariance matrix is given by  $\mathbb{E}\{\mathbf{v}'_m \mathbf{v}'_m{}^T\} = (\beta_m(\omega_m) - \alpha_m^2(\omega_m)) P_m \mathbf{I}_K$ . An example of the values of  $\alpha_m$  and  $\beta_m$  can be found in [ZF05] as the following:

$$\alpha_m = 1 - e^{-\omega_m} + \frac{\sqrt{\pi\omega_m}}{2} \operatorname{erfc}(\sqrt{\omega_m}), \quad (4.2)$$

$$\beta_m = 1 - e^{-\omega_m}. \quad (4.3)$$

The signal vector received at the  $n$ -th antenna, after cyclic prefix re-

moval, can then be expressed as

$$\mathbf{y}'_n = \sum_{m=1}^M \mathbf{H}'_{m,n} \left( \alpha_m(\omega_m) \mathbf{x}'_m + \mathbf{v}'_m \right) + \mathbf{n}'_n, \quad (4.4)$$

where  $\mathbf{H}'_{m,n} \in \mathbb{C}^{K \times K}$  is a circulant matrix representing the channel between the  $m$ th transmit antenna and the  $n$ th receive antenna and  $\mathbf{n}'_n$  is the thermal noise vector with covariance matrix  $\mathbb{E} \{ \mathbf{n}'_n \mathbf{n}'_n{}^* \} = \sigma^2 \mathbf{I}_K$ . Eventually, after performing conventional fast fourier transform, we get

$$\mathbf{y}_n = \mathbf{W}_{\text{DFT}} \mathbf{y}'_n = \sum_{m=1}^M \alpha_m \mathbf{H}_{m,n} \mathbf{x}_m + \sum_{m=1}^M \mathbf{H}_{m,n} \mathbf{v}_m + \mathbf{n}_n, \quad (4.5)$$

where  $\mathbf{v}_m = \mathbf{W}_{\text{DFT}} \mathbf{v}'_m$  and  $\mathbf{n}_n = \mathbf{W}_{\text{DFT}} \mathbf{n}'_n$  are the DFT of the distortion noise and the thermal noise respectively, and  $\mathbf{H}_{m,n} = \mathbf{W}_{\text{DFT}} \mathbf{H}'_{m,n} \mathbf{W}_{\text{DFT}}^H$  is a diagonal matrix representing the channel transfer matrix between the  $m$ -th transmit antenna and  $n$ -th receiving antenna in the frequency domain.

Now, for the sake of readability, denote with  $\mathbf{y}_{(k)} \in \mathbb{C}^N$  the received signal vector associated with the  $k$ -th subcarrier, so that

$$[\mathbf{y}_{(1)}^T, \dots, \mathbf{y}_{(K)}^T]^T = \mathbf{\Pi} [\mathbf{y}_1^T, \dots, \mathbf{y}_N^T]^T \quad (4.6)$$

where  $\mathbf{\Pi}$  is a properly defined permutation matrix whose aim is merely to reorder the elements of the vector  $\mathbf{y} = [\mathbf{y}_1, \dots, \mathbf{y}_N]$ . It follows that

$$\mathbf{y}_{(k)} = \mathbf{H}_{(k)} \mathbf{A} \mathbf{x}_{(k)} + \mathbf{H}_{(k)} \mathbf{v}_{(k)} + \mathbf{n}_{(k)}. \quad (4.7)$$

where  $\mathbf{A} = \text{diag}\{\alpha(\omega_1), \alpha(\omega_2), \dots, \alpha(\omega_M)\}$ ,  $\mathbf{x}_{(k)} = [\mathbf{x}_1(k), \dots, \mathbf{x}_M(k)]^T$ ,  $\mathbf{v}_{(k)} = [\mathbf{v}_1(k), \dots, \mathbf{v}_M(k)]^T$ ,  $\mathbf{n}_{(k)} = [\mathbf{n}_1(k), \dots, \mathbf{n}_M(k)]^T$  and  $\mathbf{H}_{(k)}(i, j) = \mathbf{H}'_{j,i}(k, k)$ . Hence, for each  $k$ ,  $\mathbf{H}_{(k)} \in \mathbb{C}^{K \times K}$ . Before proceeding further, please note that the symbol vector feeding the HPA relevant to the generic  $m$ -th transmit antenna is nothing else that the weighted sum of  $K$  precoded data symbols. Hence, if the number of OFDM subchannels  $K$  is sufficiently large, we can invoke the Lyapunov central limit theorem and approximate the time domain symbol covariance with  $\mathbb{E}\{\mathbf{x}'_m \mathbf{x}'_m{}^T\} \simeq P \mathbf{I}_K, \forall m \in 1, 2, \dots, M$ . It follows that  $\omega_m \simeq \omega, \forall m$  and, consequently  $\mathbf{A} \simeq \alpha(\omega) \mathbf{I}_M$ ,

if a common clipping level is assumed across all antennas ( $A_m = A$ ). In the following sections we make use of this assumption to formalize the precoding optimization problem and solve it through as the solution of a simple fixed point problem.

### 4.3 Problem formulation

To formalize the rate maximization problem, we first denote the data precoding matrix with  $\mathbf{B} = \text{Diag}\{\mathbf{B}_{(1)}, \mathbf{B}_{(2)}, \dots, \mathbf{B}_{(K)}\}$ , so that  $\mathbf{x}_{(k)} = \mathbf{B}_{(k)}\mathbf{s}_{(k)}$  with  $\mathbb{E}\{\mathbf{s}_{(k)}\mathbf{s}_{(k)}^H\} = \mathbf{I}_M$ . According to (4.7), it follows that the information rate of the link is given by

$$R(\mathbf{B}) = \sum_{k=1}^K \log_2 \left| \mathbf{I} + \mathbf{B}_{(k)}^H \mathbf{A}^H \mathbf{H}_{(k)}^H \mathbf{R}_{(k)}^{-1} \mathbf{H}_{(k)} \mathbf{A} \mathbf{B}_{(k)} \right| \quad (4.8)$$

where

$$\mathbf{R}_{(k)} = \gamma(\omega, \mathbf{B}) \mathbf{H}_{(k)} \mathbf{H}_{(k)}^H + \sigma^2 \mathbf{I}_N \quad (4.9)$$

with

$$\gamma(\omega, \mathbf{B}) = \frac{\text{tr}(\mathbf{B})}{KM} (\beta(\omega) - \alpha^2(\omega)). \quad (4.10)$$

From (4.9) and (4.10), we can note that the presence of a nonlinear distortion noise produces a self-interference whose average power is monotonically increasing with the average power of the signal delivered to the HPA.

To analyze the impact of the self-interference on the optimal precoding strategy, we first express  $\mathbf{H}_{(k)}$  through its SVD, i.e.  $\mathbf{H}_{(k)} = \mathbf{U}_k \mathbf{\Lambda}_k^{1/2} \mathbf{V}_k^H$ , where  $\mathbf{U}_k \in \mathbb{C}^{N \times N}$ ,  $\mathbf{\Lambda}_k^{1/2} \in \mathbb{C}^{N \times M}$ , and  $\mathbf{V}_k \in \mathbb{C}^{M \times M}$ . Therefore,

$$R(\mathbf{B}) = \sum_{k=1}^K \log_2 \left| \mathbf{I} + \alpha^2(\omega) \mathbf{B}_{(k)}^H \mathbf{V}_k \mathbf{\Lambda}_k (\gamma(\omega, \mathbf{B}) \mathbf{\Lambda}_k + \sigma^2 \mathbf{I}_N)^{-1} \mathbf{V}_k^H \mathbf{B}_{(k)} \right|. \quad (4.11)$$

Taking advantage of the Hadamard's inequality, the optimal precoder must be such that  $\mathbf{B}_{(k)} = \mathbf{V}_k \mathbf{\Sigma}_k, \forall k$ , with  $\mathbf{\Sigma}_k$  being a diagonal matrix. Hence,

without loss of generality, we can model the MIMO-OFDM link as  $I$  parallel subchannels with *effective SNR* equal to

$$g_i(\omega, \mathbf{B}) = \frac{\alpha^2(\omega) \lambda_i}{\gamma(\omega, \mathbf{B}) \lambda_i + \sigma^2}, \quad (4.12)$$

where  $\lambda_i$ , with  $i = 1, \dots, I$ , are the diagonal entries of the matrix  $\mathbf{\Lambda} = \text{Diag}\{\mathbf{\Lambda}_{(1)}, \mathbf{\Lambda}_{(2)}, \dots, \mathbf{\Lambda}_{(K)}\}$ . Thus,  $I = K \times \min\{M, N\}$ .

Defining  $\mathbf{\Sigma} = \text{Diag}\{\mathbf{\Sigma}_{(1)}, \mathbf{\Sigma}_{(2)}, \dots, \mathbf{\Sigma}_{(K)}\}$  and denoting with  $\Sigma(i, i) = \sqrt{p_i}$  the  $i$ th diagonal entry of  $\mathbf{\Sigma}$ , we have  $\text{tr}(\mathbf{B}) = \|\mathbf{p}\|_1$ , with  $\mathbf{p} = [p_1, p_2, \dots, p_I]^T$ . Hence, after diagonalization, we are only left with the following power allocation problem:

$$\max_{\omega, \mathbf{p}} \sum_{i=1}^I \log(1 + g_i(\omega, \mathbf{p}) p_i) \quad (4.13)$$

$$s.t. \quad \omega \|\mathbf{p}\|_1 = \sum_{m=1}^M A^2 \quad (4.14)$$

$$\omega \geq 1 \quad (4.15)$$

$$p_i \geq 0 \quad \text{for } i = 1, \dots, I. \quad (4.16)$$

*Remark:* Note that the (4.14) represents a constraint on the global power consumption. Since the clipping level of the HPAs,  $A$ , are assumed to be fixed, the solution of the power allocation problem stated above will provide an upper bound on the actual attainable link performance. Nonetheless, for values of  $K$  sufficiently large to invoke the Lyapunov central limit theorem the achieved solution will coincide with the one that would be obtained with individual power constraints.

## 4.4 Power allocation algorithm

In this section, we first derive the optimum structure of the power allocation vector  $\mathbf{p}$ , then give a sufficient condition of concavity of the rate function, and finally we propose an algorithm to find the optimum solution.

### 4.4.1 Optimal precoding strategy

First, observe that, from (4.14), the effective SNR defined in (4.12) can be rewritten as

$$g_i(\mathbf{p}) = \frac{\alpha^2 \left( \frac{P_{\text{am}}}{\|\mathbf{p}\|_1} \right) \lambda_i}{\gamma \left( \frac{P_{\text{am}}}{\|\mathbf{p}\|_1}, \mathbf{p} \right) \lambda_i + \sigma^2}, \quad (4.17)$$

where  $P_{\text{am}} = \sum_{m=1}^M A_m^2$ . Hence, the problem in (4.13) can be rewritten as

$$\max_{\omega, \mathbf{p}} \sum_{i=1}^I \log(1 + g_i(\mathbf{p}) p_i) \quad (4.18)$$

$$s.t. \quad \|\mathbf{p}\|_1 \leq P_{\text{am}} \quad (4.19)$$

$$p_i \geq 0 \quad \text{for } i = 1, \dots, I \quad (4.20)$$

$$\omega = \frac{P_{\text{am}}}{\|\mathbf{p}\|_1} \quad (4.21)$$

Trivially, one can demonstrate that the optimal solution  $(\mathbf{p}^*, \omega^*)$  can be found by relaxing the constraint (4.21), so that  $\mathbf{p}^*$  is solution of the following problem

$$\max_{\mathbf{p}} R(\mathbf{p}) = \sum_{i=1}^I \log(1 + g_i(\mathbf{p}) p_i) \quad (4.22)$$

$$s.t. \quad \|\mathbf{p}\|_1 \leq P_{\text{am}} \quad (4.23)$$

$$p_i \geq 0 \quad \text{for } i = 1, \dots, I \quad (4.24)$$

and  $\omega^* = \frac{P_{\text{am}}}{\|\mathbf{p}^*\|_1}$ . The Lagrangian function associated with the problem defined in (4.22)-(4.24) is then given by

$$L(\mathbf{p}, \nu, \eta_1, \eta_2, \dots, \eta_I) = R(\mathbf{p}) - \nu \left( \sum_{i=1}^I p_i - P_{\text{am}} \right) + \sum_{i=1}^I \eta_i p_i \quad (4.25)$$

where  $\nu \geq 0$  and  $\eta_i \geq 0, \forall i$ . Now, for the sake of readability, let

$$g'_j = \frac{\partial g_j}{\partial p_i} = \frac{\partial g_j}{\partial \|\mathbf{p}\|_1} \frac{\partial \|\mathbf{p}\|_1}{\partial p_i} = \frac{\partial g_j}{\partial P} \quad \forall i, j \quad (4.26)$$

and

$$g_j'' = \frac{\partial^2 g_j}{\partial p_i \partial p_l} = \frac{\partial^2 g_j}{(\partial \|\mathbf{p}\|_1)^2} \quad \forall i, j, l \quad (4.27)$$

denote the first and the second derivative of the effective SNR, respectively. Please, note that the dependence of  $g_j$ ,  $g_j'$  and  $g_j''$  on  $\mathbf{p}$  has been omitted in the notation. Moreover, it is worth remarking that, since  $g_j$  depends on  $\mathbf{p}$  through its norm one,  $\partial g_j / \partial p_i$  does not depend on the index  $i$ .

It follows that

$$\begin{aligned} \frac{\partial L(\mathbf{p}^*, \nu, \eta_1, \eta_2, \dots, \eta_I)}{\partial p_i^*} &= \frac{\partial R(\mathbf{p}^*)}{\partial p_i^*} - \nu + \eta_i \\ &= \frac{1}{\ln 2} \left( \frac{g_i^*}{1 + g_i^* p_i^*} + \sum_{j=1}^L \frac{g_j' p_j^*}{1 + g_j^* p_j^*} \right) - \nu + \eta_i = 0, \end{aligned} \quad (4.28)$$

where  $\eta_i$  is such that  $\eta_i p_i^* = 0$  for  $i = 1, \dots, I$ . Therefore, since  $\eta_i > 0$  only if  $p_i^* = 0$ , we can remove  $\eta_i = 0$  and the optimal power allocation vector can be found as the solution of the following fixed point problem

$$\mathbf{p}^* = \mathbf{wf}(\mu(\mathbf{p}^*)) \quad (4.29)$$

where  $\mathbf{wf} : \mathbb{R} \rightarrow \mathbb{R}^I$  represents the waterfilling operator, whose generic  $i$ th component is defined as

$$\mathbf{wf}_i(\mu(\mathbf{p}^*)) = \left[ \mu(\mathbf{p}^*) - \frac{1}{g_i^*} \right]^+ \quad (4.30)$$

and

$$\mu(\mathbf{p}^*) = \frac{1}{\nu \ln 2 - \sum_{j=1}^I \frac{g_j' p_j^*}{1 + g_j^* p_j^*}} \quad (4.31)$$

represents the water level. Interestingly, one can note that, due to the self interference caused by the nonlinear distortion noise, the water level now depends on the solution itself.

## 4.4.2 Concavity condition

Unfortunately, as a result of the nonlinear distortion, the rate function might be non-concave, thus implying a non-zero duality gap. For this reason, in the remainder of this section, we provide the reader with a sufficient

concavity condition for the rate function. To achieve this goal, we first derive the Hessian matrix of the rate function, whose generic element  $(i, j)$  is defined as

$$\frac{\partial R(\mathbf{p})}{\partial p_i \partial p_j} = \frac{\partial}{\partial p_j} \frac{g_i}{1 + g_i p_i} + \sum_{i=1}^I \frac{\partial}{\partial p_j} \frac{g'_i p_i}{1 + g_i p_i} \quad (4.32)$$

After some manipulations, one can easily find that

$$\frac{\partial R(\mathbf{p})}{\partial p_i \partial p_j} = \mathbf{D}(i, j) + \mathbf{\Omega}_1(i, j) + \mathbf{\Omega}_2(i, j) \quad (4.33)$$

where

$$\mathbf{D}(i, j) = \frac{g_i^2 \delta [i - j]}{(1 + g_i p_i)^2} \quad (4.34)$$

$$\mathbf{\Omega}_1(i, j) = \frac{g'_i}{1 + g_i p_i} + \frac{g'_j}{1 + g_j p_j} \quad (4.35)$$

and

$$\mathbf{\Omega}_2(i, j) = \sum_{i=1}^I \frac{g''_i p_i (1 + g_i p_i) - (g'_i p_i)^2}{(1 + g_i p_i)^2}. \quad (4.36)$$

A necessary and sufficient condition of concavity is that the largest eigenvalue of the Hessian matrix is negative. Since the Hessian matrix  $\nabla^2 R$  is real and symmetric, according to [KT01], its maximum eigenvalue is bounded by

$$\pi_1(\nabla^2 R) \leq \pi_1(\mathbf{D}) + \pi_1(\mathbf{\Omega}_1) + \pi_1(\mathbf{\Omega}_2), \quad (4.37)$$

where  $\pi_1(\mathbf{A})$  denotes the largest eigenvalue of the matrix  $\mathbf{A}$ . Observe that  $\mathbf{D}$  is a diagonal matrix, so that its largest eigenvalue is

$$\pi_1(\mathbf{D}) = \max \left( \left\{ -\frac{g_i^2}{(1 + g_i p_i)^2} \right\}_{i=1}^I \right) \quad (4.38)$$

As far as  $\Omega_1$  is concerned, one can easily note that  $\Omega_1$  is a real and symmetric matrix, so that from [Zha05], for  $I \geq 2$  we get

$$\pi_1(\Omega_1) \leq \frac{I(b-a)}{2} \quad (4.39)$$

where

$$a = \min \left( 2 \left\{ \frac{g'_i}{1 + g_i p_i} \right\}_{i=1}^I \right) \quad (4.40)$$

and

$$b = \max \left( 2 \left\{ \frac{g'_i}{1 + g_i p_i} \right\}_{i=1}^I \right). \quad (4.41)$$

For the case of  $I = 1$ , the maximum eigenvalue is the only entry of the matrix. The result will be given directly in (4.50).

Finally,  $\Omega_2$  is a matrix whose entries have the same value and it has only one non-zero eigenvalue equal to

$$\pi_1(\Omega_2) = \max \left( I \sum_{i=1}^I \frac{g''_i p_i (1 + g_i p_i) - (g'_i p_i)^2}{(1 + g_i p_i)^2}, 0 \right). \quad (4.42)$$

Unfortunately, the bound obtained by substituting (4.38),(4.39), (4.42) into (4.37) still depends on the vector  $\mathbf{p}$ . In order to obtain a meaningful result, we first define the subspace  $\mathcal{P} = \{\mathbf{p} \in \mathbb{R}_+^I : \|\mathbf{p}\|_1 = P_T\}$  and we observe that for a fixed total radiated power the efficient SNR  $g(\mathbf{p})$  remains constant. Obviously, this implies that the function  $R(\cdot)$  is concave on that subspace and its unique maximum value is obtained at  $\mathbf{p}^* = \mathbf{wf}(\delta(P_T))$ , where  $\delta(P_T)$  is a scalar parameter such that  $\|\mathbf{p}^*\|_1 = P_T$ . Hence, (4.29) provides the global optimal solution if there exists only one value of  $\mathbf{p}^*$  such that (4.29) holds true, i.e. the function  $R(\cdot)$  is concave on the subspace defined as

$$\mathcal{P}^* = \{\mathbf{p}^* \in \mathbb{R}_+^I : \mathbf{p}^* = \mathbf{wf}(\delta(P_T)), \forall P_T \in (0, P_{\text{am}}]\}. \quad (4.43)$$

Let us define  $\mathbf{p}^{[N_{\text{ac}}]}$  as the first  $N_{\text{ac}}$  entries of the vector  $\mathbf{p}$  and  $N_{\text{ac}}$  is the number of active subchannels which is changing with  $P_T$ . Note that if the

function is concave with respect to  $\mathbf{p}^{[N_{ac}]}$  for different values of  $N_{ac}$  respectively, then it is easy to show that it is concave with respect to  $P_T$  on the subspace defined as in (4.43) for different values of  $N_{ac}$  respectively, because  $P_T$  is the sum of all the entries of  $\mathbf{p}^{[N_{ac}]}$ . On the other hand, the first derivative of the rate function on this subspace is continuous when  $N_{ac}$  changes. Therefore the rate function is concave in the subspace of (4.43).

By only considering  $\mathbf{p}$  which are in the subspace defined in (4.43),  $\mathbf{p}$  is replaced by  $\mathbf{p}^{[N_{ac}]}$ . From (4.38), we have

$$\pi_1(\mathbf{D}) = -\frac{1}{(\delta(P_T))^2}. \quad (4.44)$$

Using Lemma 1 in the following, (4.39) becomes

$$\pi_1(\boldsymbol{\Omega}_1) = \frac{N_{ac}}{\delta(P_T)} \left( \frac{|g'_1|}{g_1} - \frac{|g'_{N_{ac}}|}{g_{N_{ac}}} \right), \quad (4.45)$$

where we denote the subchannels in a descending order,  $\lambda_1 \geq \dots \geq \lambda_L$ , and  $g_l$  comes from  $\lambda_l$  using (4.12).

**Lemma 4.1.** *If  $\lambda_i > \lambda_j$  for  $i \neq j$  and  $p_i, p_j > 0$ , then  $\frac{g'_i}{1+g_i p_i} < \frac{g'_j}{1+g_j p_j}$ .*

*Proof.* From (4.12) we know that  $g_l = \frac{\alpha^2 \lambda_l^2}{\gamma \lambda_l^2 + \sigma^2}$ , where for the sake of readability we do not write  $g_l$  as a function of  $\omega$  and  $\mathbf{p}$ , but keep in mind that  $g_l$  is always a function of  $\omega$  and  $\mathbf{p}$  since  $\alpha$  and  $\gamma$  depends on  $\omega$  and  $\mathbf{p}$ . Its derivative with respect to  $\|\mathbf{p}\|_1$  is

$$g'_l = \frac{\lambda_l^4((\alpha^2)'\gamma - \alpha^2\gamma') + \lambda_l^2(\alpha^2)'\sigma^2}{(\gamma\lambda_l^2 + \sigma^2)^2}. \quad (4.46)$$

Therefore

$$\frac{g'_l}{g_l} = \frac{1}{\alpha^2} \frac{((\alpha^2)'\gamma - \alpha^2\gamma')\lambda_l^2 + (\alpha^2)'\sigma^2}{\gamma\lambda_l^2 + \sigma^2}. \quad (4.47)$$

Since  $\lambda_i > \lambda_j > 0$  for  $i \neq j$ , using (4.47), we have

$$\begin{aligned} \frac{g'_i}{1+g_i p_i} - \frac{g'_j}{1+g_j p_j} &= \frac{g'_i}{\delta(\mathbf{p})g_i} - \frac{g'_j}{\delta(\mathbf{p})g_j} \\ &= \frac{1}{\delta(\mathbf{p})\alpha^2} \frac{(((\alpha^2)'\gamma - \alpha^2\gamma')\sigma^2 - (\alpha^2)'\sigma^2\gamma)(\lambda_i^2 - \lambda_j^2)}{(\gamma\lambda_i^2 + \sigma^2)(\gamma\lambda_j^2 + \sigma^2)} \\ &= -\frac{\gamma'\sigma^2(\lambda_i^2 - \lambda_j^2)}{\delta(\mathbf{p})(\gamma\lambda_i^2 + \sigma^2)(\gamma\lambda_j^2 + \sigma^2)} < 0. \end{aligned} \quad (4.48)$$

Therefore  $\frac{g'_i}{1+g_i p_i} < \frac{g'_j}{1+g_j p_j}$ .  $\square$

Substituting (4.44), (4.45), (4.42) into (4.37), we obtain a sufficient condition for the rate function  $R(\mathbf{p})$  to be concave in the subspace of (4.43),

$$\begin{aligned} \pi_1(\nabla^2 R) &\leq -\frac{1}{\delta(\mathbf{p})^2} + \frac{N_{ac}}{\delta(\mathbf{p})} \left( \frac{|g'_1|}{g_1} - \frac{|g'_{N_{ac}}|}{g_{N_{ac}}} \right) \\ &\quad + \max \left( N_{ac} \sum_{i=1}^{N_{ac}} \frac{g''_i p_i (1+g_i p_i) - (g'_i p_i)^2}{(1+g_i p_i)^2}, 0 \right) \\ &< 0, \quad \text{if } N_{ac} \geq 2, \end{aligned} \quad (4.49)$$

and

$$\pi_1(\nabla^2 R) = -\frac{1}{\delta(\mathbf{p})^2} + \frac{2g'_1}{\delta(\mathbf{p})g_1} + \frac{\delta(\mathbf{p})p_1 g''_1 g_1 - (g'_1)^2 p_1^2}{\delta(\mathbf{p})^2 g_1^2} < 0, \quad \text{if } N_{ac} = 1. \quad (4.50)$$

If one can guarantee  $g''_i \leq 0$ , then  $\pi_1(\nabla^2 R) < 0$  for  $N_{ac} = 1$ . From (4.49), we get, for  $N_{ac} \geq 2$ , the condition

$$\frac{|g'_1|}{g_1} - \frac{|g'_{N_{ac}}|}{g_{N_{ac}}} < \frac{1}{\delta(P_T) \cdot N_{ac}}. \quad (4.51)$$

*Remarks:* Now the condition does not depend on the solution itself, but only on the total power  $P_T$  because every effective SNR  $g_i$  and the number of active subchannels  $N_{ac}$  only depends on  $P_T$ . This implies that if the property of the nonlinear distortion is known, one can easily examine the concavity of the rate function.

### 4.4.3 Algorithm

When the total power is small, the IBO ( $\omega$ ) is large, therefore the amplifiers are in the linear zone. The rate function first increases as the classical case without nonlinear distortion. As the power increases, the IBO decreases, therefore the power of effective signal  $\alpha^2$  in the Busgang theorem decreases and the noise due to the distortion  $\gamma$  increases. As a result, the rate increases more slowly and then begins to decrease.

We use the Dichotomous search to find the solution [Kim97]. When the concavity condition in (4.51) is satisfied, the global maximum is found, otherwise, a local maximum is found. We will see in the numerical results that the rate function is always quasi-concave and the Dichotomous method always finds the best IBO.

## 4.5 Numerical results

In this section, we illustrate our analytical findings by means of numerical results. The system parameters are set as follows: the bandwidth for each subcarrier is set to  $B = 10\text{KHz}$ .  $K = 10$ ,  $M = 4$  and  $N = 4$ . We also select the following values:  $n = 3.5$ ,  $G_{0dB} = -(G_{1dB} + M_{1dB}) = -70\text{dB}$  where  $G_{1dB} = 30\text{dB}$  is the gain factor at  $d = 1\text{m}$ ,  $M_{1dB} = 40\text{dB}$ , the noise power spectral density is set to  $N_{0dB} = -170\text{dBm/Hz}$ , and the noise figure to  $N_{f_{dB}} = 10\text{dB}$  [CGB05]. Finally, we set  $\delta = 1\text{mW}$  as the tolerance of the Dichotomous algorithm. We use of the approximation of  $\alpha(\cdot)$  and  $\beta(\cdot)$  that can be found in [ZF05]. The results are averaged over 1000 different channel realizations.

In Fig. 4.1, we plot the rate function versus  $\omega$  and  $P_{am}$ . As  $10/\omega$  increases from 1 to 10, the HPA tends to saturation. We observe that when  $d$  is small, for example the case  $d = 30$ , the rate first increases and then decreases for each  $P_{am}$ . When  $d$  is large, for example the case  $d = 200$ , the rate increases monotonically. This is because the original channel gain  $g_l$  is strong for small  $d$ , and thus the detrimental term  $\gamma g_l^2$  in the effective subchannel gain, which is resulted from the distortion noise component, is dominant compared with the receiver noise  $\sigma^2$ . Therefore when the transmit power increases to saturation, the effective subchannel gains decrease rapidly. However for large  $d$ , the term  $\gamma g_l^2$  is small compared with  $\sigma^2$ . In

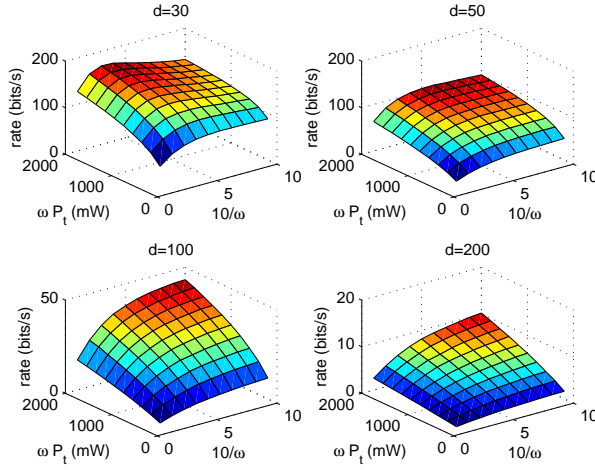


Figure 4.1: Rate as a function of IBO ( $\omega$ ) and HPA power ( $P_{am}$ ). Plot for different transceiver distance  $d$ .

this case, the IBO has only impact on  $\alpha$  and the rate keeps monotonically increasing as without distortion.

In Fig. 4.2, we plot the optimum rate versus  $P_{am}$  using the Dichotomous search. We see that in all cases the optimum rate grows with  $P_{am}$ . This is because a larger  $P_{am}$  provides more space for the HPA within saturation. With respect to optimization, larger  $P_{am}$  provides larger feasible space for the solution of the maximization problem.

Performance comparison for different IBOs is provided in Fig. 4.3 and Fig. 4.4. The adaptive IBO ( $\text{IBO}^*$ ) is plotted as a reference. We observe that  $\text{IBO}^*$  always outperforms other fixed IBOs, behaving as an envelope of all the other lines.

In Fig. 4.3, the rate for a small IBO value, for example 1, becomes inferior to that for large IBO values when  $P_{am}$  increases, which means that a larger  $P_{am}$  requires a larger IBO to maximize the rate. This implies that when more power is available in HPA, eliminating the effect of nonlinear distortion becomes more important in the trade-off between increasing IBO or increasing transmit power.

Fig. 4.4 shows that the rate for small IBO becomes superior to that achieved with large IBO values when  $d$  increases, because as explained in

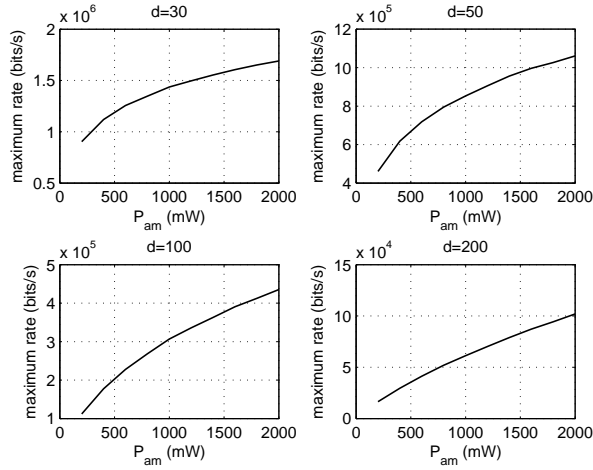


Figure 4.2: Maximum rate as a function of HPA power ( $P_{am}$ ). Plot for different transceiver distance  $d$ .

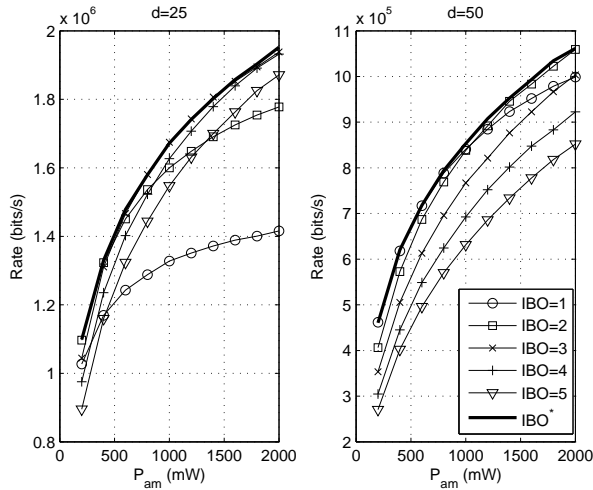


Figure 4.3: Rate performance versus HPA power ( $P_{am}$ ) for different IBO.

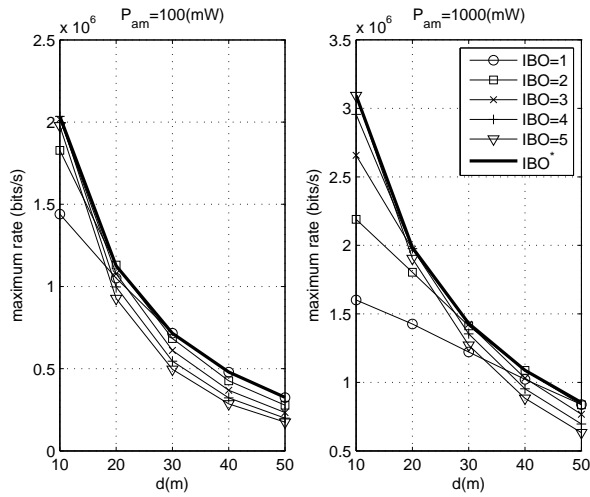


Figure 4.4: Rate performance versus  $d$  for different IBO.

Fig.4.1, nonlinear distortion has smaller effect on larger  $d$ ; therefore smaller IBO which provides more power outperforms big IBO.

## 4.6 Conclusion

We studied the rate maximization problem for MIMO-OFDM systems in the presence of nonlinear distortion noise due to the HPAs at the transmitter side. We demonstrated that the optimum precoding and power allocation strategies rely on the channel SVD decomposition and a generalized version of the water filling strategy. In particular, due to the self interference term, the generalized water filling operator presents a water level that depends on the solution itself. Then, a sufficient condition for the global optimality of the proposed solution is given. Eventually, numerical results show the advantages of our approach in comparison with traditional fixed-IBO precoding strategy.



# Chapter 5

## EE maximization in MIMO-OFDMA downlink systems

### 5.1 Related works and chapter review

In this chapter, we consider the EE maximization problem in a MIMO-OFDMA downlink. Studies on sum rate maximization for OFDMA systems can be found in [SMC06, WGLV13] and for MIMO-OFDMA systems in [LCL<sup>+</sup>07, WCLM99]. Different from the rate maximization problem in single-input-single-output (SISO)-OFDMA where each subcarrier is straightforwardly allocated to the user with the maximum channel gain, sum rate maximization for MIMO-OFDMA is not concave. Because the subcarrier allocation will change for various transmit power values, the rate should be maximized by jointly optimizing over power allocation and subcarrier allocation. The authors in [SMC06] proposed a Lagrangian dual decomposition method, while the authors in [LCL<sup>+</sup>07, WCLM99] adopted the time-sharing concept to reformulate the problem.

Several studies on precoder design and RA for EE maximization in multi-user setups are reported in [TSA<sup>+</sup>15, OHI13, YBC14, SH14, XTL15, XYL<sup>+</sup>13, XQ13, XLZ<sup>+</sup>11, VTFH16, MB16, LTY15, XLZ<sup>+</sup>12]. Papers [OHI13, YBC14, XQ13] considered multi-user MIMO systems. Zero-forcing (ZF) semiorthogonal user selection (SUS) was implemented in [YBC14] to design the pre-

coder and select favorable users for multi-user MIMO systems. Uplink-downlink duality can be used for downlink EE maximization [XQ13]. Paper [XLZ<sup>+</sup>11] studied the trade-off between spectrum efficiency (SE) and EE in OFDMA systems and some basic properties on how the system parameters impact the EE performance were investigated. EE maximization in OFDMA systems was studied by analyzing an upper bound and an lower bound of the EE function [XLZ<sup>+</sup>12]. Instead of studying stationary channels, paper [MB16] considered fast fading channels in a MIMO-OFDM network with multiple co-existing connections. The authors proposed a learning method to gradually adapt to the channel. Papers [TSA<sup>+</sup>15, SH14, XTL15, XYL<sup>+</sup>13] studied MIMO-OFDMA systems. ZF precoder was assumed in [SH14] and then subcarriers were allocated. The authors in [TSA<sup>+</sup>15] considered a circuit power changing with the number of antennas and users, and dirty paper coding (DPC) for the multi-user symbols at each subcarrier, which make EE maximization non-concave. Paper [XTL15] maximized EE through optimizing resource block (RB) allocation, where the RB is defined as in the long-term evolution (LTE) standard. In [XYL<sup>+</sup>13], the authors also considered a MIMO-OFDMA system and minimized power for a given capacity by optimizing various system parameters such as the number of subcarriers and number of RF chains, etc. However, channel state information at the transmitter (CSIT) was assumed to be unavailable and therefore precoding was not considered. Base station selection was implemented and zero-forcing precoding is assumed for an EE maximization problem of a macro-cell system with the presence of small-cell networks [VTFH16]. The energy-efficient precoder design for multi-cell networks can be solved by introducing a lower bound of the EE function [LTY15].

In this thesis, we jointly optimize the subcarrier allocation and the precoder design. Different from the previous works about MIMO-OFDMA reported in [TSA<sup>+</sup>15] and [XYL<sup>+</sup>13], we fix the number of antennas and focus on the quasi-concavity of the EE function that we obtained. An important difference compared to paper [XYL<sup>+</sup>13] is that, in this chapter, we assume perfect CSIT while paper [XYL<sup>+</sup>13] operates on the basis of statistical CSI. As a consequence, our subcarrier allocation changes with the power consumption, while on the contrary, there is no subcarrier allocation to users (only fractions of spectrum are allocated) in [XYL<sup>+</sup>13]. Moreover, one of the constraints of [XYL<sup>+</sup>13] prescribes a target for the ergodic capacity while

the this chapter targets an instantaneous rate. Besides the differences associated with CSI, the optimization problem in [XYL<sup>+</sup>13] is to minimize power consumption for a prescribed achievable ergodic capacity, while our optimization objective is the global EE maximum for a given power constraint. Therefore the study of the EE as a function of the power consumption is of primary importance, and is one of the challenges in this chapter. Compared to paper [XLZ<sup>+</sup>12] where an upper bound was analyzed for an OFDMA system, we study the exact EE function based on a closed form strategy for subcarrier allocation. As our mathematical results will reveal, the resulting EE function has properties similar to quasi-concave functions. We come up with the following key contributions.

- To the best of our knowledge, no author has jointly considered the EE-optimized subcarrier allocation and precoder design for a MIMO-OFDMA downlink system. While the precoder optimization is widely known as a quasi-concave problem [PD10, WSV15], the quasi-concavity property for MIMO-OFDMA downlink system is worth substantial theoretical analysis. This chapter provides mathematical proofs to obtain the property of the problem.
- We obtain a condition on the subcarrier allocation and the precoder at the base station at the optimum EE and show the optimality of the condition for fixed transmit power.
- We then show that the subcarrier allocation scheme makes the EE function a discontinuous quasi-concave function of the transmit power. Finally, we give an upper bound for the EE when the optimum transmit power does not fulfill the proposed condition of subcarrier allocation and power allocation. The quasi-concavity and the upper bound guarantee the convergence and the global optimality of the proposed algorithm.

The chapter is organized as follows. In Section II, we give the transmission model and EE formulation. In Section III, we first show that the optimal precoder for each subcarrier and each user is based on SVD, and then give the conditions that the optimum EE should satisfy after reformulation of the problem with time-sharing. In Section IV, we analyze the EE function and

propose an algorithm to obtain maximum EE. Section V reports the numerical results and is followed by the conclusion in Section VI.

## 5.2 System model

### 5.2.1 Transmission model

Consider a MIMO-OFDMA system with one base station and a total of  $K$  subcarriers to be allocated to  $U$  users. Each subcarrier is allocated to one user at maximum in one coherence time slot. Therefore, there is no intra-cell interference among different users at each subcarrier. We assume that perfect CSI is available at both the transmitter and the users. The base station is equipped with  $M$  antennas and each user terminal has  $N$  antennas. During the transmission, slow fading is assumed so that within each coherence time the channel remains invariant. Denote by matrix  $\mathbf{H}_{k,u} \in \mathbb{C}^{N \times M}$ ,  $k \in 1, \dots, K$  and  $u \in 1, \dots, U$  the downlink MIMO channel matrix of the  $k$ -th subcarrier for the  $u$ -th user. The transmission over the  $k$ -th subcarrier can be expressed as

$$\mathbf{y}_k = \mathbf{W}_{k,u(k)} \mathbf{H}_{k,u(k)} \mathbf{F}_{k,u(k)} \mathbf{x}_k + \mathbf{W}_{k,u(k)} \mathbf{n}_k, \quad (5.1)$$

where  $\mathbf{x}_k \in \mathbb{C}^{\min\{M,N\} \times 1}$  is the source symbol vector with a covariance matrix  $\mathbb{E} \{ \mathbf{x}_k \mathbf{x}_k^H \} = \mathbf{I}_{\min\{M,N\}}$  where we assume full multiplexing gain is always used.  $\mathbf{y}_k \in \mathbb{C}^{\min\{M,N\}}$  is the vector received at user  $u(k)$ , where  $u(k)$  denotes the user to whom the  $k$ -th subcarrier is allocated.  $\mathbf{F}_{k,u(k)} \in \mathbb{C}^{M \times \min\{M,N\}}$  is the precoding matrix,  $\mathbf{W}_{k,u(k)} \in \mathbb{C}^{\min\{M,N\} \times N}$  the decoding matrix, and  $\mathbf{n}_k$  the noise vector at the user  $u(k)$  with a covariance matrix  $\mathbb{E} \{ \mathbf{n}_k \mathbf{n}_k^H \} = \sigma^2 \mathbf{I}_N$ . We assume all the users have the same noise power  $\sigma^2$ .

### 5.2.2 EE model

The power consumption at the transmitter consists of the transmit power in the power amplifier at each antenna and the power consumed for base-band control, such as the synchronization, that depends on the number of antennas. The EE is defined as the transmitted information bits per energy

consumed, which, in this downlink channel, can be expressed as

$$\text{EE} = \frac{\sum_{k=1}^K r(\mathbf{H}_{k,u(k)}, \mathbf{F}_{k,u(k)})}{\phi \sum_{k=1}^K \text{tr} \left\{ \mathbf{F}_{k,u(k)}^H \mathbf{F}_{k,u(k)} \right\} + P_C}, \quad (5.2)$$

where  $\phi \geq 1$  is the inverse of the amplifier efficiency. Because  $U \ll K$  in practical MIMO-OFDMA systems, we assume that all users are active and therefore we model the circuit power  $P_C$  as  $\rho_B M + \rho_U U N$  [CGB05], where  $\rho_B$  and  $\rho_U$  are respectively the power consumption at each transmit antenna of the base station and receive antenna at the user terminals.

The rate function is defined as

$$r(\mathbf{H}, \mathbf{F}) = \log_2 \left| \mathbf{I} + \frac{\mathbf{H} \mathbf{F} \mathbf{F}^H \mathbf{H}^H}{\sigma^2 \Gamma} \right|, \quad (5.3)$$

where  $\Gamma \geq 1$  is the SNR gap depending on the modulation mode, channel coding rate and the expected bit error rate (BER) [MHL10].  $\mathbf{H}$  is the channel matrix and  $\mathbf{F}$  is the precoder.

## 5.3 EE maximization problem

In this section, we show that EE is upper bounded with precoding matrices and decoding matrices that diagonalize the channel matrices. The EE maximization problem is then reformulated as a power allocation and subcarrier allocation problem. We adopt time-sharing to transform the original problem into a quasi-concave problem and obtain solutions for power allocation and subcarrier allocation.

### 5.3.1 Optimal precoder

The channel matrix  $\mathbf{H}$  can be decomposed by means of the SVD as  $\mathbf{H} = \mathbf{U} \mathbf{A} \mathbf{V}^H$ . Since  $\mathbf{I} + \frac{\mathbf{H} \mathbf{F} \mathbf{F}^H \mathbf{H}^H}{\sigma^2 \Gamma}$  is a positive-definite matrix, then according to

Hadamard's inequality, we have, for the rate,

$$\begin{aligned} & \log_2 \left| \mathbf{I} + \frac{\mathbf{H}\mathbf{F}\mathbf{F}^H\mathbf{H}^H}{\sigma^2\Gamma} \right| = \log_2 \left| \mathbf{I} + \frac{\mathbf{V}^H\mathbf{F}\mathbf{F}^H\mathbf{V}\Lambda^2}{\sigma^2\Gamma} \right| \\ & \leq \sum_{n=1}^N \log_2 \left| 1 + \frac{(\mathbf{V}^H\mathbf{F}\mathbf{F}^H\mathbf{V}\Lambda^2)_{(n,n)}}{\sigma^2\Gamma} \right| = \sum_{n=1}^N \log_2 \left| 1 + \frac{(\mathbf{V}^H\mathbf{F}\mathbf{F}^H\mathbf{V})_{(n,n)}(\Lambda^2)_{(n,n)}}{\sigma^2\Gamma} \right|, \end{aligned} \quad (5.4)$$

where the equality holds if and only if the matrix  $\mathbf{V}^H\mathbf{F}\mathbf{F}^H\mathbf{V}\Lambda^2$  is diagonal, which is equivalent to the matrix  $\mathbf{V}^H\mathbf{F}\mathbf{F}^H\mathbf{V}$  being diagonal.

Let us now consider the EE objective function. Assume that for subcarrier  $k$ , we have that  $\mathbf{P}_{k,u(k)} = \mathbf{V}_{k,u(k)}^H\mathbf{F}_{k,u(k)}\mathbf{F}_{k,u(k)}^H\mathbf{V}_{k,u(k)}$  is not diagonal. Then define a diagonal matrix  $\hat{\mathbf{P}}_{k,u(k)} = \text{diag}\{\mathbf{P}_{k,u(k)}\}$ , meaning that  $\text{tr}\{\mathbf{P}_{k,u(k)}\} = \text{tr}\{\hat{\mathbf{P}}_{k,u(k)}\}$ . By using (5.4) for subcarrier  $k$ , (5.5) is obtained:

$$\begin{aligned} & \frac{\sum_{l=1}^K \log_2 \left| \mathbf{I} + \frac{\mathbf{P}_{l,u(l)}\Lambda_{l,u(l)}^2}{\sigma^2\Gamma} \right|}{\phi \sum_{l=1}^K \text{tr}\{\mathbf{P}_{l,u(l)}\} + P_C} \\ & < \frac{\sum_{l=1, l \neq k}^K \log_2 \left| \mathbf{I} + \frac{\mathbf{P}_{l,u(l)}\Lambda_{l,u(l)}^2}{\sigma^2\Gamma} \right| + \log_2 \left| \mathbf{I} + \frac{\hat{\mathbf{P}}_{k,u(k)}\Lambda_{k,u(k)}^2}{\sigma^2\Gamma} \right|}{\phi \sum_{l=1, l \neq k}^K \text{tr}\{\mathbf{P}_{l,u(l)}\} + \phi \text{tr}\{\hat{\mathbf{P}}_{k,u(k)}\} + P_C}, \end{aligned} \quad (5.5)$$

which means that the EE function is upper-bounded by the EE with every precoder  $\mathbf{F}_{k,u(k)}$  satisfying the structure  $\mathbf{F}_{k,u(k)} = \mathbf{V}_{k,u(k)}\mathbf{P}_{k,u(k)}^{\frac{1}{2}}$  where  $\mathbf{P}_{k,u(k)}$  is diagonal. On the other hand, according to [Tel99], the rate function for subcarrier  $k$  is maximized by water filling power allocation, which is,

$$(\mathbf{P}_{k,u(k)})_{(m,m)} = \left( \kappa_{k,u(k)} - \frac{\sigma^2\Gamma}{(\Lambda_{k,u(k)})_{(m,m)}^2} \right)^+, \quad (5.6)$$

where  $(x)^+ = \max\{x, 0\}$  and  $\kappa_{k,u(k)}$  is the water level. That is, for each given  $\text{tr}\{\hat{\mathbf{P}}_{k,u(k)}\}$ , the optimal power allocation strategy for each user that maximizes EE is water filling. Therefore the rate function in (5.3) can be rewritten as a function of the channel matrix and the transmit power  $r(\mathbf{H}, p)$ .

### 5.3.2 Time-sharing approach

Based on the previous section, the problem is formulated as the maximization of the system EE defined in (5.2) subject to a sum power constraint at the base station, with variables which are the power allocation among all subcarriers and the subcarrier allocation. Defining  $P_{k,u(k)}$  and  $r_{k,u(k)} = r(\mathbf{H}_{k,u(k)}, P_{k,u(k)})$  as the transmit power and rate for subcarrier  $k$ , the problem can be stated as:

$$\max_{\{u(k)\}, \{P_{k,u(k)}\}} \frac{\sum_{k=1}^K r_{k,u(k)}}{\phi \sum_{k=1}^K P_{k,u(k)} + P_C} \quad (5.7)$$

$$s.t. \quad u(k) \in \{1, \dots, U\}, \quad k = 1, \dots, K \quad (5.8)$$

$$\sum_{k=1}^K P_{k,u(k)} \leq P_{max} \quad (5.9)$$

$$P_{k,u(k)} \geq 0. \quad (5.10)$$

This is not a concave-convex fractional program as in [ICJF12] because the variables  $u(k)$  are discontinuous. We relax the constraint that one subcarrier is only allocated to one user by using time-sharing as in [WCLM99]. The original problem in (5.7) is reformulated as

$$\max_{\{\rho_{k,u}\}, \{p_{k,u}\}} \frac{\sum_{u=1}^U \sum_{k=1}^K \rho_{k,u} r_{k,u}}{\phi \sum_{u=1}^U \sum_{k=1}^K p_{k,u} + P_C} \quad (5.11)$$

$$s.t. \quad \sum_{u=1}^U \rho_{k,u} = 1, \quad k = 1, \dots, K \quad (5.12)$$

$$\sum_{u=1}^U \sum_{k=1}^K p_{k,u} \leq P_{max} \quad (5.13)$$

$$p_{k,u} \geq 0, \quad (5.14)$$

$$0 < \rho_{k,u} \leq 1 \quad (5.15)$$

where  $\rho_{k,u}$  is the time fraction allocated to user  $u$  by subcarrier  $k$  and  $p_{k,u}$  is the total power consumed by user  $u$  at subcarrier  $k$  during this fraction. Therefore we have

$$r_{k,u} = r\left(\mathbf{H}_{k,u}, \frac{p_{k,u}}{\rho_{k,u}}\right). \quad (5.16)$$

$\rho_{k,u}r_{k,u}$  is a perspective function of  $r(\mathbf{H}_{k,u}, p_{k,u})$ , and therefore it is a concave function of  $p_{k,u}, \rho_{k,u}$ . (5.11) is quasi-concave w.r.t  $p_{k,u}, \rho_{k,u}$ .

In the following, we will show that no local maximum exists for the reformulated problem because a local maximum would require that  $\rho_{k,u} = 0$  for some  $u$  which is not compatible with (5.15). Despite this result, the KKT conditions which are derived will be used to obtain our solution and the properties of this solution will be discussed in the next section.

The corresponding Lagrangian function of (5.11)-(5.15) is

$$\begin{aligned} L = & \frac{\sum_{u=1}^U \sum_{k=1}^K \rho_{k,u} r_{k,u}}{\phi \sum_{u=1}^U \sum_{k=1}^K p_{k,u} + P_C} - \mu \left( \sum_{u=1}^U \sum_{k=1}^K p_{k,u} - P_{max} \right) \\ & + \sum_{k=1}^K \nu_k \left( \sum_{u=1}^U \rho_{k,u} - 1 \right) + \sum_{u=1}^U \sum_{k=1}^K \eta_{k,u} p_{k,u} \\ & - \sum_{u=1}^U \sum_{k=1}^K \alpha_{k,u} (\rho_{k,u} - 1) + \sum_{u=1}^U \sum_{k=1}^K \beta_{k,u} \rho_{k,u}. \end{aligned} \quad (5.17)$$

$\mu, \nu_k, \eta_{k,u}, \alpha_{k,u}$  and  $\beta_{k,u}$  are all non-negative. Denote  $r'(\mathbf{H}, p)$  as the derivative of the function  $r(\mathbf{H}, p)$  w.r.t  $p$ . A necessary KKT condition for a local maximum is that

$$\begin{aligned} \frac{\partial L}{\partial p_{k,u}} = & \frac{r' \left( \mathbf{H}_{k,u}, \frac{p_{k,u}}{\rho_{k,u}} \right)}{\phi \sum_{u=1}^U \sum_{k=1}^K p_{k,u} + P_C} \\ & - \frac{\phi \sum_{u=1}^U \sum_{k=1}^K \rho_{k,u} r_{k,u}}{\left( \phi \sum_{u=1}^U \sum_{k=1}^K p_{k,u} + P_C \right)^2} - \mu + \eta_{k,u} = 0, \end{aligned} \quad (5.18)$$

where  $\mu \left( \sum_{u=1}^U \sum_{k=1}^K p_{k,u} - P_{max} \right) = 0$  and  $\eta_{k,u} p_{k,u} = 0$ , therefore  $r' \left( \mathbf{H}_{k,u}, \frac{p_{k,u}}{\rho_{k,u}} \right)$  is the same for every  $k, u$  for which  $p_{k,u} > 0$  because  $\eta_{k,u} = 0$  in this case. From [WSV15], we know that

$$r' \left( \mathbf{H}_{k,u}, \frac{p_{k,u}}{\rho_{k,u}} \right) = \frac{1}{\ln 2 \cdot \kappa_{k,u}}. \quad (5.19)$$

Therefore  $\kappa_{k,u}$  are all the same for every  $k, u$  for which  $p_{k,u} > 0$ . Denote this common water level as  $\kappa$  in the following.

Another necessary condition is that

$$\frac{\partial L}{\partial \rho_{k,u}} = \frac{r_{k,u} + \rho_{k,u} r' \left( \mathbf{H}_{k,u}, \frac{p_{k,u}}{\rho_{k,u}} \right) \left( \frac{-p_{k,u}}{\rho_{k,u}^2} \right)}{\phi \sum_{u=1}^U \sum_{k=1}^K p_{k,u} + P_C} + \nu_k - \alpha_{k,u} + \beta_{k,u} = 0, \quad (5.20)$$

where  $\nu_k \left( \sum_{u=1}^U \rho_{k,u} - 1 \right) = 0$ ,  $\alpha_{k,u} (\rho_{k,u} - 1)$  and  $\beta_{k,u} \rho_{k,u} = 0$ . Note that when  $U \geq 2$  and if  $\rho_{k,u} < 1$  for some  $k, u$ , then  $\alpha_{k,u} = \beta_{k,u} = 0$ . Thus, for a local maximum, a  $\rho_{k,u} \in (0, 1)$  should satisfy that

$$\frac{r_{k,u} - \frac{p_{k,u}}{\rho_{k,u}} r' \left( \mathbf{H}_{k,u}, \frac{p_{k,u}}{\rho_{k,u}} \right)}{\phi \sum_{u=1}^U \sum_{k=1}^K p_{k,u} + P_C} + \nu_k = 0. \quad (5.21)$$

Let us define

$$\Theta(k, u) \triangleq r_{k,u} - \frac{p_{k,u}}{\rho_{k,u}} r' \left( \mathbf{H}_{k,u}, \frac{p_{k,u}}{\rho_{k,u}} \right). \quad (5.22)$$

For each  $k$ , when  $U \geq 2$ , if all  $\Theta(k, u)$  are different from each other, (5.21) can only be satisfied by at most one  $u$ , all the other users should have  $\rho_{k,u} = 0$  or  $\rho_{k,u} = 1$ . Because of the fact that  $\sum_{u=1}^U \rho_{k,u} = 1$ , there is no local maximum for  $0 < \rho_{k,u} < 1$ . Then, there is only one  $u$  for each specific  $k$  such that  $\rho_{k,u} = 1$ . For this  $(k, u)$ ,  $\alpha_{k,u} > 0$  and  $\beta_{k,u} = 0$  which results in

$$\Theta(k, u) + \nu_k \left( \phi \sum_{\tilde{u}=1}^U \sum_{\tilde{k}=1}^K p_{\tilde{k}, \tilde{u}} + P_C \right) > 0, \quad (5.23)$$

while for any other  $u$  and the same  $k$ ,  $\alpha_{k,u} = 0$  and  $\beta_{k,u} > 0$  due to  $\rho_{k,u} = 0$ , and thus

$$\Theta(k, u) + \nu_k \left( \phi \sum_{\tilde{u}=1}^U \sum_{\tilde{k}=1}^K p_{\tilde{k}, \tilde{u}} + P_C \right) < 0. \quad (5.24)$$

Therefore, we have

$$u(k) = \arg \max_u \Theta(k, u), \quad (5.25)$$

where, for each  $p_{k,u} > 0$ , according to (5.19), the following condition should be satisfied

$$r' \left( \mathbf{H}_{k,u}, \frac{p_{k,u}}{\rho_{k,u}} \right) = \frac{1}{\ln 2 \cdot \kappa}. \quad (5.26)$$

If  $U = 1$ , all subcarriers will be allocated to this user. When  $U \geq 2$ , if for a specific subcarrier  $k$  there are  $z$  users such that  $\Theta(k, u)$  are the same and they are the largest among all users, then  $\rho_{k,u} = 1/z$  for these users and  $\rho_{k,u} = 0$  for all other users. This means that this subcarrier  $k$  should be equally allocated to these  $z$  users in the current time slot. Alternatively, this subcarrier can randomly be allocated to any of the  $z$  users. Note that this case happens with a 0 probability since exactly the same  $\Theta(k, u)$  implies the same  $\mathbf{H}_{k,u}$ .

### 5.3.3 Remarks

From a programming viewpoint, the EE maximization problem does not have a local maximum with respect to  $\rho_{k,u}$  for  $\rho_{k,u} \in (0, 1]$ . The user selection in (5.25) tells us that if all users are allocated a non-zero portion of time  $\rho_{k,u}$ , then the user with the largest  $\Theta(k, u)$  should be given a  $\rho_{k,u} \rightarrow 1$  and all the other users be given a  $\rho_{k,u} \rightarrow 0$ . However, when  $\rho_{k,u} = 0$ , we obviously have  $p_{k,u} = 0$ , which means that  $\eta_{k,u}$  in (5.18) is not necessarily 0. Therefore, the condition in (5.26) is not a necessary condition for  $\rho_{k,u} \in [0, 1]$ , which means there may exist some local maximums that the user selection in (5.25) cannot find. As the analysis in the next section will reveal, this makes the EE function discontinuous. On the other hand, because the objective function is not concave, it is not certain whether the conditions in (5.25) and (5.26) make it possible to find a global maximum.

In the next section, we will see that there is always more than one local maximum near the point when the user selection switches, which is intuitively correct because  $\Theta(k, u)$  in (5.25) for different  $u$  can be very close in this case. However, as we will show in the next section, this user selection and the proposed algorithm have mathematical essential properties that guarantee a global maximum.

## 5.4 Optimal EE solution

In this section, the exact behavior and property of the EE function is given. We will first show the optimality of the subcarrier allocation and power allocation in (5.25), that is, the EE that satisfies the conditions in

(5.25) and (5.26) is the largest among all other possible subcarrier allocations. Then we show the discontinuous quasi-concavity of the EE function and show that the EE is upper bounded when the global optimum exists in the gap of the EE function. Finally we propose an algorithm to obtain the optimum.

Before stating the following theorems, let us define some notations.  $S$  is a certain user selection defined in the set of all possibilities of the user selections, while  $S^*(\kappa)$  is the user selection from (5.25) with the water level  $\kappa$ .  $EE(S, \kappa)$ ,  $R(S, \kappa)$  and  $P(S, \kappa)$  are respectively the EE, rate and transmit power consumption with the user selection  $S$  and water level  $\kappa$ .  $Q(S, P) = R(S, \kappa)$ , where  $P = P(S, \kappa)$ , is the rate with the user selection  $S$  and power  $P$ . Define  $Q'(S, P)$  as the derivative of  $Q(S, P)$  w.r.t  $P$ . Finally,  $G(S, P) = \frac{Q(S, P)}{\phi P + P_C}$ .

We will first show in the following theorem that any point that satisfies simultaneously the conditions provided in (5.25) and (5.26) gives the largest EE for a given transmit power  $P$ .

**Theorem 5.1.** *For each  $\kappa_0$ ,  $EE(S^*(\kappa_0), \kappa_0)$  is the largest among all the user selections with the same power consumption, that is,*

$$EE(S^*(\kappa_0), \kappa_0) \geq EE(S, \kappa'), \quad (5.27)$$

for any  $S, \kappa'$ , such that

$$P(S, \kappa') = P(S^*(\kappa_0), \kappa_0). \quad (5.28)$$

Theorem 5.1 is proved in subsection A of the appendix.

Theorem 5.1 actually renders the EE function a sole function of the transmit power: for every water level  $\kappa_0$ , a unique subcarrier allocation and power allocation can be calculated from (5.25) and (5.26). Any other water level different from  $\kappa_0$  will result in a different transmit power. Therefore there exists one unique EE for each transmit power. Let us define the one-dimensional EE function as

$$f(P) = G(S^+, P), \quad (5.29)$$

where  $S^+$  is such that there exists a  $\kappa$  satisfying  $S^+ = S^*(\kappa)$  and  $P = P(S^+, \kappa)$  simultaneously. To characterize this EE function, we first introduce the following two lemmas.

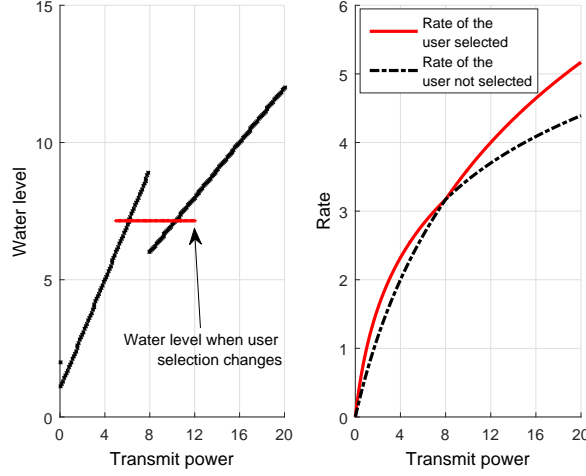


Figure 5.1: User selection and the transmission power of the MIMO channel versus the water level. The channel is  $[1, 0]$  for user 1 and  $[0.5, 0.5]$  for user 2. In the first stage, user 1 is selected and user 2 is silent. In the second stage, user 2 is selected and user 1 is silent.

**Lemma 5.1.** *As  $\kappa$  increases, if at  $\kappa_c$ , the user selection for subcarrier  $k$  changes from  $u_1$  to  $u_2$ , transmit power from  $q_1$  to  $q_2$ , and rate from  $r(\mathbf{H}_{k,u_1}, q_1)$  to  $r(\mathbf{H}_{k,u_2}, q_2)$ , then we have  $q_1 \leq q_2$  and  $r(\mathbf{H}_{k,u_1}, q_1) \leq r(\mathbf{H}_{k,u_2}, q_2)$ .*

Lemma 5.1 is proved in subsection B of the appendix.

As it is well known,  $\kappa$  is increasing with the transmit power for a fixed user selection. Therefore Lemma 5.1 demonstrates that for each subcarrier, the rate and power grow till the switching point and then may 'jump' to other values. This will be demonstrated in detail in the next section.

**Lemma 5.2.** *If  $g(x) (x \geq 0)$  is concave, then  $h(x) = \frac{g(x)}{ax+b}$ , where  $a$  and  $b$  are positive constant, is quasi-concave. In addition,  $h(x)$  is concave in the region where  $h(x)$  is increasing.*

Lemma 5.2 is proved in subsection C of the appendix.

The next theorem intends to discuss the behavior of the EE function.

**Theorem 5.2.**  *$f(P)$  is a discontinuous quasi-concave function of the transmit power  $P$ .*

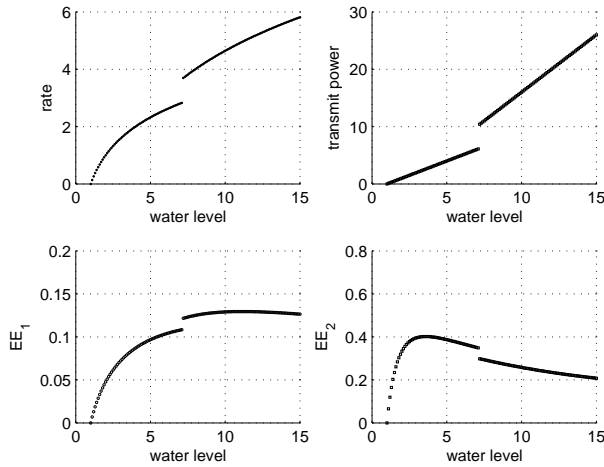


Figure 5.2: The rate, transmit power and EE vs. water level. Gaps can be observed in all the figures when user changes.

Theorem 5.2 is proved in subsection D of the appendix.

Up to this point, we have well understood the EE function  $f(P)$  for values of  $P$  belonging to the discontinuous definition set.

We give an example of subcarrier allocation to better understand the behavior of a MIMO system with subcarrier allocation. Let us assume a system with one subcarrier and two users where each user has a  $2 \times 2$  MIMO downlink channel. For simplicity, we consider the eigenchannels after SVD. For user 1, the channel is  $[1, 0]$  and for user 2, the channel is  $[0.5, 0.5]$ . Note that in this example we assume  $\Gamma = 1$  and  $\sigma^2 = 1$ . If the waterlevel is below 2, user 1 will obviously be selected since the power for user 2 is zero. As the power grows, the water level grows, the channel for user 2 becomes more and more advantageous because it has two eigenchannels while user 1 has always only one. When the power reaches the value 8, one can calculate that both user 1 and user 2 have a rate = 9. Note that at this point, user 1 has a water level 9, and user 2 has a water level 6. And after, as power continues to grow, user 2 is always selected. The 'water level dropping' can also be inferred by Lemma 5.1. Because from this point, user 2 has a faster rate growth, so it has a lower water level ( $\kappa$ ). The performance with user selection can be observed in Fig. 5.1.

Fig. 5.2 shows the performance of rate, power and EE versus water level with the user selection strategy in (5.25).  $EE_1$  and  $EE_2$  represent respectively the cases where EE increases and decreases due to a different circuit power. Gaps can be observed in all the figures when user changes. It is interesting to see that the EE has a positive gap when it is increasing, and has a negative gap when it is decreasing, which is consistent with Theorem 5.2.

The next theorem provides an upper-bound on the EE function evaluated for values of  $P$  which do not belong to this discontinuous set.

**Theorem 5.3.** *If the user selection changes from  $S_1$  to  $S_2$  at  $\kappa_c$ , and  $P(S_1, \kappa_c) < P(S_2, \kappa_c)$ , for any  $P$  such that  $P(S_1, \kappa_c) < P < P(S_2, \kappa_c)$  and any  $S$ , the following is true:*

$$\frac{Q(S, P)}{\phi P + P_C} < \max \{EE(S_1, \kappa_c), EE(S_2, \kappa_c)\}. \quad (5.30)$$

Theorem 5.3 is proved in subsection E of the appendix.

From (5.70) of the appendix, the exact value of EE function outside the discontinuous set is upper bounded. From the fact that there is only one subcarrier changing its user selection at each interval (a  $\kappa$  can usually satisfy only one equation of (5.44) of the appendix), we can largely reduce the complexity of finding the exact value of EE by searching all possibilities of user selection of this subcarrier, instead of searching all possibilities of all subcarriers. To this end, we can explicitly describe the EE function  $f(P)$ : the definition set  $P$  is discontinuous with several intervals. Within each interval, there are only  $U$  possibilities left of quasi-concave EE functions which are all upper bounded by (5.70). The optimal EE within each interval is the maximum among these  $U$  functions.

From (5.25), we see that maximizing the EE (and also the rate) for a certain subcarrier is impacted by other subcarriers' selection through the change of water level. In SISO systems, the user selection only depends on the channel gains. On the contrary, in MIMO systems such as the one under consideration, the user selection will depend both on channel gains and available power, which is impacted by the other users.

The next proposition intends to show that the user selection for MIMO in (5.25) is consistent with the SISO strategy mentioned above, that is, selection of the maximum channel gain, when  $\min\{M, N\} = 1$ .

---

**Algorithm 5.1:** Calculate  $\text{EE}^*$ 

---

- 1: Set  $\kappa_l = 0$ ;  $\kappa_u = 1$ ;  $\Pi_l = \Pi_u = \emptyset$ ;  $P_l = P_u = 0$ ; **Mode=Fast** or **Slow**
  - 2: For every channel  $\mathbf{H}_{k,u}$ , calculate the eigenvalues using SVD.
  - 3: Go to Algorithm 2 with  $\kappa = \kappa_u$ ;  $\Pi_u = \Pi$  and  $P_u = P_T$
  - 4: **while**  $P_u < P_{max}$  **do**
  - 5:      $\kappa_u = \kappa_u \times 2$
  - 6:     Go to Algorithm 2
  - 7: **end while**
  - 8: **while**  $\kappa_u - \kappa_l > \delta$  **do**
  - 9:      $\kappa_c = 0.5(\kappa_l + \kappa_u)$
  - 10:     Go to Algorithm 2 with  $\kappa = \kappa_c$
  - 11:     In (5.56) of the appendix, substitute  $P_l$  with  $P_T$ ,  $Q(S_1, P_1)$  with  $R$ , and  $Q'(S_1, P_1)$  with  $\frac{1}{\ln 2 \cdot \kappa_c}$ ; Calculate  $f'(P_T)$
  - 12:     **if**  $f'(P_T) < 0$  or  $P_c > P_{max}$  **then**
  - 13:          $\kappa_u = \kappa_c$ ;  $\Pi_u = \Pi$ ;  $P_u = P_T$
  - 14:     **else**
  - 15:          $\kappa_l = \kappa_c$ ;  $\Pi_l = \Pi$ ;  $P_l = P_T$
  - 16:     **end if**
  - 17: **end while**
  - 18: **if**  $P_u - P_l > \eta$  and  $P_u > P_{max}$  and **Mode=Slow** **then**
  - 19:     Find  $k$  that  $u(k)$  in  $\Pi_l$  and  $u(k)$  in  $\Pi_u$  are different.
  - 20:     Between  $P_l$  and  $P_{max}$ , for each  $u(k) = 1, \dots, U$ , get  $\text{EE}_1, \dots, \text{EE}_U$  using bisection method
  - 21:      $\text{EE}^* = \max\{\text{EE}_1, \dots, \text{EE}_U\}$
  - 22: **else**
  - 23:      $\text{EE}^* = \frac{R_l}{\phi P_l + P_C}$
  - 24: **end if**
- 

---

**Algorithm 5.2:** Subcarrier allocation

---

- 1: Calculate  $\Theta(k, u)$  in (5.22) for the given  $\kappa$ .
  - 2: For every  $k$ , find  $u(k) = \arg \max_u \Theta(k, u)$
  - 3: Calculate  $P_T = \sum_{k=1}^K p_{k,u(k)}$
  - 4: Calculate  $R = \sum_{k=1}^K r_{k,u(k)}$
  - 5:  $\Pi = \{u(k)\}$
-

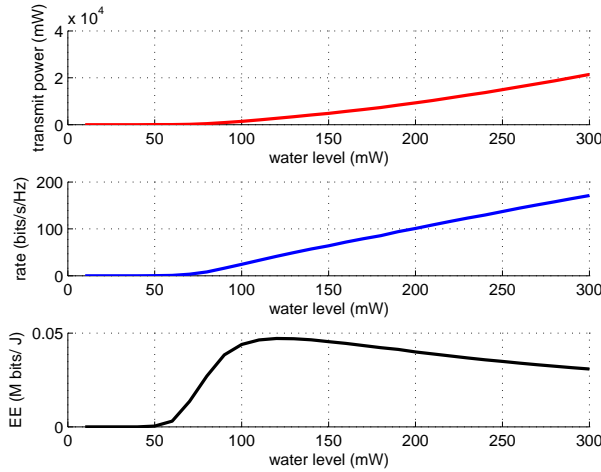


Figure 5.3: Transmit power, rate, and EE versus water level when  $K = 64$ .

**Proposition 5.1.** *The user selection in (5.22) and (5.25) corresponds to selecting the maximum channel gain if  $\min\{M, N\} = 1$ .*

Proposition 1 is proved in subsection F of the appendix.

Based on the whole characterization of the EE function, we propose Algorithm 5.1 (see the last page) for its maximization. From the analysis reported above, the algorithm in 'Fast Mode' always converges, except if the optimum  $P$  does not belong to the discontinuous definition set. In this case, the algorithm switches to 'Slow Mode' and exhaustively tries the allocation of the switching subcarrier to all users. Please note that for practical values of  $K$ , this situation almost never happen. We can observe this in Fig. 5.3.

## 5.5 Numerical results

In this section we show the numerical results. The parameters are set as follows:  $B = 10\text{KHz}$  is the bandwidth for each OFDM subcarrier,  $M = N = 4$  and  $U = 10$  is the number of users.  $\phi = 2.5$  is the inverse of the amplifier efficiency and  $\Gamma = 1$ . The channel is assumed to be Rayleigh distributed and has an average channel gain  $G_0 d^{-n}$  where the pass loss exponent  $n = 4$ ,  $G_0 = -(G_1 M_l) = -70\text{dB}$  in which  $G_1 = 30\text{dB}$  is the gain

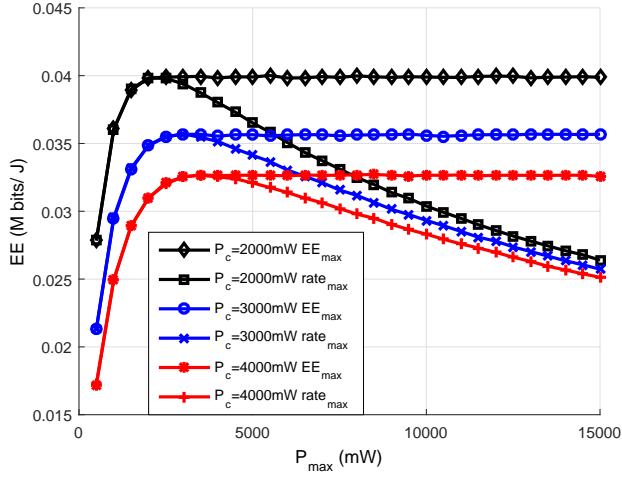


Figure 5.4: Performance comparison between EE maximization and rate maximization for different  $P_C$ .  $\phi = 2.5$ ,  $K = 32$ .

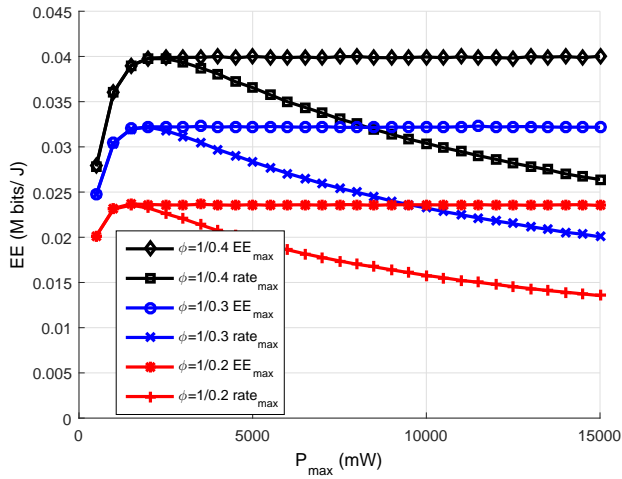


Figure 5.5: Performance comparison between EE maximization and rate maximization for different inverse of amplifier efficiency  $\phi$ .  $P_C = 2000\text{mW}$ ,  $K = 32$ .

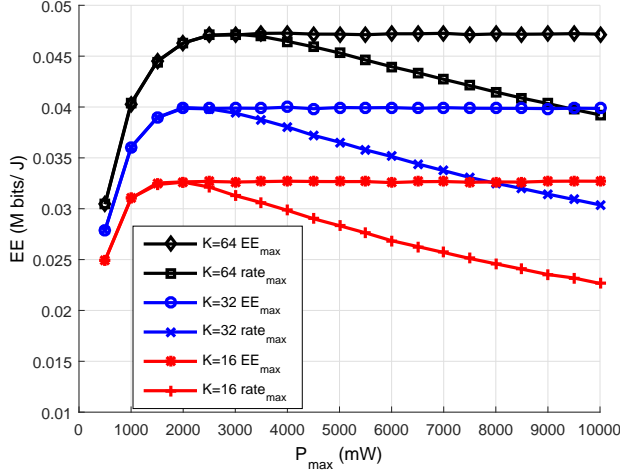


Figure 5.6: Performance comparison between EE maximization and rate maximization for different  $K$ .  $\phi = 2.5$ ,  $P_C = 2000\text{mW}$ .

factor at  $d = 1\text{m}$ .  $M_l = 40\text{dB}$  is the link margin compensating the hardware process variations and other noise and interference, the noise power  $\sigma^2 = BN_0N_f$  where  $N_0 = -170\text{dBm/Hz}$  is the noise power spectral density and  $N_f = 10\text{dB}$  is the noise figure [CGB05]. The results are averaged over 1000 channel realizations.

Fig. 5.3 shows the rate, power and EE versus water level as in Fig. 5.2. We observe that the gap in Fig. 5.2 cannot be seen in this case where the number of subcarriers is large. And we also see that the EE function is quasi-concave as analysed in Theorem 5.2 which allows us to use the bisection method to find its maximum.

In Fig. 5.4, we compare the proposed algorithm of EE maximization with rate maximization [LCL<sup>+</sup>07] for various values of  $P_c$ . The optimum transmit power increases when the circuit power  $P_c$  increases. This is consistent with the conclusion for MIMO-OFDM in [WSV15]. One can easily extend the conclusion to the case for MIMO-OFDMA. This is also consistent with the result for MIMO as shown in [BL11] that the optimal transmit power is zero for zero circuit power.

In Fig. 5.5, we compare the proposed EE maximization algorithm with a rate maximization one, for various amplifier efficiency values. The op-

timal transmit power increases when the amplifier efficiency increases. In Fig. 5.6, we compare the proposed EE maximization algorithm with a rate maximization one for various numbers of subcarriers. The optimal transmit power increases when the number of subcarriers  $K$  increases. Since we fix the bandwidth for each subcarrier, increasing  $K$  enlarges the set of feasible solutions, which is beneficial for the EE.

In Fig. 5.4, Fig. 5.5, and Fig. 5.6, we observe that in the region where EE is an increasing function, EE maximization follows rate maximization. In the power region where rate maximization leads to decreasing EE, EE maximization outperforms rate maximization. This is due to the fact that full transmit power is always used in rate maximization, which is not the case in EE maximization.

## 5.6 Conclusion

We have considered joint precoder design and subcarrier allocation in a MIMO-OFDMA downlink optimized for the EE criterion. We have shown that the EE function is discontinuous and quasi-concave. Conditions have been identified for the optimal power and subcarrier allocation. For the few cases where the optimal allocation cannot be found by these conditions, the EE can be upper bounded and the allocation can be solved by means of an exhaustive step. An algorithm has been proposed to find the globally optimal EE. Its performance has been illustrated by means of numerical results.

## 5.7 Appendix

### 5.7.1 Proof of Theorem 5.1

*Proof.* Assume that  $\text{EE}(S^*(\kappa_0), \kappa_0) < \text{EE}(S_1, \kappa_1)$  where  $P(S_1, \kappa_1) = P(S^*(\kappa_0), \kappa_0) = P_0$ . Since

$$\text{EE}(S, \kappa) = \frac{R(S, \kappa)}{\phi P(S, \kappa) + P_C}, \quad (5.31)$$

we have

$$\frac{R(S^*(\kappa_0), \kappa_0)}{\phi P(S^*(\kappa_0), \kappa_0) + P_C} < \frac{R(S_1, \kappa_1)}{\phi P(S_1, \kappa_1) + P_C}. \quad (5.32)$$

Thus  $R(S^*(\kappa_0), \kappa_0) < R(S_1, \kappa_1)$ . Find  $P_1$  such that  $Q'(S_1, P_1) = Q'(S^*(\kappa_0), P_0)$ . Because  $Q(S_1, P)$  is concave w.r.t  $P$ , we have

$$Q(S^*(\kappa_0), P_0) < Q(S_1, P_0) \leq Q(S_1, P_1) + Q'(S_1, P_1)(P_0 - P_1), \quad (5.33)$$

and therefore

$$\begin{aligned} Q(S^*(\kappa_0), P_0) - Q'(S^*(\kappa_0), P_0)P_0 &= Q(S^*(\kappa_0), P_0) - Q'(S_1, P_1)P_0 \\ &< Q(S_1, P_1) - Q'(S_1, P_1)P_1. \end{aligned} \quad (5.34)$$

On the other hand, for every  $k$ ,  $r_{k,u_0(k)} - r'_{k,u_0(k)}p_{k,u_0(k)}$  is the largest among all  $r_{k,u} - r'_{k,u}p_{k,u}$  satisfying  $r'_{k,u} = \frac{1}{\ln 2 \cdot \kappa_0}$ , where  $r'_{k,u} \triangleq r'(\mathbf{H}_{k,u}, p_{k,u})$  and  $u_0(k)$  is the user selection for subcarrier  $k$  with water level  $\kappa_0$ . Note also the fact that

$$r'_{1,u(1)} = \dots = r'_{K,u_0(K)} = Q'(S^*(\kappa_0), P_0) \quad (5.35)$$

$$\sum_{k=1}^K r_{k,u_0(k)} = Q(S^*(\kappa_0), P_0) \quad (5.36)$$

$$\sum_{k=1}^K p_{k,u_0(k)} = P_0. \quad (5.37)$$

Therefore

$$Q(S^*(\kappa_0), P_0) - Q'(S^*(\kappa_0), P_0)P_0 = \sum_{k=1}^K r_{k,u_0(k)} - \sum_{k=1}^K r'_{k,u_0(k)}p_{k,u_0(k)}. \quad (5.38)$$

Similarly, we have the fact that

$$Q(S_1, P_1) - Q'(S_1, P_1)P_1 = \sum_{k=1}^K r_{k,\hat{u}_k} - \sum_{k=1}^K r'_{k,\hat{u}_k}p_{k,\hat{u}_k}, \quad (5.39)$$

where  $\widehat{u}_k$  are elements of  $S_1$  and

$$r'_{1,\widehat{u}_1} = \dots = r'_{K,\widehat{u}_K} = Q'(S_1, P_1) \quad (5.40)$$

$$\sum_{k=1}^K r_{k,\widehat{u}_k} = Q(S_1, P_1) \quad (5.41)$$

$$\sum_{k=1}^K p_{k,\widehat{u}_k} = P_1. \quad (5.42)$$

From (5.34), there exists at least one  $k$  such that

$$r_{k,u_0(k)} - r'_{k,u_0(k)} p_{k,u_0(k)} < r_{k,\widehat{u}_k} - r'_{k,\widehat{u}_k} p_{k,\widehat{u}_k}, \quad (5.43)$$

which is contradictory with the fact that for every  $k$ ,  $r_{k,u_0(k)} - r'_{k,u_0(k)} p_{k,u_0(k)}$  is the largest among all  $r_{k,u} - r'_{k,u} p_{k,u}$  satisfying  $r'_{k,u} = r'_{k,u_0(k)}$ . Thus there exists no such  $S_1, \kappa_1$ .  $\square$

## 5.7.2 Proof of Lemma 5.1

*Proof.* Since the user selection changes at  $\kappa_c$ , we have

$$r(\mathbf{H}_{k,u_1}, q_1) - \frac{q_1}{\ln 2 \cdot \kappa_c} = r(\mathbf{H}_{k,u_2}, q_2) - \frac{q_2}{\ln 2 \cdot \kappa_c}. \quad (5.44)$$

Assume that  $q_1 > q_2$ . We can always find  $\delta_1, \delta_2 > 0$  small enough such that  $q_1 + \delta_1 > q_1 > q_2 + \delta_2$ , and

$$r'(\mathbf{H}_{k,u_1}, q_1 + \delta_1) = r'(\mathbf{H}_{k,u_2}, q_2 + \delta_2) < r'(\mathbf{H}_{k,u_1}, q_1) = r'(\mathbf{H}_{k,u_2}, q_2). \quad (5.45)$$

Let us denote  $r'(\mathbf{H}_{k,u_1}, q_1 + \delta_1) = \frac{1}{\ln 2 \cdot \kappa_d}$  in the following. Since  $\kappa$  is increasing with power and user selection changes from  $u_1$  to  $u_2$ , we have

$$r(\mathbf{H}_{k,u_1}, q_1 + \delta_1) - \frac{q_1 + \delta_1}{\ln 2 \cdot \kappa_d} < r(\mathbf{H}_{k,u_2}, q_2 + \delta_2) - \frac{q_2 + \delta_2}{\ln 2 \cdot \kappa_d}. \quad (5.46)$$

From (5.46) we have

$$\frac{1}{\ln 2 \cdot \kappa_d} > \frac{r(\mathbf{H}_{k,u_2}, q_2 + \delta_2) - r(\mathbf{H}_{k,u_1}, q_1 + \delta_1)}{(q_2 + \delta_2) - (q_1 + \delta_1)} \quad (5.47)$$

On the other hand, since the functions  $r(\mathbf{H}_{k,u_1}, p)$  and  $r(\mathbf{H}_{k,u_2}, p)$  are both concave, we have

$$r(\mathbf{H}_{k,u_1}, q_1) < r(\mathbf{H}_{k,u_1}, q_1 + \delta_1) - \frac{\delta_1}{\ln 2 \cdot \kappa_d} \quad (5.48)$$

and

$$\begin{aligned} r(\mathbf{H}_{k,u_2}, q_2 + \delta_2) &< r(\mathbf{H}_{k,u_2}, q_2) + \frac{\delta_2}{\ln 2 \cdot \kappa_c} \\ &= r(\mathbf{H}_{k,u_1}, q_1) + \frac{q_2 + \delta_2 - q_1}{\ln 2 \cdot \kappa_c} \\ &< r(\mathbf{H}_{k,u_1}, q_1 + \delta_1) - \frac{\delta_1}{\ln 2 \cdot \kappa_d} + \frac{q_2 + \delta_2 - q_1}{\ln 2 \cdot \kappa_c} \\ &< r(\mathbf{H}_{k,u_1}, q_1 + \delta_1) + \frac{q_2 + \delta_2 - q_1 - \delta_1}{\ln 2 \cdot \kappa_d}. \end{aligned} \quad (5.49)$$

Thus

$$\frac{1}{\ln 2 \cdot \kappa_d} < \frac{r(\mathbf{H}_{k,u_2}, q_2 + \delta_2) - r(\mathbf{H}_{k,u_1}, q_1 + \delta_1)}{(q_2 + \delta_2) - (q_1 + \delta_1)}, \quad (5.50)$$

which is in contradiction with (5.47). Thus  $q_1 \leq q_2$  and from (5.44) we have  $r(\mathbf{H}_{k,u_1}, q_1) \leq r(\mathbf{H}_{k,u_2}, q_2)$ .  $\square$

### 5.7.3 Proof of Lemma 5.2

*Proof.* Many papers have shown the quasi-concavity of  $h(x)$  [WSV15]. Let us show the second claim directly. The first derivative of  $h(x)$  is

$$h'(x) = \frac{g'(x)(ax + b) - ag(x)}{(ax + b)^2}. \quad (5.51)$$

The second derivative of  $h(x)$  is

$$h''(x) = \frac{g''(x)(ax + b)^2 - 2a(ax + b)(g'(x)(ax + b) - ag(x))}{(ax + b)^3}. \quad (5.52)$$

Due to the fact that  $g''(x) < 0$  and  $ax + b > 0$ , if  $h'(x) \geq 0$ , then  $h''(x) < 0$ . Thus we have the second claim.  $\square$

### 5.7.4 Proof of Theorem 5.2

*Proof.* On one hand, when the user selection  $S^*(\kappa)$  does not change, the rate function  $Q(S^*(\kappa), P)$  is concave w.r.t  $P$  for the region, and  $\kappa$  should be such that  $P = P(S^*(\kappa), \kappa)$ . Therefore the EE function

$$f(P) = G(S^*(\kappa), P) = \frac{Q(S^*(\kappa), P)}{\phi P + P_C} \quad (5.53)$$

is quasi-concave w.r.t.  $P$ .

On the other hand, assume that one or more subcarrier have a modified user allocation when  $\kappa = \kappa_c$ , and let us denote the former and new set by  $S_1$  and  $S_2$  respectively. From Lemma 5.1, we have

$$\begin{aligned} P_1 = P(S_1, \kappa_c) &= \sum_{k=1}^K \left[ \left( r'(\mathbf{H}_{k,u_1(k)}, p_{k,u_1(k)}) \right)^{-1} \left( \frac{1}{\ln 2 \cdot \kappa_c} \right) \right] \\ &\leq \sum_{k=1}^K \left[ \left( r'(\mathbf{H}_{k,u_2(k)}, p_{k,u_2(k)}) \right)^{-1} \left( \frac{1}{\ln 2 \cdot \kappa_c} \right) \right] \\ &= P(S_2, \kappa_c) = P_2, \end{aligned} \quad (5.54)$$

where  $(\cdot)^{-1}$  stands for the inverse function and  $u_1(k)$  and  $u_2(k)$  are respectively the elements of  $S_1$  and  $S_2$ . Similarly, we also have  $Q(S_1, P_1) = R(S_1, \kappa_c) \leq R(S_2, \kappa_c) = Q(S_2, P_2)$ , and from (5.44), we also have

$$Q(S_1, P_1) - Q'(S_1, P_1)P_1 = Q(S_2, P_2) - Q'(S_2, P_2)P_2. \quad (5.55)$$

Then

$$f'(P_1) = \frac{Q'(S_1, P_1)(\phi P_1 + P_C) - \phi Q(S_1, P_1)}{(\phi P_1 + P_C)^2} \quad (5.56)$$

and using (5.55) we have

$$\begin{aligned} f'(P_2) &= \frac{Q'(S_2, P_2)(\phi P_2 + P_C) - \phi Q(S_2, P_2)}{(\phi P_2 + P_C)^2} \\ &= \frac{Q'(S_1, P_1)(\phi P_1 + P_C) - \phi Q(S_1, P_1)}{(\phi P_2 + P_C)^2}, \end{aligned} \quad (5.57)$$

and

$$\begin{aligned} f(P_2) - f(P_1) &= \frac{Q(S_2, P_2)}{\phi P_2 + P_C} - \frac{Q(S_1, P_1)}{\phi P_1 + P_C} \\ &= \frac{(P_2 - P_1)(Q'(S_1, P_1)(\phi P_1 + P_C) - \phi Q(S_1, P_1))}{(\phi P_1 + P_C)(\phi P_2 + P_C)}. \end{aligned} \quad (5.58)$$

If  $P_1 = P_2$ , then  $Q(S_1, P_1) = Q(S_2, P_2)$  from (5.55) since  $Q'(S_1, P_1) = Q'(S_2, P_2)$ . Therefore the EE function is continuous at  $P_1 (= P_2)$ . From (5.56) and (5.57), the first derivatives before and after user switching are simultaneously either 0, positive, or negative, that is,

$$\lim_{P \rightarrow P_1^-} f'(P_1) > 0 \Leftrightarrow \lim_{P \rightarrow P_1^+} f'(P_1) > 0 \quad (5.59)$$

$$\lim_{P \rightarrow P_1^-} f'(P_1) = 0 \Leftrightarrow \lim_{P \rightarrow P_1^+} f'(P_1) = 0 \quad (5.60)$$

$$\lim_{P \rightarrow P_1^-} f'(P_1) < 0 \Leftrightarrow \lim_{P \rightarrow P_1^+} f'(P_1) < 0. \quad (5.61)$$

On the other hand, if  $P_1 < P_2$ , we have

$$f(P_1) < f(P_2) \Leftrightarrow f'(P_1) > 0 \Leftrightarrow f'(P_2) > 0 \quad (5.62)$$

$$f(P_1) = f(P_2) \Leftrightarrow f'(P_1) = 0 \Leftrightarrow f'(P_2) = 0 \quad (5.63)$$

$$f(P_1) > f(P_2) \Leftrightarrow f'(P_1) < 0 \Leftrightarrow f'(P_2) < 0. \quad (5.64)$$

Let us define the discontinuous definition set of  $f(P)$  by  $P \in [u_{11}, u_{12}] \cup [u_{21}, u_{22}] \cup \dots \cup [u_{T1}, u_{T2}]$ , where  $u_{11} < u_{12} < u_{21} < u_{22} < \dots < u_{T1} < u_{T2}$ . Assume that there exists  $\bar{P} \in (u_{t1}, u_{t2})$ , where  $1 < t < T$ , such that  $f(\bar{P}) < \min\{f(u_{11}), f(u_{T2})\}$ . From (5.62-5.64), there must exist  $\bar{P}_1 \in [u_{i1}, u_{i2}]$ , where  $i < t$ , such that  $f'(\bar{P}_1) < 0$ , and there must exist  $\bar{P}_2 \in [u_{j1}, u_{j2}]$ , where  $j > t$ , such that  $f'(\bar{P}_2) > 0$ . Then from Lemma 5.2, we have  $\lim_{P \rightarrow \bar{P}^-} f'(P) \leq 0$  and  $\lim_{P \rightarrow \bar{P}^+} f'(P) > 0$ , which is contradictory with the fact that  $f'(P)$  exists. The same reasoning is also valid for the special cases where  $\bar{P} = u_{t1}$ , or  $\bar{P} = u_{t2}$  and  $t = 1$  or  $t = T$ .

Thus for any  $P \in [u_{11}, u_{12}] \cup [u_{21}, u_{22}] \cup \dots \cup [u_{T1}, u_{T2}]$ , we have

$$f(P) \geq \min\{f(u_{11}), f(u_{T2})\}. \quad (5.65)$$

Hence  $f(P)$  is a discontinuous but quasi-concave function.  $\square$

### 5.7.5 Proof of Theorem 5.3

*Proof.* From Theorem 5.1, for all  $S$ ,  $Q(S, P(S_1, \kappa_c)) \leq R(S_1, \kappa_c)$  and  $Q(S, P(S_2, \kappa_c)) \leq R(S_2, \kappa_c)$ . If, for a certain  $S_0$  and a certain  $P_a$ , the following condition is fulfilled,

$$Q(S_0, P_a) \geq \frac{P(S_2, \kappa_c) - P_a}{P(S_2, \kappa_c) - P(S_1, \kappa_c)} R(S_1, \kappa_c) + \frac{P_a - P(S_1, \kappa_c)}{P(S_2, \kappa_c) - P(S_1, \kappa_c)} R(S_2, \kappa_c), \quad (5.66)$$

then, because of the continuity of  $Q'(S_0, P)$  and the fact that  $Q(S_0, P(S_1, \kappa_c)) \leq R(S_1, \kappa_c)$  and  $Q(S_0, P(S_2, \kappa_c)) \leq R(S_2, \kappa_c)$ , there exists a  $P(S_1, \kappa_c) < P_b < P(S_2, \kappa_c)$  such that

$$Q'(S_0, P_b) = Q'(S_1, P(S_1, \kappa_c)) \quad (5.67)$$

and

$$Q(S_0, P_b) \geq \frac{P(S_2, \kappa_c) - P_b}{P(S_2, \kappa_c) - P(S_1, \kappa_c)} R(S_1, \kappa_c) + \frac{P_b - P(S_1, \kappa_c)}{P(S_2, \kappa_c) - P(S_1, \kappa_c)} R(S_2, \kappa_c). \quad (5.68)$$

Therefore, by using (5.55) and after some manipulations, we have

$$Q(S_0, P_b) - Q'(S_0, P_b)P_b \geq R(S_1, \kappa_c) - Q'(S_1, P(S_1, \kappa_c))P(S_1, \kappa_c). \quad (5.69)$$

Thus the user selection changes from  $S_1$  to  $S_0$ , which is contradictory with the fact that the user selection changes from  $S_1$  to  $S_2$ .

Therefore, for all  $P, S$ , we must have that

$$Q(S, P) < \frac{P(S_2, \kappa_c) - P}{P(S_2, \kappa_c) - P(S_1, \kappa_c)} R(S_1, \kappa_c) + \frac{P - P(S_1, \kappa_c)}{P(S_2, \kappa_c) - P(S_1, \kappa_c)} R(S_2, \kappa_c). \quad (5.70)$$

If  $\frac{Q(S,P)}{\phi P + P_C} \geq \text{EE}(S_1, \kappa_c)$ , substituting into (5.70), we have

$$R(S_1, \kappa_c) \frac{\phi P(S_2, \kappa_c) + P_C}{\phi P(S_1, \kappa_c) + P_C} < R(S_2, \kappa_c). \quad (5.71)$$

If  $\frac{Q(S,P)}{\phi P + P_C} \geq \text{EE}(S_2, \kappa_c)$ , substituting into (5.70), we have

$$R(S_2, \kappa_c) \frac{\phi P(S_1, \kappa_c) + P_C}{\phi P(S_2, \kappa_c) + P_C} < R(S_1, \kappa_c). \quad (5.72)$$

Equations (5.71) and (5.72) cannot be fulfilled simultaneously, meaning that claim (5.30) is true.  $\square$

### 5.7.6 Proof of Proposition 1

*Proof.* If  $\min\{M, N\} = 1$ , there is only one eigenvalue of the channel matrix,  $\lambda_{k,u}$ . With the water level  $\kappa$ , the allocated power is  $p_{k,u} = \kappa - \frac{\Gamma}{\lambda_{k,u}}$ . From (5.22) we have

$$\Theta(k, u) = \log_2 \left( \frac{\kappa \lambda_{k,u}}{\Gamma} \right) - \frac{1}{\ln 2 \cdot \kappa} \left( \kappa - \frac{\Gamma}{\lambda_{k,u}} \right). \quad (5.73)$$

The derivative of  $\Theta(k, u)$  w.r.t.  $\lambda_{k,u}$  is given by

$$\frac{\partial \Theta(k, u)}{\partial \lambda_{k,u}} = \frac{1}{\ln 2 \cdot \lambda_{k,u}} - \frac{\Gamma}{\ln 2 \cdot \kappa} \frac{1}{\lambda_{k,u}^2} = \frac{p_{k,u}}{\ln 2 \cdot \kappa \lambda_{k,u}} \geq 0. \quad (5.74)$$

It appears that  $\Theta(k, u)$  is an increasing function of  $\lambda_{k,u}$  meaning that the algorithm will always select the user with the largest channel gain.  $\square$

# Chapter 6

## Power allocation and relay selection in MIMO relay channels

### 6.1 Related works and chapter review

In this chapter, we consider the EE maximization problem for MIMO-relay channels with relay selection and individual power constraints for each node. Among the works of the EE maximization problem, a number of papers have studied the scenarios with assisting relays to forward the signal because relays can increase the coverage distance. Two well known relaying technologies are amplify-and-forward (AF) and decode-and-forward (DF) respectively. Papers [PBS15, CYH14, KWT13] considered EE maximization problem for DF relaying, while papers [ZCJ14a, CYH13, ZJB14, HCCZ13, ZCJB13, ZBJ11, ZCJ14b, ZBCH14] considered AF relaying. Paper [ZJB14] studied the interference channel with multiple users and one single relay, while paper [ZCJB13] studied the interference channel for a MIMO channel with single-stream source symbols. Papers [ZBJ11] and [HCCZ13] consider SISO channels. In paper [HCCZ13], the authors showed that the EE functions for no direct link or with direct link are both quasi-concavity. Paper [CYH13] studied the EE maximization problem for multi-relay OFDMA networks. However, a high SNR approximation is used to show the quasi-concavity of the EE function and a total power constraint is considered instead of individual power constraints for the different nodes. The authors in [ZBCH14] investigate antenna selection at the relay for MIMO chan-

nels assuming uniform power allocation at the source. Papers [ZCJ14a] and [ZCJ14b] studied MIMO-relay channels without direct link. The authors show that the EE function is quasi-concave w.r.t. the amplifying coefficients for a fixed power allocation at the source and vice versa. Therefore an alternating method can be implemented to find the optimal EE.

Instead of calculating the individual EE for each active relay, we implement Dinkelbach's method for the whole system to reduce calculation complexity. Different from [ZCJ14a] and [ZCJ14b], we obtain the closed-form expressions of the precoding matrix at the source and the beamforming matrix at the selected relay thanks to the concavity of the objective function using Dinkelbach's method. The expressions, which are functions of the Lagrangian multipliers, give deeper insights on the power allocations for each eigenchannel. We also give the mathematical property of monotonicity which guarantees that the values of Lagrangian multipliers can always be found. Finally, we report numerical results illustrating the performance gain due to relay selection.

## 6.2 System model

Consider a wireless transmission system consisting of one source node communicating to one destination node with the help of  $K$  relay nodes. Assuming severe large-scale fading, direct link between the source and the destination is ignored. The source selects one relay in a centralized manner to help the transmission. The criterion is to maximize the EE of the whole system. The source node and the destination node are both assumed to be equipped with  $N_t$  antennas. All the relays are assumed to be equipped with  $N_r$  antennas without loss of generality and implement AF mechanism. The transmission consists of two time slots, that is, the selected relay receives signal from the source in the first time-slot and forward the signal to the destination in the second time-slot.

Assume that the  $k$ -th relay is selected, the observation model of the first time-slot is:

$$\mathbf{r}_k = \mathbf{H}_k \mathbf{F}_k \mathbf{s} + \mathbf{n}_k, \quad (6.1)$$

where  $M = \min\{N_t, N_r\}$  is the number of streams,  $\mathbf{s} \in \mathbb{C}^{M \times 1}$  is the source symbol vector with a covariance matrix  $\mathbb{E}\{\mathbf{s}\mathbf{s}^H\} = \mathbf{I}_M$ ,  $\mathbf{F}_k \in \mathbb{C}^{N_t \times M}$  is the

precoding matrix,  $\mathbf{H}_k \in \mathbb{C}^{N_r \times N_t}$  is the backward channel matrix between the source and the  $k$ -th relay,  $\mathbf{n}_k$  is the noise vector with  $\mathbb{E} \{ \mathbf{n}_k \mathbf{n}_k^H \} = \sigma^2 \mathbf{I}_{N_r}$ , and  $\mathbf{r}_k$  denotes the received signal at the  $k$ -th relay.

The observation model of the second time-slot is

$$\mathbf{y} = \mathbf{G}_k \mathbf{A}_k \mathbf{r}_k + \mathbf{n}_D, \quad (6.2)$$

where  $\mathbf{A}_k$  is the AF beamforming matrix which corresponds to the precoding of  $\mathbf{r}_k$ ,  $\mathbf{G}_k \in \mathbb{C}^{N_t \times N_r}$  is the forward channel matrix between the  $k$ -th relay and the destination,  $\mathbf{n}_D$  is the noise at the destination with  $\mathbb{E} \{ \mathbf{n}_D \mathbf{n}_D^H \} = \sigma^2 \mathbf{I}_{N_t}$ , and finally  $\mathbf{y}$  is the received symbol at the destination.

The rate of the system is

$$R(k, \mathbf{F}_k, \mathbf{A}_k) = \log |\mathbf{I}_M + \mathbf{N}^{-1} \mathbf{G}_k \mathbf{A}_k \mathbf{H}_k \mathbf{F}_k \mathbf{F}_k^H \mathbf{H}_k^H \mathbf{A}_k^H \mathbf{G}_k^H|, \quad (6.3)$$

where

$$\mathbf{N} = \sigma^2 \mathbf{I}_M + \sigma^2 \mathbf{G}_k \mathbf{A}_k \mathbf{A}_k^H \mathbf{G}_k^H. \quad (6.4)$$

The power consumption of the whole system is

$$P(k, \mathbf{F}_k, \mathbf{A}_k) = \rho_S \text{tr}(\mathbf{F}_k \mathbf{F}_k^H) + \rho_k \text{tr}(\mathbf{A}_k (\mathbf{H}_k \mathbf{F}_k \mathbf{F}_k^H \mathbf{H}_k^H + \sigma^2 \mathbf{I}_M) \mathbf{A}_k^H) + D_k^C, \quad (6.5)$$

where  $D_k^C = D^{SD} + D_k^R$ ,  $D^{SD}$  is the constant circuit power at the source and the destination and  $D_k^R$  is the constant circuit power at the  $k$ -th relay.  $\rho_S$  and  $\rho_k$  denotes respectively the inverse of amplifier efficiency of the source node and the  $k$ -th relay node.

Assuming the bandwidth is  $B$ Hz, the EE maximization problem can be formulated as

$$\begin{aligned} \max_{k, \{\mathbf{F}_k\}, \{\mathbf{A}_k\}} & \frac{B \cdot R(k, \mathbf{F}_k, \mathbf{A}_k)}{P(k, \mathbf{F}_k, \mathbf{A}_k)} \\ \text{s.t.} & \text{tr}(\mathbf{F}_k \mathbf{F}_k^H) \leq P^S \\ & \text{tr}(\mathbf{A}_k (\mathbf{H}_k \mathbf{F}_k \mathbf{F}_k^H \mathbf{H}_k^H + \sigma^2 \mathbf{I}_M) \mathbf{A}_k^H) \leq P_k^R, \end{aligned} \quad (6.6)$$

where  $P^S$  and  $P_k^R$  are respectively the transmit power constraint at the source and the  $k$ -th relay.

## 6.3 EE maximization

In this section, a new formulation will be provided for problem (6.6). Especially, for a given  $k$ , the objective function will be concave w.r.t  $\mathbf{Q}_k$  (resp.  $\Theta_k$ ) for given  $\Theta_k$  (resp.  $\mathbf{Q}_k$ ), where  $\mathbf{Q}_k$  and  $\Theta_k$  will be defined after equation (6.10). The structure of the power allocation will be obtained thanks to the KKT conditions. Finally, we will propose an algorithm made of multiple sub-algorithms to find the maximum EE.

### 6.3.1 Problem reformulation

Using Dinkelbach's method [ICJF12], the original objective function can be reformulated as finding  $\mu^*$ , which is the root of  $F(\mu)$ , where

$$F(\mu) = \max_{k, \{\mathbf{F}_k\}, \{\mathbf{A}_k\}} [R(k, \mathbf{F}_k, \mathbf{A}_k) - \mu P(k, \mathbf{F}_k, \mathbf{A}_k)]. \quad (6.7)$$

The obtained EE will be  $B\mu^*$ . Denote the SVD of the channel matrices as:  $\mathbf{H}_k = \mathbf{U}_{\mathbf{H}_k} \Lambda_{\mathbf{H}_k} \mathbf{V}_{\mathbf{H}_k}^H$  and  $\mathbf{G}_k = \mathbf{U}_{\mathbf{G}_k} \Lambda_{\mathbf{G}_k} \mathbf{V}_{\mathbf{G}_k}^H$ . According to the proposition 1 in [ZCJ14a], the function  $R(k, \mathbf{F}_k, \mathbf{A}_k)$  is maximized and the function  $P(k, \mathbf{F}_k, \mathbf{A}_k)$  is minimized simultaneously when the following conditions are satisfied:  $\mathbf{U}_{\mathbf{F}_k} = \mathbf{V}_{\mathbf{H}_k}$ ,  $\mathbf{U}_{\mathbf{A}_k} = \mathbf{V}_{\mathbf{G}_k}$ , and  $\mathbf{V}_{\mathbf{A}_k} = \mathbf{U}_{\mathbf{H}_k}$ , where we denote the SVD of  $\mathbf{F}_k$  and  $\mathbf{A}_k$  as  $\mathbf{F}_k = \mathbf{U}_{\mathbf{F}_k} \Lambda_{\mathbf{F}_k} \mathbf{V}_{\mathbf{F}_k}^H$  and  $\mathbf{A}_k = \mathbf{U}_{\mathbf{A}_k} \Lambda_{\mathbf{A}_k} \mathbf{V}_{\mathbf{A}_k}^H$ . Thus we only consider  $\mathbf{F}_k$  and  $\mathbf{A}_k$  fulfilling the above conditions. Denote the  $m$ -th eigenvalue of  $\mathbf{F}_k \mathbf{F}_k^H$ ,  $\mathbf{H}_k \mathbf{H}_k^H$ ,  $\mathbf{A}_k \mathbf{A}_k^H$ , and  $\mathbf{G}_k \mathbf{G}_k^H$  respectively as  $q_m^{(k)}$ ,  $h_m^{(k)}$ ,  $\theta_m^{(k)}$  and  $g_m^{(k)}$ . We have

$$F(\mu) = \max_{k, \mathbf{Q}_k, \Theta_k} [R(k, \mathbf{Q}_k, \Theta_k) - \mu P(k, \mathbf{Q}_k, \Theta_k)], \quad (6.8)$$

where

$$R(k, \mathbf{Q}_k, \Theta_k) = \sum_{m=1}^M \log \left( 1 + \frac{\theta_m^{(k)} q_m^{(k)} h_m^{(k)} g_m^{(k)}}{\sigma^2 + \sigma^2 \theta_m^{(k)} g_m^{(k)}} \right) \quad (6.9)$$

and

$$P(k, \mathbf{Q}_k, \Theta_k) = \rho_S \sum_{m=1}^M q_m^{(k)} + \rho_k \sum_{m=1}^M \theta_m^{(k)} (h_m^{(k)} q_m^{(k)} + \sigma^2) + D_k^C, \quad (6.10)$$

with  $\mathbf{Q}_k = \text{diag}\{q_1^{(k)}, \dots, q_M^{(k)}\}$  and  $\mathbf{\Theta}_k = \text{diag}\{\theta_1^{(k)}, \dots, \theta_M^{(k)}\}$ . The constraints of the original problem become

$$\sum_{m=1}^M q_m^{(k)} \leq P^S, \quad (6.11)$$

and

$$\sum_{m=1}^M \theta_m^{(k)} (h_m^{(k)} q_m^{(k)} + \sigma^2) \leq P_k^R. \quad (6.12)$$

For given  $\hat{\mu}$ , the objective function of (6.7) for relay  $k$  is

$$\epsilon_k(\hat{\mu}) = \max_{\mathbf{Q}_k, \mathbf{\Theta}_k} [R(\mathbf{Q}_k, \mathbf{\Theta}_k) - \hat{\mu}P(\mathbf{Q}_k, \mathbf{\Theta}_k)]. \quad (6.13)$$

Because this objective function is a sum of several functions of orthogonal eigenchannels, according to [ZCJ14a] and [HCCZ13], the problem is strictly concave w.r.t.  $\mathbf{Q}_k$  for given  $\mathbf{\Theta}_k$  and strictly concave w.r.t.  $\mathbf{\Theta}_k$  for given  $\mathbf{Q}_k$ . In the following, we will respectively investigate the two sets of KKT conditions and study the structure of power allocation.

### 6.3.2 Optimization of $\mathbf{Q}_k$ for given $\mathbf{\Theta}_k$

For each  $k$  and  $m$ , given  $\hat{\mu}$  and  $\mathbf{\Theta}_k$ , the Lagrangian of the problem in (6.13) with constraints (6.11) and (6.12) is

$$\begin{aligned} L(\mathbf{Q}_k, \beta_k, \alpha_k) = & R(\mathbf{Q}_k, \mathbf{\Theta}_k) - \hat{\mu}P(\mathbf{Q}_k, \mathbf{\Theta}_k) \\ & - \beta_k \left( \sum_{m=1}^M q_m^{(k)} - P^S \right) - \alpha_k \left( \sum_{m=1}^M \theta_m^{(k)} (h_m^{(k)} q_m^{(k)} + \sigma^2) - P_k^R \right). \end{aligned} \quad (6.14)$$

The KKT condition in (6.14) for  $\mathbf{Q}_k$  is

$$\begin{aligned} & \frac{\theta_m^{(k)} h_m^{(k)} g_m^{(k)}}{\ln 2 \left( \theta_m^{(k)} h_m^{(k)} g_m^{(k)} q_m^{(k)} + \sigma^2 (\theta_m^{(k)} g_m^{(k)} + 1) \right)} \\ = & \hat{\mu} (\rho_S + \rho_k \theta_m^{(k)} h_m^{(k)}) + \beta_k + \alpha_k \rho_k \theta_m^{(k)} h_m^{(k)}, \end{aligned} \quad (6.15)$$

where  $\beta_k \geq 0, \alpha_k \geq 0$ . If  $\theta_m^{(k)} = 0$ , then  $q_m^{(k)} = 0$ . Otherwise we have

$$q_m^{(k)} = \left[ \nu(m, \beta_k, \alpha_k) - \frac{\sigma^2(1 + \theta_m^{(k)} g_m^{(k)})}{\theta_m^{(k)} h_m^{(k)} g_m^{(k)}} \right]_0^+, \quad (6.16)$$

where

$$\nu(m, \beta_k, \alpha_k) = \left[ \ln 2 \left( \hat{\mu} (\rho_S + \rho_k \theta_m^{(k)} h_m^{(k)}) + \beta_k + \alpha_k \rho_k \theta_m^{(k)} h_m^{(k)} \right) \right]^{-1}. \quad (6.17)$$

There are 4 cases w.r.t.  $\alpha_k$  and  $\beta_k$ , indicating whether the two equalities regarding the power constraints are active or inactive:

- $\beta_k = \alpha_k = 0$

In this case, both  $\sum_{m=1}^M q_m^{(k)} < P^S$  and  $\sum_{m=1}^M \theta_m^{(k)} (h_m^{(k)} q_m^{(k)} + \sigma^2) < P_k^R$  should be satisfied.

- $\beta_k > 0, \alpha_k = 0$

In this case, both  $\sum_{m=1}^M q_m^{(k)} = P^S$  and  $\sum_{m=1}^M \theta_m^{(k)} (h_m^{(k)} q_m^{(k)} + \sigma^2) < P_k^R$  should be satisfied.

In the following, we derive the structure of power allocation at the source node and propose an algorithm to find the  $\beta_k$  such that  $\sum_{m=1}^M q_m^{(k)} = P^S$ . For the  $k$ -th relay, for each  $m$ , calculate

$$z_m^{(k)} = \frac{\theta_m^{(k)} h_m^{(k)} g_m^{(k)}}{\ln 2 \sigma^2 (1 + \theta_m^{(k)} g_m^{(k)})} - \hat{\mu} (\rho_S + \rho_k \theta_m^{(k)} h_m^{(k)}), \quad (6.18)$$

which is the maximum value of  $\beta_k$  for a non-zero  $q_m^{(k)}$  according to (6.16) and (6.17). For each  $k$ , order them in descending order

$$z_{\tau_1}^{(k)} > z_{\tau_2}^{(k)} > \dots > z_{\tau_M}^{(k)}, \quad (6.19)$$

which means the eigenchannel  $\tau_1$  will be the first one to be active. Define

$$a_m^{(k)} = \sum_{i=1}^{m-1} \left( \nu(\tau_i, z_{\tau_m}^{(k)}, 0) - \frac{\sigma^2(1 + \theta_{\tau_i}^{(k)} g_{\tau_i}^{(k)})}{\theta_{\tau_i}^{(k)} h_{\tau_i}^{(k)} g_{\tau_i}^{(k)}} \right), \quad (6.20)$$

which is the total power allocation above which the  $\tau_m$ -th eigenchannel starts to be active. Compare each  $a_m^{(k)}$  with  $P^S$  to find the number of active eigenchannels. We will propose an algorithm to find  $\beta_k^*$  such that  $\sum_{m=1}^M q_m^{(k)} = P^S$ . That is to find  $\beta_k$  such that  $\tilde{a}^{(k)}(\beta_k) = P^S$ , where

$$\tilde{a}^{(k)}(\beta_k) = \sum_{m=1}^M \left[ \nu(\tau_m, \beta_k, 0) - \frac{\sigma^2(1 + \theta_{\tau_m}^{(k)} g_{\tau_m}^{(k)})}{\theta_{\tau_m}^{(k)} h_{\tau_m}^{(k)} g_{\tau_m}^{(k)}} \right]_0^+. \quad (6.21)$$

The detailed algorithm can be found in Algorithm 6.5.

- $\beta_k = 0, \alpha_k > 0$

In this case, both  $\sum_{m=1}^M q_m^{(k)} < P^S$  and  $\sum_{m=1}^M \theta_m^{(k)} (h_m^{(k)} q_m^{(k)} + \sigma^2) = P_k^R$  should be satisfied.

Similarly as in Case 2, for each  $k, m$ , calculate

$$w_m^{(k)} = \left[ \frac{\theta_m^{(k)} h_m^{(k)} g_m^{(k)}}{\ln 2 \sigma^2 (1 + \theta_m^{(k)} g_m^{(k)})} - \hat{\mu} (\rho_S + \rho_k \theta_m^{(k)} h_m^{(k)}) \right] \cdot (\rho_k \theta_m^{(k)} h_m^{(k)})^{-1}, \quad (6.22)$$

which is the maximum value of  $\alpha_k$  for a non-zero  $q_m^{(k)}$  according to (6.16) and (6.17). For each  $k$ , order them in descending order

$$w_{\eta_1}^{(k)} > w_{\eta_2}^{(k)} > \dots > w_{\eta_M}^{(k)} \quad (6.23)$$

and define

$$c_m^{(k)} = \sum_{i=1}^{m-1} \theta_{\eta_i} \left( h_{\eta_i} \left( \nu(\eta_i, 0, w_{\eta_m}^{(k)}) - \frac{\sigma^2(1 + \theta_{\eta_i}^{(k)} g_{\eta_i}^{(k)})}{\theta_{\eta_i}^{(k)} h_{\eta_i}^{(k)} g_{\eta_i}^{(k)}} \right) + \sigma^2 \right), \quad (6.24)$$

which is the total power allocation above which the  $\eta_m$ -th eigenchannel starts to be active. Compare each  $c_m^{(k)}$  with  $P_k^R$  to find the number of active eigenchannels. The algorithm will find  $\alpha_k^*$  such that

$\sum_{m=1}^M \theta_m^{(k)} (h_m^{(k)} q_m^{(k)} + \sigma^2) = P_k^R$ . As in Case 2, this is equivalent to find  $\alpha_k$  such that  $\tilde{c}^{(k)}(\alpha_k) = P_k^R$ , where

$$\tilde{c}^{(k)}(\alpha_k) = \sum_{m=1}^M \theta_{\eta_m} \left( h_{\eta_m} \left[ \nu(\eta_m, 0, \alpha_k) - \frac{\sigma^2(1 + \theta_{\eta_m}^{(k)} g_{\eta_m}^{(k)})}{\theta_{\eta_m}^{(k)} h_{\eta_m}^{(k)} g_{\eta_m}^{(k)}} \right]_0^+ + \sigma^2 \right). \quad (6.25)$$

The detailed algorithm can be found in Algorithm 6.6.

- $\beta_k, \alpha_k > 0$

In this case, both  $\sum_{m=1}^M q_m^{(k)} = P^S$  and  $\sum_{m=1}^M \theta_m^{(k)} (h_m^{(k)} q_m^{(k)} + \sigma^2) = P_k^R$  should be satisfied.

Before introducing the algorithm, we first give the following theorem.

**Theorem 6.1. Monotonicity:** Assume that  $\beta_k^{(1)}$  and  $\alpha_k^{(1)}$  change to  $\beta_k^{(2)}$  and  $\alpha_k^{(2)}$ , if the following equations are true:

$$\sum_{m=1}^M q_m^{(k)(1)} = P^S \quad (6.26)$$

and

$$\sum_{m=1}^M q_m^{(k)(2)} = P^S, \quad (6.27)$$

then it is if and only if when  $\alpha_k^{(1)} < \alpha_k^{(2)}$  that the following is true:

$$\sum_{m=1}^M \theta_m^{(k)} (h_m^{(k)} q_m^{(k)(1)} + \sigma^2) > \sum_{m=1}^M \theta_m^{(k)} (h_m^{(k)} q_m^{(k)(2)} + \sigma^2). \quad (6.28)$$

Then, from (6.26) and (6.27), we must have  $\beta_k^{(1)} > \beta_k^{(2)}$ .

Therefore, it can be concluded that a higher relay power comes with a lower value of  $\alpha_k$  which is the monotonicity property announced.

Similarly, we have the following theorem:

**Theorem 6.2. Monotonicity:** For  $\beta_k^{(1)}, \alpha_k^{(1)}, \beta_k^{(2)}$ , and  $\alpha_k^{(2)}$ , if the following equations are true:

$$\sum_{m=1}^M \theta_m^{(k)} (h_m^{(k)} q_m^{(k)(1)} + \sigma^2) = P_k^R \quad (6.29)$$

and

$$\sum_{m=1}^M \theta_m^{(k)} (h_m^{(k)} q_m^{(k)(2)} + \sigma^2) = P_k^R, \quad (6.30)$$

then it is if and only if when  $\beta_k^{(1)} < \beta_k^{(2)}$  that the following is true:

$$\sum_{m=1}^M q_m^{(k)(1)} > \sum_{m=1}^M q_m^{(k)(2)}. \quad (6.31)$$

Then, from (6.29) and (6.30), we must have  $\alpha_k^{(1)} > \alpha_k^{(2)}$ .

Therefore, it can also be concluded that a higher source power comes with a lower value of  $\beta_k$  which is the monotonicity property announced.

The proof is provided in the appendix.

Let us denote by  $\alpha_k^+$  and  $\beta_k^+$  respectively as the  $\alpha_k$  and  $\beta_k$  satisfying  $\sum_{m=1}^M q_m^{(k)} = P^S$  and  $\sum_{m=1}^M \theta_m^{(k)} (h_m^{(k)} q_m^{(k)} + \sigma^2) = P_k^R$ .  $\alpha_k^*$  denotes the  $\alpha_k$  found in Case 3 satisfying  $\sum_{m=1}^M q_m^{(k)} > P^S$  and  $\beta_k^*$  denotes the  $\beta_k$  found in Case 2 satisfying  $\sum_{m=1}^M \theta_m^{(k)} (h_m^{(k)} q_m^{(k)} + \sigma^2) > P_k^R$ . From Theorem 6.1, we know that  $\beta_k^+ < \beta_k^*$ ,  $\alpha_k^+ > 0$  and from Theorem 6.2  $\alpha_k^+ < \alpha_k^*$ ,  $\beta_k^+ > 0$ , which means  $0 < \alpha_k^+ < \alpha_k^*$  and  $0 < \beta_k^+ < \beta_k^*$ .

Therefore, in the algorithm, we will implement Algorithm 6.5 for each given  $\bar{\alpha}_k$ . The only differences with case 2 are that  $z_m^{(k)}$  becomes

$$z_m^{(k)} = \frac{\theta_m^{(k)} h_m^{(k)} g_m^{(k)}}{\ln 2 \sigma^2 \left( 1 + \theta_m^{(k)} g_m^{(k)} \right)} - \hat{\mu} \left( \rho_S + \rho_k \theta_m^{(k)} h_m^{(k)} \right) - \bar{\alpha}_k \rho_k \theta_m^{(k)} h_m^{(k)}, \quad (6.32)$$

$\alpha_m^{(k)}$  becomes

$$\alpha_m^{(k)} = \sum_{i=1}^{m-1} \left( \nu(\tau_i, z_{\tau_m}^{(k)}, \bar{\alpha}_k) - \frac{\sigma^2(1 + \theta_{\tau_i}^{(k)} g_{\tau_i}^{(k)})}{\theta_{\tau_i}^{(k)} h_{\tau_i}^{(k)} g_{\tau_i}^{(k)}} \right). \quad (6.33)$$

and finally  $\tilde{a}^{(k)}(\beta_k)$  becomes

$$\tilde{a}^{(k)}(\beta_k) = \sum_{m=1}^M \left[ \nu(\tau_m, \beta_k, \bar{\alpha}_k) - \frac{\sigma^2(1 + \theta_{\tau_m}^{(k)} g_{\tau_m}^{(k)})}{\theta_{\tau_m}^{(k)} h_{\tau_m}^{(k)} g_{\tau_m}^{(k)}} \right]_0^+. \quad (6.34)$$

If the power consumed at the relay  $k$  is larger than  $P_k^R$ , we will increase  $\bar{\alpha}_k$  according to Theorem 1. If the power consumed at the relay  $k$  is less than  $P_k^R$ , we will decrease  $\bar{\alpha}_k$ . The algorithm in detail can be found in Algorithm 6.7.

### 6.3.3 Optimization of $\Theta_k$ for given $\mathbf{Q}_k$

For given  $\mathbf{Q}_k$ , for each  $k$  and  $m$ , the Lagrangian of the problem in (6.13) with constraints (6.11) and (6.12) is

$$\begin{aligned} L(\Theta_k, \beta_k, \alpha_k) = & R(\mathbf{Q}_k, \Theta_k) - \hat{\mu}P(\mathbf{Q}_k, \Theta_k) \\ & - \gamma_k \left( \sum_{m=1}^M \theta_m^{(k)} (h_m^{(k)} q_m^{(k)} + \sigma^2) - P_k^R \right). \end{aligned} \quad (6.35)$$

The KKT condition in (6.35) for  $\Theta_k$  is

$$\begin{aligned} & \frac{q_m^{(k)} h_m^{(k)} g_m^{(k)}}{\ln 2 \left( 1 + \theta_m^{(k)} g_m^{(k)} \right) \left( \theta_m^{(k)} h_m^{(k)} g_m^{(k)} q_m^{(k)} + \sigma^2(1 + \theta_m^{(k)} g_m^{(k)}) \right)} \\ = & \hat{\mu} \rho_k \left( q_m^{(k)} h_m^{(k)} + \sigma^2 \right) + \gamma_k \left( q_m^{(k)} h_m^{(k)} + \sigma^2 \right), \end{aligned} \quad (6.36)$$

which, after some manipulations, becomes

$$A_m \left( \theta_m^{(k)} \right)^2 + B_m \theta_m^{(k)} + C_m(\gamma_k) = 0, \quad (6.37)$$

where

$$A_m = g_m^{(k)2} (h_m^{(k)} q_m^{(k)} + \sigma^2) \quad (6.38)$$

$$B_m = 2\sigma^2 g_m^{(k)} + h_m^{(k)} g_m^{(k)} q_m^{(k)} \quad (6.39)$$

$$C_m(\gamma_k) = \sigma^2 - \frac{g_m^{(k)} q_m^{(k)} h_m^{(k)}}{\ln 2 (\hat{\mu}\rho_k + \gamma_k) (q_m^{(k)} h_m^{(k)} + \sigma^2)}. \quad (6.40)$$

Then

$$\theta_m^{(k)} = \frac{-B_m + \sqrt{B_m^2 - 4A_m C_m(\gamma_k)}}{2A_m}, \quad (6.41)$$

where  $\theta_m^{(k)} = 0$  if  $C_m(\gamma_k) \geq 0$ .  $\gamma_k$  should be chosen to satisfy the  $k$ -th relay power constraint. We first define

$$y_m^{(k)} = \frac{g_m^{(k)} q_m^{(k)} h_m^{(k)}}{\sigma^2 \ln 2 (q_m^{(k)} h_m^{(k)} + \sigma^2)} - \hat{\mu}\rho_k, \quad (6.42)$$

which is the maximum value of  $\gamma_k$  for a non-zero  $\theta_m^{(k)}$  according to (6.40). Order them in descending order

$$y_{\kappa_1}^{(k)} > y_{\kappa_2}^{(k)} > \dots > y_{\kappa_M}^{(k)}. \quad (6.43)$$

Similarly with  $\mathbf{Q}_k$  optimization, calculate  $b_m^{(k)}$  according to (6.41) as

$$b_m^{(k)} = \sum_{i=1}^{m-1} \frac{-B_{\kappa_i} + \sqrt{B_{\kappa_i}^2 - 4A_{\kappa_i} C_{\kappa_i}(y_{\kappa_m}^{(k)})}}{2A_{\kappa_i}} (h_{\kappa_i}^{(k)} q_{\kappa_i}^{(k)} + \sigma^2). \quad (6.44)$$

Compare each  $b_m^{(k)}$  to  $P_k^R$  to determine the number of active eigenchannels. Define

$$\tilde{b}^{(k)}(\gamma_k) = \sum_{i=1}^{m-1} \frac{-B_{\kappa_i} + \sqrt{B_{\kappa_i}^2 - 4A_{\kappa_i} C_{\kappa_i}(\gamma_k)}}{2A_{\kappa_i}} (h_{\kappa_i}^{(k)} q_{\kappa_i}^{(k)} + \sigma^2). \quad (6.45)$$

This value will be used to find the  $\gamma_k$  such that the relay power constraint is satisfied with equality. The detailed algorithm can be found in Algorithm 6.3.

### 6.3.4 Algorithm for EE maximization

We propose an algorithm for relay selection and power allocation according to the analysis reported above. In each iteration in Algorithm 6.1,  $\mu^{(i)}$  is updated according to Newton's method as introduced in [ICJF12]. As  $\mu^{(i)}$  increases, certain relays will be discarded, therefore reducing calculation complexity. In Algorithm 6.2,  $\mathbf{Q}_k$  and  $\Theta_k$  are optimized alternately. The concavity and the KKT conditions guarantee the objective function  $\epsilon_k^{(j)}(\mu^{(i)})$  increases monotonically. In Algorithms 6.3, 6.5, 6.6, 6.7, the common idea is to first order the eigenchannels, then find the number of active eigenchannels, and finally calculate the exact power allocation using bisection method by implementing Algorithm 6.8. Note that Case 1 in  $\mathbf{Q}_k$  optimization is involved in Algorithm 6.5 when  $\beta_k^* = 0$ .

---

#### Algorithm 6.1: EE maximization with relay selection

---

- 1: Initialize  $S = \{1, \dots, K\}$ .  $i = 0$ ,  $\mu^{(0)} = 0$ , Set  $\delta_\mu$
  - 2: **repeat**
  - 3:   For each  $k \in S$ , implement Algorithm 6.2
  - 4:    $S = \{S/\{\bar{k}\}\}$ , where  $\{\bar{k}\}$  are such that
 
$$F_{\bar{k}}(\mu^{(i)}) < 0$$
  - 5:    $i = i + 1$
  - 6:    $\mu^{(i)} = \max_k \frac{R(\mathbf{Q}_k, \Theta_k)}{P(\mathbf{Q}_k, \Theta_k)}$
  - 7: **until**  $\frac{|\mu^{(i)} - \mu^{(i-1)}|}{\mu^{(i)}} < \delta_\mu$  and  $|S| = 1$
  - 8: Output  $S = \{k^*\}$ ,  $\mu^{(i)}$  (= EE<sub>max</sub>),  $\mathbf{Q}_{k^*}$ ,  $\Theta_{k^*}$
- 

## 6.4 Numerical results

In this section we report the numerical results. The parameters are set as follows:  $B = 10\text{kHz}$  is the bandwidth for each OFDM subcarrier. The channel is assumed to be Rayleigh distributed and has an average channel gain  $G_0 d^{-n}$  where the path loss exponent  $n = 4$ ,  $G_0 = -(G_1 M_l) = -70\text{dB}$  in which  $G_1 = 30\text{dB}$  is the gain factor at  $d = 1\text{m}$ .  $M_l = 40\text{dB}$  is the link margin compensating the hardware process variations and other noise and interference, the noise power  $\sigma^2 = BN_0 N_f$  where  $N_0 = -170\text{dBm/Hz}$  is the

---

**Algorithm 6.2:** Individual EE maximization using alternating maximization, INPUT:  $k, \mu^{(i)}$ ; OUTPUT:  $\mathbf{Q}_k, \Theta_k$

---

- 1: Initialize  $j = 0$  and  $\mathbf{Q}_k^{(0)} = \frac{PS}{M} \mathbf{I}_M$ ; Set  $\delta_\epsilon$ ; Initialize  $\epsilon_k^{(0)}(\mu^{(i)}) = 0$
  - 2: **repeat**
  - 3:   Implement Algorithm 6.3 using the current  $\mathbf{Q}_k^{(j)}$ , get  $\Theta_k^{(j+1)}$
  - 4:   Implement Algorithm 6.4 using  $\Theta_k^{(j+1)}$ , get  $\mathbf{Q}_k^{(j+1)}$
  - 5:    $j = j + 1$
  - 6:   Calculate  $\epsilon_k^{(j)}(\mu^{(i)})$  in (6.13)
  - 7: **until**  $\frac{|\epsilon_k^{(j)}(\mu^{(i)}) - \epsilon_k^{(j-1)}(\mu^{(i)})|}{|\epsilon_k^{(j)}(\mu^{(i)})|} < \delta_\epsilon$
  - 8:  $\mathbf{Q}_k = \mathbf{Q}_k^{(j)}$  and  $\Theta_k = \Theta_k^{(j)}$ ,  $F_k(\mu^{(i)}) = \epsilon_k^{(j)}(\mu^{(i)})$
- 

---

**Algorithm 6.3:** Find  $\Theta_k$  for given  $\mathbf{Q}_k$

---

- 1: For each  $m \in \{1, \dots, M\}$ , calculate  $y_m^{(k)}$  in (6.42)
  - 2: Order them in descending order
 
$$y_{\kappa_1}^{(k)} > y_{\kappa_2}^{(k)} > \dots > y_{\kappa_M}^{(k)}$$
  - 3: Remove  $y_{\kappa_m}^{(k)}$  where  $y_{\kappa_m}^{(k)} \leq 0$ , remaining  $m = 1, \dots, L_1$
  - 4: For each  $1 \leq m \leq L_1$ , calculate  $b_m^{(k)}$  in (6.44)
  - 5: Define  $b_{L_1+1}^{(k)} = \tilde{b}^{(k)}(0)$  in (6.45) and set  $y_{\kappa_{L_1+1}}^{(k)} = 0$
  - 6: **if**  $P_k^R \geq b_{L_1+1}^{(k)}$  **then**
  - 7:    $\gamma_k = 0$
  - 8: **else**
  - 9:   Find  $\tilde{m} \in \{1, \dots, L_1\}$  such that  $b_{\tilde{m}}^{(k)} \leq P_k^R < b_{\tilde{m}+1}^{(k)}$
  - 10:   **if**  $b_{\tilde{m}}^{(k)} = P_k^R$  **then**
  - 11:      $\gamma_k = y_{\tau_{\tilde{m}}}^{(k)}$
  - 12:   **else**
  - 13:     Implementing Algorithm 6.8 by setting  $x_l = y_{\tau_{\tilde{m}}}^{(k)}$ ,  $x_u = y_{\tau_{\tilde{m}+1}}^{(k)}$ ,  
 $x = \gamma_k$  in (6.45) and  $f(x) = \tilde{b}^{(k)}(x) - P_k^R$  to find  
 $\gamma_k \in (y_{\tau_{\tilde{m}}}^{(k)}, y_{\tau_{\tilde{m}+1}}^{(k)})$ ;
  - 14:   **end if**
  - 15: **end if**
  - 16: Calculate  $\Theta_k$  using (6.41) with  $\gamma_k = x^*$
-

---

**Algorithm 6.4:** Find  $\mathbf{Q}_k$  for given  $\Theta_k$ 


---

- 1: Implement Algorithm 6.5 and calculate power consumed at relay  $k$   
 $\sum_{m=1}^M \theta_m^{(k)} (h_m^{(k)} q_m^{(k)} + \sigma^2)$
  - 2: **if**  $\sum_{m=1}^M \theta_m^{(k)} (h_m^{(k)} q_m^{(k)} + \sigma^2) > P_k^R$  **then**
  - 3:   Implement Algorithm 6.6 and calculate power consumed at the  
source  $\sum_{m=1}^M q_m^{(k)}$
  - 4:   **if**  $\sum_{m=1}^M q_m^{(k)} > P^S$  **then**
  - 5:     Implement Algorithm 6.7
  - 6:   **end if**
  - 7: **end if**
- 

---

**Algorithm 6.5:** Case 1 and case 2

---

- 1: For each  $m \in \{1, \dots, M\}$ , calculate  $z_m^{(k)}$  in (6.18)
  - 2: Order them in descending order  

$$z_{\tau_1}^{(k)} > z_{\tau_2}^{(k)} > \dots > z_{\tau_M}^{(k)}$$
  - 3: Remove  $z_{\kappa_m}^{(k)}$  where  $z_{\kappa_m}^{(k)} \leq 0$ , remaining  $m = 1, \dots, L_2$
  - 4: For each  $1 \leq m \leq L_2$ , calculate  $a_m^{(k)}$  in (6.20)
  - 5: Define  $a_{L_2+1}^{(k)} = \tilde{a}^{(k)}(0)$  in (6.21) and set  $z_{\tau_{L_2+1}}^{(k)} = 0$
  - 6: **if**  $P^S \geq a_{L_2+1}^{(k)}$  **then**
  - 7:    $\beta_k^* = 0$
  - 8: **else**
  - 9:   Find  $\tilde{m} \in \{1, \dots, L_2\}$  such that  $a_{\tilde{m}}^{(k)} \leq P^S < a_{\tilde{m}+1}^{(k)}$
  - 10:   **if**  $a_{\tilde{m}}^{(k)} = P^S$  **then**
  - 11:      $\beta_k^* = z_{\tau_{\tilde{m}}}^{(k)}$
  - 12:   **else**
  - 13:     Implementing Algorithm 6.8 by setting  $x_l = z_{\tau_{\tilde{m}}}^{(k)}$ ,  $x_u = z_{\tau_{\tilde{m}+1}}^{(k)}$ ,  
 $x = \beta_k$  in (6.21) and  $f(x) = \tilde{a}^{(k)}(x) - P^S$  to find  
 $\beta_k \in (z_{\tau_{\tilde{m}}}^{(k)}, z_{\tau_{\tilde{m}+1}}^{(k)})$
  - 14:   **end if**
  - 15: **end if**
  - 16: Calculate  $\mathbf{Q}_k$  in (6.16) with  $\beta_k = \beta_k^* = x^*$  and  $\alpha_k = 0$
-

---

**Algorithm 6.6:** Case 3
 

---

- 1: For each  $m$ , calculate  $w_m^{(k)}$  in (6.22)
  - 2: Order them in descending order
 
$$w_{\eta_1}^{(k)} > w_{\eta_2}^{(k)} > \dots > w_{\eta_M}^{(k)}$$
  - 3: Remove  $w_{\eta_m}^{(k)}$  where  $w_{\eta_m}^{(k)} \leq 0$ , remaining  $m = 1, \dots, L_3$
  - 4: For each  $1 \leq m \leq L_3$ , calculate  $c_m^{(k)}$  in (6.24)
  - 5: Define  $c_{L_3+1}^{(k)} = \tilde{c}^{(k)}(0)$  in (6.25) and set  $w_{\eta_{L_3+1}}^{(k)} = 0$
  - 6: **if**  $P_k^R \geq a_{L_3+1}^{(k)}$  **then**
  - 7:    $\alpha_k^* = 0$
  - 8: **else**
  - 9:   Find  $\tilde{m} \in \{1, \dots, L_3\}$  such that  $c_{\tilde{m}}^{(k)} \leq P_k^R < c_{\tilde{m}+1}^{(k)}$
  - 10:   **if**  $c_{\tilde{m}}^{(k)} = P_k^R$  **then**
  - 11:      $\alpha_k^* = w_{\eta_{\tilde{m}}}^{(k)}$
  - 12:   **else**
  - 13:     Implementing Algorithm 6.8 by setting  $x_l = w_{\eta_{\tilde{m}}}^{(k)}$ ,  $x_u = w_{\eta_{\tilde{m}+1}}^{(k)}$ ,  
 $x = \alpha_k$  in (6.25) and  $f(x) = \tilde{c}^{(k)}(x) - P_k^R$  to find  
 $\alpha_k \in (w_{\eta_{\tilde{m}}}^{(k)}, w_{\eta_{\tilde{m}+1}}^{(k)})$
  - 14:   **end if**
  - 15: **end if**
  - 16: Calculate  $\mathbf{Q}_k$  in (6.16) with  $\alpha_k = \alpha_k^* = x^*$  and  $\beta_k = 0$
-

---

**Algorithm 6.7:** Case 4

---

- 1: Set  $\delta_\alpha$ ;  $\alpha_l = 0$ ,  $\alpha_k^+ = \alpha_u = \alpha_k^*$
  - 2: **while**  $\alpha_u - \alpha_l > \delta_\alpha$  **do**
  - 3:    $\alpha_t = (\alpha_l + \alpha_u)/2$
  - 4:   Calculate  $\beta_k^+$  by substituting (6.18), (6.20) and (6.21) respectively by (6.32), (6.33) and (6.34) and implementing an algorithm similar to Algorithm 6.5
  - 5:   Calculate the total power consumed at the relay  $k$  and denote it by  $P_t$
  - 6:   **if**  $P_t = P_k^R$  **then**
  - 7:      $\alpha_k^+ = \alpha_t$ ; **break**
  - 8:   **else if**  $P_t > P_k^R$  **then**
  - 9:      $\alpha_l = \alpha_t$
  - 10:   **else**
  - 11:      $\alpha_u = \alpha_t$ ;  $\alpha_k^+ = \alpha_u$
  - 12:   **end if**
  - 13: **end while**
  - 14: Calculate  $\mathbf{Q}_k$  in (6.16) with  $\alpha_k = \alpha_k^+$  and  $\beta_k = \beta_k^+$
- 

---

**Algorithm 6.8:** Bisection method to find  $f(x^*) = 0$ 

---

- 1: Set  $\delta_B$ ;  $x^* = x_u$
  - 2: **while**  $x_u - x_l > \delta_B$  **do**
  - 3:    $x_t = (x_l + x_u)/2$
  - 4:   **if**  $f(x_t) = 0$  **then**
  - 5:      $x^* = x_t$ ; **break**
  - 6:   **else if**  $f(x_t) < 0$  **then**
  - 7:      $x_l = x_t$
  - 8:   **else**
  - 9:      $x_u = x_t$ ;  $x^* = x_u$
  - 10:   **end if**
  - 11: **end while**
  - 12: Output  $x^*$
- 

noise power spectral density and  $N_f = 10\text{dB}$  is the noise figure [CGB05]. In all the figures,  $a \times b$  means  $N_t = a$  and  $N_r = b$ .

In Fig. 6.1, we compare the EE performance versus the number of relays. We observe that EE increases as the number of relays increases due to enlarged searching space of the EE optimization problem. It is interesting to see that the EE gain due to the increase of relays becomes less prominent as the number of antenna increases. This is due to the fact that more antennas already improves the diversity gain and the channels for each relay are more 'averaged'. The impact of relay selection on EE is lower when the number of antennas increases.

Fig. 6.2 demonstrates the averaged number of remaining relays at each iteration. We observe that the algorithm stops within about 7 iterations. Moreover, the number of remaining relays significantly decreases after 3 iterations, which reduces the calculation complexity.

In Fig. 6.3, we show the percentage of each relay being selected, where the relays differ in the efficiency of their amplifier. We observe that more antennas results in unevenly distribution of relay selection. As a matter of fact, increasing the number of antennas leads to an optimum EE which is obtained at a higher transmit power value. Consequently, we also have a higher sensitivity to the amplifier efficiency.

In Fig. 6.4, we show the percentage of each relay being selected, where the relays differ in their distance to the source and the destination. The figure shows that every antenna configuration favors the relay nodes at approximately the middle point between the source and the destination. It is interesting to observe that when more antennas are used, this leads to selecting the relays located close to the source. This is because if the average SNR is enhanced, the SNR of the whole system will be more dominated by its backward channel.

## 6.5 Conclusion

In this chapter, we have considered the EE maximization problem for MIMO-relay channels with relay selection. We first implemented Dinkelbach's method to iteratively select the relays. We then derived the closed-form expressions of the precoding matrix at the source and the beamforming matrix at the selected relay using the respective KKT conditions. The optimization of precoder involves two independent Lagrangian multipliers and

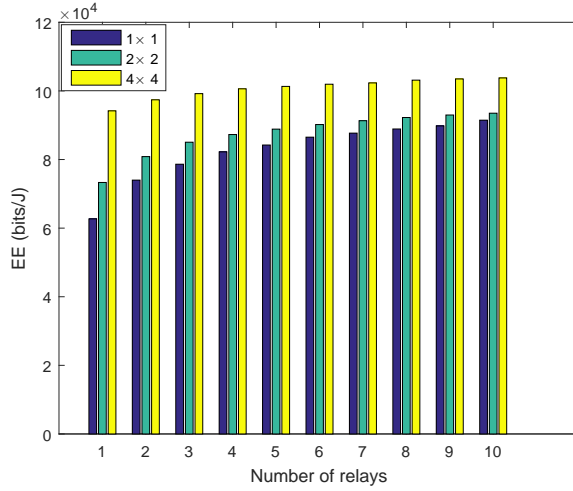


Figure 6.1: EE increases as the number of relays.  $P^S = 2000$  mW and  $P_k^R = 500$  mW.  $D^{SD} = 200 \times M$  mW and  $D_k^R = 100 \times M$  mW.  $\rho_S = 2.5$  and  $\rho_k = 3$ .

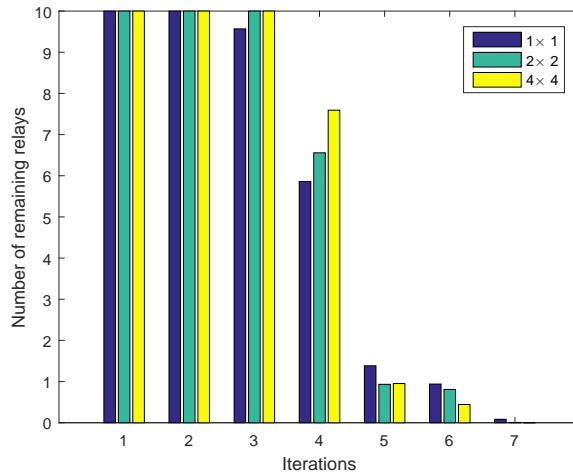


Figure 6.2: Number of remaining relays at each iteration.  $K = 10$ .  $P^S = 2000$  mW and  $P_k^R = 500$  mW.  $D^{SD} = 200 \times M$  mW and  $D_k^R = 100 \times M$  mW.  $\rho_S = 2.5$  and  $\rho_k = 3$ .

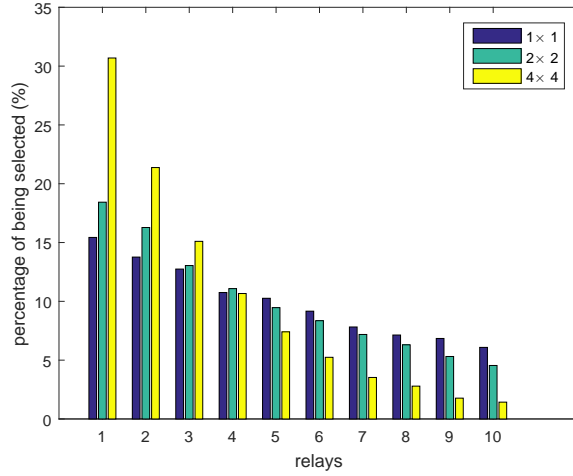


Figure 6.3: Percentage of each relay being selected.  $K = 10$ .  $P^S = 2000$  mW and  $P_k^R = 500$  mW.  $D^{SD} = 200 \times M$  mW and  $D_k^R = 100 \times M$  mW.  $\rho_S = 2.5$  and  $\rho_k = 3 + 0.3(k - 1)$ .

the optimization of the beamforming involves a quadratic equation. Finally, the numerical results demonstrate the impact of relay location, and of the number of antennas and of relays.

## 6.6 Appendix

### 6.6.1 Proof of Theorem 6.1

Assume not all  $\theta_m^{(k)} h_m^{(k)}$  are the same. Then apparently for some  $m$ ,  $q_m^{(k)(1)} \neq q_m^{(k)(2)}$ . Without loss of generality, let us assume that  $q_m^{(k)(1)} \neq q_m^{(k)(2)}$  for all  $m$  except when  $q_m^{(k)(1)} = q_m^{(k)(2)} = 0$ . On the other hand, if  $\alpha_k^{(1)} < \alpha_k^{(2)}$ , then  $\beta_k^{(1)} > \beta_k^{(2)}$ , and if  $\alpha_k^{(1)} > \alpha_k^{(2)}$ , then  $\beta_k^{(1)} < \beta_k^{(2)}$ .

Let us reorder  $\theta_m^{(k)} h_m^{(k)}$  in a descending order, that  $\theta_{\omega_1}^{(k)} h_{\omega_1}^{(k)} \geq \dots \geq$

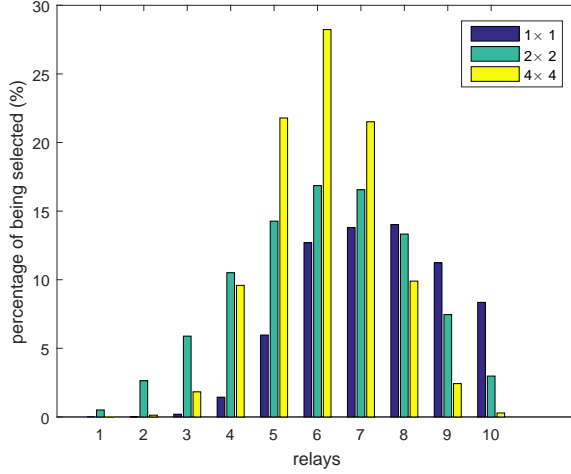


Figure 6.4: Percentage of each relay being selected.  $K = 10$ .  $P^S = 2000$  mW and  $P_k^R = 500$  mW.  $D^{SD} = 200 \times M$  mW and  $D_k^R = 100 \times M$  mW.  $\rho_S = 2.5$  and  $\rho_k = 3$ . Assume the distance between the source and the  $k$ -th relay is  $d_1 = 10 \times k$ (m), and the distance between the  $k$ -th relay and the destination is  $d_2 = 10 \times (11 - k)$ (m).

$\theta_{\omega_M}^{(k)} h_{\omega_M}^{(k)}$ . If  $\alpha_k^{(1)} < \alpha_k^{(2)}$ , then there exist  $M_1$  such that

$$\begin{aligned}
& \left( \alpha_k^{(2)} - \alpha_k^{(1)} \right) \theta_{\omega_1}^{(k)} h_{\omega_1}^{(k)} \geq \dots \geq \left( \alpha_k^{(2)} - \alpha_k^{(1)} \right) \theta_{\omega_{M_1}}^{(k)} h_{\omega_{M_1}}^{(k)} \\
& > \beta_k^{(1)} - \beta_k^{(2)} \\
& > \left( \alpha_k^{(2)} - \alpha_k^{(1)} \right) \theta_{\omega_{M_1+1}}^{(k)} h_{\omega_{M_1+1}}^{(k)} \geq \dots \geq \left( \alpha_k^{(2)} - \alpha_k^{(1)} \right) \theta_{\omega_M}^{(k)} h_{\omega_M}^{(k)}. \quad (6.46)
\end{aligned}$$

Therefore,  $q_{\omega_m}^{(k)(1)} > q_{\omega_m}^{(k)(2)}$  for  $1 \leq m \leq M_1$  and  $q_{\omega_m}^{(k)(1)} < q_{\omega_m}^{(k)(2)}$  for

$M_1 + 1 \leq m \leq M$  except when  $q_{\omega_m}^{(k)(1)} = q_{\omega_m}^{(k)(2)} = 0$ . Then we have

$$\begin{aligned}
& \sum_{m=1}^M q_{\omega_m}^{(k)(1)} \theta_{\omega_m}^{(k)} h_{\omega_m}^{(k)} \\
& > \sum_{m=1}^{M_1} q_{\omega_m}^{(k)(2)} \theta_{\omega_m}^{(k)} h_{\omega_m}^{(k)} + \left( \sum_{m=1}^{M_1} \left( q_{\omega_m}^{(k)(1)} - q_{\omega_m}^{(k)(2)} \right) \right) \theta_{\omega_{M_1}}^{(k)} h_{\omega_{M_1}}^{(k)} \\
& + \sum_{m=M_1+1}^M q_{\omega_m}^{(k)(1)} \theta_{\omega_m}^{(k)} h_{\omega_m}^{(k)} \\
& > \sum_{m=1}^{M_1} q_{\omega_m}^{(k)(2)} \theta_{\omega_m}^{(k)} h_{\omega_m}^{(k)} + \left( \sum_{m=M_1+1}^M \left( q_{\omega_m}^{(k)(2)} - q_{\omega_m}^{(k)(1)} \right) \right) \theta_{\omega_{M_1+1}}^{(k)} h_{\omega_{M_1+1}}^{(k)} \\
& + \sum_{m=M_1+1}^M q_{\omega_m}^{(k)(1)} \theta_{\omega_m}^{(k)} h_{\omega_m}^{(k)} > \sum_{m=1}^M q_{\omega_m}^{(k)(2)} \theta_{\omega_m}^{(k)} h_{\omega_m}^{(k)} \tag{6.47}
\end{aligned}$$

Thus we have

$$\sum_{m=1}^M \theta_m^{(k)} (h_m^{(k)} q_m^{(k)(1)} + \sigma^2) > \sum_{m=1}^M \theta_m^{(k)} (h_m^{(k)} q_m^{(k)(2)} + \sigma^2). \tag{6.48}$$

Similarly, if  $\alpha_k^{(1)} > \alpha_k^{(2)}$ , we have

$$\sum_{m=1}^M \theta_m^{(k)} (h_m^{(k)} q_m^{(k)(1)} + \sigma^2) < \sum_{m=1}^M \theta_m^{(k)} (h_m^{(k)} q_m^{(k)(2)} + \sigma^2). \tag{6.49}$$

## 6.6.2 Proof of Theorem 6.2

If  $\beta_k^{(1)} < \beta_k^{(2)}$ , then there exist  $M_2$  such that

$$\begin{aligned}
& \left( \alpha_k^{(1)} - \alpha_k^{(2)} \right) \theta_{\omega_1}^{(k)} h_{\omega_1}^{(k)} \geq \dots \geq \left( \alpha_k^{(1)} - \alpha_k^{(2)} \right) \theta_{\omega_{M_2}}^{(k)} h_{\omega_{M_2}}^{(k)} \\
& > \beta_k^{(2)} - \beta_k^{(1)} \\
& > \left( \alpha_k^{(1)} - \alpha_k^{(2)} \right) \theta_{\omega_{M_2+1}}^{(k)} h_{\omega_{M_2+1}}^{(k)} \geq \dots \geq \left( \alpha_k^{(1)} - \alpha_k^{(2)} \right) \theta_{\omega_M}^{(k)} h_{\omega_M}^{(k)}. \tag{6.50}
\end{aligned}$$

Therefore,  $q_{\omega_m}^{(k)(1)} < q_{\omega_m}^{(k)(2)}$  for  $1 \leq m \leq M_2$  and  $q_{\omega_m}^{(k)(1)} > q_{\omega_m}^{(k)(2)}$  for  $M_2 + 1 \leq m \leq M$ , which is equivalent to  $q_{\omega_m}^{(k)(1)} \theta_{\omega_m}^{(k)} h_{\omega_m}^{(k)} < q_{\omega_m}^{(k)(2)} \theta_{\omega_m}^{(k)} h_{\omega_m}^{(k)}$  for  $1 \leq m \leq M_2$  and  $q_{\omega_m}^{(k)(1)} \theta_{\omega_m}^{(k)} h_{\omega_m}^{(k)} > q_{\omega_m}^{(k)(2)} \theta_{\omega_m}^{(k)} h_{\omega_m}^{(k)}$  for  $M_2 + 1 \leq m \leq M$ . Then we have...

# Chapter 7

## RA and SP in Relay-Assisted OFDMA Downlink Systems

### 7.1 Related works and chapter review

In this chapter, we consider EE maximization in single-relay multi-user systems with OFDMA and the AF technique. A number of papers have already investigated EE in scenarios with assisting relays. AF relaying was considered in papers [CYH14, CYH13, BAH<sup>+</sup>15, XLL15, CFH14]. Papers [CYH14, CYH13] have studied EE maximization in multi-relay downlink systems. The authors of [BAH<sup>+</sup>15] maximized the worst EE among all users of an uplink under individual power constraints. EE maximization was also studied in [XLL15] for two-way relay channels. In [CFH14], EE was optimized by the proper selection of the modulation level out of a discrete set. While all these contributions assume multicarrier modulation, none of them has considered SP at the relay. Optimized SP leads to stronger link combinations and therefore a higher rate [WGLV13]. Paper [LMB14] has studied the joint problem of SP and allocation for an AF downlink system, but with a total power constraint across the base station and the relay. Moreover, an approximated SNR expression was used in [LMB14] for high SNR as in [CYH13]. Paper [SNN<sup>+</sup>16] considered decode-and-forward (DF) relaying with SP but also with a total power constraint.

We optimize the exact value of EE instead of an approximated value for high SNR in this work. Individual power constraints at the base station and

the relay node are considered which is of more practical significance. The problem is solved in an alternating way by means of an iterative algorithm and within only a few iterations. To the best of our knowledge, no work has studied this alternating SP method for maximizing EE. Thanks to the discontinuous quasi-concavity of the obtained EE function of each subproblem, the optimal EE value of each iteration is guaranteed and is obtained by a one-dimension search with bisection method. Different from the problem with total power constraint, where the rate function has to be approximated to be concave, the problem with individual power constraints can be solved by using the exact rate expression. Numerical results show that the proposed algorithm outperforms two benchmarks, especially at low SNR. A first one is based on the approximation of the rate function. Concerning the second one, for both hops the carriers are first sorted according to a gain decreasing order. Then sorted subcarrier  $k$  of the first hop is paired with sorted subcarrier  $k$  in the second hop.

Perfect CSI is assumed in this chapter as in [LMB14]. An extension to robust precoder designs considering imperfect CSI can be easily obtained by adding an additional term in the power of noise associated with the gap between real CSI and CSI estimation [BV12]. However, this is beyond the scope of this chapter. The focus of this chapter is on perfect CSI systems which provide an upper bound on the performance achievable in practice.

## 7.2 System Model and Problem Formulation

### 7.2.1 System model

Consider an OFDMA downlink system with a single cell equipped with one base station, one AF relay and a total of  $K$  subcarriers to be allocated to  $N$  users. The relay is assumed to be half-duplex and the transmission is divided to two time slots. The relay receives the signal from the base station in the first time slot and broadcasts an amplified signal to all users in the second time slot. Each subcarrier is allocated to one user at maximum in the second time slot. Therefore, there is no interference among different users at each subcarrier. We assume that perfect CSI is available at all transmission nodes and all nodes are equipped with a single antenna. During the transmission,

slow fading is assumed so that within the two time slots the channel remains invariant. Direct link is ignored due to severe fading.

In cellular networks, the base station and the relay node have individual power constraints. We assume that their power constraints are  $P_s$  and  $P_r$  respectively in this chapter.

In the first time slot, at the subcarrier  $i$ , the signal received at the relay is given by  $r_i = h_i s_i + n_i^R$ , where  $s_i$  is the source symbol with  $\mathbb{E}\{s_i s_i^*\} = p_i$ ,  $h_i$  denotes the channel gain at the  $i$ -th subcarrier, and  $n_i^R$  is the noise with  $\mathbb{E}\{n_i^R n_i^{R*}\} = \sigma^2$ . In the second time slot, the relay transmits over carrier  $j$  the value  $r_i$  amplified to  $a_{i,j} r_i$ . It is subsequently received by user  $n$  as  $y_{i,j,n} = g_{j,n} a_{i,j} r_i + n_{j,n}^D$ , where  $\mathbb{E}\{a_{i,j}^2 r_i r_i^*\} = q_{i,j}$  is the transmission power at subcarrier  $j$  in the second time slot if it is paired with subcarrier  $i$  in the first time slot,  $g_{j,n}$  denotes the channel gain between the relay and user  $n$  at subcarrier  $j$ , and  $n_{j,n}^D$  is the noise with  $\mathbb{E}\{n_{j,n}^D n_{j,n}^{D*}\} = \sigma^2$ . Here we assume the noise power at the relay and at each user is the same without loss of generality. Since each subcarrier in the second time slot is paired with a unique subcarrier in the first time slot, we will remove the subscript  $i$  and denote  $q_{i,j}$  as  $q_j$  hereafter. Thus, the signal-to-noise ratio (SNR) of the link from the subcarrier  $i$  at the first time slot to the subcarrier  $j$  which is allocated to user  $n$  at the second time slot is

$$\gamma_{i,j,n} = \frac{p_i |h_i|^2 q_j |g_{j,n}|^2}{\sigma^2 (\sigma^2 + p_i |h_i|^2 + q_j |g_{j,n}|^2)}. \quad (7.1)$$

## 7.2.2 EE model

The EE of the system is defined as the transmission rate normalized by the power consumption [ICJF12], which is

$$\epsilon = \frac{\frac{1}{2} \sum_{i=1}^K \sum_{j=1}^K \sum_{n=1}^N \alpha_{i,j,n} \cdot w(n) \cdot \log(1 + \gamma_{i,j,n})}{\phi_S \sum_{i=1}^K p_i + \phi_R \sum_{j=1}^K q_j + P_C}, \quad (7.2)$$

where  $\alpha_{i,j,n} = 1$  if subcarrier  $j$  at the second time slot is paired with subcarrier  $i$  at the first time slot and is allocated to user  $n$ , otherwise  $\alpha_{i,j,n} = 0$ ;  $\phi_S$  and  $\phi_R$  are respectively the inverse of the efficiency of the HPA of the base station and the relay,  $P_C$  denotes the sum of the constant circuit power of all nodes,  $w(n)$  is the rate weight for user  $n$ , which provides different priorities

for each user. The penalty term  $\frac{1}{2}$  is due to the fact that the total transmission takes two time slots.

### 7.2.3 Problem formulation

The EE problem is formulated as maximizing the EE of the system with individual source and relay power constraints, that is,

$$\max_{\{p_i\}, \{q_j\}, \{\alpha_{i,j,n}\} \in \{0,1\}} \epsilon \quad (7.3)$$

$$s.t. \quad \sum_{i=1}^K p_i \leq P_s \quad (7.4)$$

$$\sum_{j=1}^K q_j \leq P_r \quad (7.5)$$

$$\sum_{j=1}^K \sum_{n=1}^N \alpha_{i,j,n} = 1 \quad i \in \{1, \dots, K\} \quad (7.6)$$

$$\sum_{i=1}^K \sum_{n=1}^N \alpha_{i,j,n} = 1 \quad j \in \{1, \dots, K\}, \quad (7.7)$$

where (7.6) and (7.7) imply that there exists a one-to-one mapping between subcarriers in the first time slot and in the second time slot, and paired subcarriers are allocated to unique user.

## 7.3 Theoretical Analysis and Algorithm

In this section, we will first analyze the original problem and then solve it in an alternating manner. An algorithm will be provided following the analysis.

Even if there is no SP nor subcarrier allocation, i.e.  $\{\alpha_{i,j,n}\}$  are fixed,  $\epsilon$  in (7.2) is neither concave nor quasi-concave w.r.t  $\mathbf{p} = [p_1, \dots, p_K]^T$  and  $\mathbf{q} = [q_1, \dots, q_K]^T$  [ZCJ14a]. However, for fixed  $\{\alpha_{i,j,n}\}$ ,  $\epsilon$  in (7.2) is concave w.r.t.  $\mathbf{p}$  for given  $\mathbf{q}$  and concave w.r.t.  $\mathbf{q}$  for given  $\mathbf{p}$  [HW07]. Because

problem (7.3) has two individual power constraints, it has been decided to solve it in an alternating manner in the sequel (see Algorithm 7.1).

One iteration is defined as the optimization over  $\mathbf{q}$ ,  $\{\alpha_{i,j,n}\}$  for given  $\mathbf{p}$  or over  $\mathbf{p}$ ,  $\{\alpha_{i,j,n}\}$  for given  $\mathbf{q}$ . In every iteration, SP, subcarrier allocation, and power allocation are jointly optimized. It is notable that the optimizations over  $\mathbf{q}$ ,  $\{\alpha_{i,j,n}\}$  for given  $\mathbf{p}$  or over  $\mathbf{p}$ ,  $\{\alpha_{i,j,n}\}$  for given  $\mathbf{q}$  are symmetric. This is because, in the optimization of the first time slot, the subcarrier allocation can also be optimized. This is confirmed by observing that  $\mathbf{p}$  and  $\mathbf{q}$  are symmetric in the SNR function in (7.1). Therefore we only discuss the optimization over  $\mathbf{q}$ ,  $\{\alpha_{i,j,n}\}$  for a given  $\mathbf{p}$ , that is to say, the RA and SP in the second time slot given a fixed power allocation at the source.

### 7.3.1 Optimize $\mathbf{q}$ , $\{\alpha_{i,j,n}\}$ for given $\mathbf{p}$

In each odd numbered iteration,  $\mathbf{q}$  and  $\{\alpha_{i,j,n}\}$  are optimized for a given  $\mathbf{p}$ . Each sub-problem is a mixed-integer nonlinear programming (MINLP). The optimal solution is to exhaustively search all combinations of subcarrier allocation and pairing, which is not practical in real-time transmission when  $K$  is large (for example, there are 1200 subcarriers within a bandwidth of 20MHz in the LTE standard [Zyr07]).

Therefore we will first relax the integer constraints to obtain a criterion for subcarrier allocation. Different from [LMB14], we take derivative to the relaxed time sharing variable, which gives a condition for subcarrier allocation that allows us to implement a one-dimension bisection search to maximize the obtained EE function. Then we will see that the Hungarian algorithm can be implemented to the result of subcarrier allocation for SP.

For time sharing, we introduce the duration  $\rho_{i,j,n}$ , which is the time fraction during which the subcarrier  $j$  in the second time slot is paired with the subcarrier  $i$  in the first time slot and allocated to user  $n$ . Denote  $\hat{q}_{i,j,n}$  as the total transmit power at the relay during the time fraction  $\rho_{i,j,n}$ . Then the EE function in (7.2) becomes [WV17]:

$$\epsilon = \frac{\frac{1}{2} \sum_{i=1}^K \sum_{j=1}^K \sum_{n=1}^N \rho_{i,j,n} w(n) R_{i,j,n}}{\phi_S \sum_{i=1}^K p_i + \phi_R \sum_{i=1}^K \sum_{j=1}^K \sum_{n=1}^N \rho_{i,j,n} Q_{i,j,n} + P_C}, \quad (7.8)$$

where  $Q_{i,j,n} = \frac{\hat{q}_{i,j,n}}{\rho_{i,j,n}}$  and

$$R_{i,j,n} = \log \left( 1 + \frac{p_i |h_i|^2 Q_{i,j,n} |g_{j,n}|^2}{\sigma^2 (\sigma^2 + p_i |h_i|^2 + Q_{i,j,n} |g_{j,n}|^2)} \right). \quad (7.9)$$

It can be shown that  $\epsilon$  is concave w.r.t.  $\rho_{i,j,n}$  and  $\hat{q}_{i,j,n}$  [BV04]. For each pair  $(i, j)$ , define  $\sum_{n=1}^N \rho_{i,j,n} = \Sigma_{i,j}$ . Then we have  $0 \leq \rho_{i,j,n} \leq \Sigma_{i,j}$ .

Similar with [WV17], checking the KKT condition of  $\epsilon$  is equivalent to checking the KKT condition of its numerator. Thus, by checking the KKT condition w.r.t  $\rho_{i^*,j^*,n^*}$  for  $0 \leq \rho_{i^*,j^*,n^*} \leq \Sigma_{i,j}$ , we have

$$\begin{aligned} & \frac{1}{2} \frac{\partial \sum_{i,j=1}^K \sum_{n=1}^N \rho_{i,j,n} w(n) R_{i,j,n}}{\partial \rho_{i^*,j^*,n^*}} \\ &= \frac{1}{2} w(n^*) \left( R_{i^*,j^*,n^*} - \rho_{i^*,j^*,n^*} \frac{\hat{q}_{i^*,j^*,n^*}}{\rho_{i^*,j^*,n^*}^2} \frac{\partial R_{i^*,j^*,n^*}}{\partial Q_{i^*,j^*,n^*}} \right) \\ &= f_{i^*,j^*,n^*}'(Q_{i^*,j^*,n^*}) - Q_{i^*,j^*,n^*} f_{i^*,j^*,n^*}'(Q_{i^*,j^*,n^*}) \\ &= \beta_{i^*,j^*,n^*} - \gamma_{i^*,j^*,n^*}, \end{aligned} \quad (7.10)$$

where  $\beta_{i^*,j^*,n^*} > 0$  if  $\rho_{i^*,j^*,n^*} = \Sigma_{i,j}$  and  $\beta_{i^*,j^*,n^*} = 0$  if  $\rho_{i^*,j^*,n^*} < \Sigma_{i,j}$ ,  $\gamma_{i^*,j^*,n^*} > 0$  if  $\rho_{i^*,j^*,n^*} = 0$  and  $\gamma_{i^*,j^*,n^*} = 0$  if  $\rho_{i^*,j^*,n^*} > 0$ , and

$$f_{i^*,j^*,n^*}(x) \triangleq \frac{1}{2} w(n^*) R_{i^*,j^*,n^*}, \quad (7.11)$$

where its derivative is w.r.t  $Q_{i^*,j^*,n^*}$ . By checking the KKT condition for  $\hat{q}_{i^*,j^*,n^*} > 0$ , we have

$$\begin{aligned} & \frac{1}{2} \frac{\partial \sum_{i,j=1}^K \sum_{n=1}^N \rho_{i,j,n} w(n) R_{i,j,n}}{\partial p_{i^*,j^*,n^*}} = \frac{1}{2} w(n^*) \rho_{i^*,j^*,n^*} \frac{\partial R_{i^*,j^*,n^*}}{\partial Q_{i^*,j^*,n^*}} \frac{\partial Q_{i^*,j^*,n^*}}{\partial p_{i^*,j^*,n^*}} \\ &= f_{i^*,j^*,n^*}'(Q_{i^*,j^*,n^*}) \triangleq \lambda. \end{aligned} \quad (7.12)$$

Similar with [LCL<sup>+</sup>07, WV17], each potential subcarrier pair  $(i, j)$  is allocated to the user  $n(i, j)$  such that

$$n(i, j) = \arg \max_n \left[ \Omega(i, j, n) = f_{i,j,n}(Q_{i,j,n}) - Q_{i,j,n} f_{i,j,n}'(Q_{i,j,n}) \right]. \quad (7.13)$$

Let us define a cost matrix  $\mathbf{A}$  by

$$\mathbf{A}_{(i,j)} = \max_n \Omega(i, j, n). \quad (7.14)$$

So far, we have allocated each subcarrier pair  $(i, j)$  to a certain user to maximize the EE (also the rate) for a given  $\lambda$ . That is, for a given  $\lambda$ ,  $f_{i,j,n}$  for each  $(i, j, n)$  can be calculated by using (7.12). For a given  $\lambda$ , we need to find the corresponding  $Q_{i,j,n}$  such that  $f'_{i,j,n}(Q_{i,j,n}) = \lambda$ . This can be obtained thanks to the following formula.

Define  $d(x) \triangleq w \log \left(1 + \frac{ax}{bx+c}\right)$ . Then

$$d'(x) = \frac{1}{\ln 2} \frac{wac}{((a+b)x+c)(bx+c)}. \quad (7.15)$$

If  $x \geq 0$ , then we have  $d'(x) \leq d'(0) = \frac{wa}{c \ln 2}$  and

$$x = \frac{\sqrt{a^2c^2 + \frac{4wabc(a+b)}{\ln 2 \cdot d'(x)}} - c(a+2b)}{2b(a+b)}. \quad (7.16)$$

For each  $(i, j, n)$ , define

$$w(i, j, n) = \frac{1}{2}w(n) \quad (7.17)$$

$$a(i, j, n) = p_i |h_i|^2 |g_{j,n}|^2 \quad (7.18)$$

$$b(i, j, n) = |g_{j,n}|^2 \sigma^2 \quad (7.19)$$

$$c(i, j, n) = (p_i |h_i|^2 + \sigma^2) \sigma^2. \quad (7.20)$$

By substituting  $w = w(i, j, n)$ ,  $a = a(i, j, n)$ ,  $b = b(i, j, n)$ ,  $c = c(i, j, n)$ , and  $d'(x) = \lambda$  into (7.16), the values of  $Q_{i,j,n}(=x)$  and  $f_{i,j,n}(Q_{i,j,n})$  can be obtained.

Then  $\Omega(i, j, n)$  are calculated and finally the matrix  $\mathbf{A}$  is obtained by using (7.14).

Performing SP consists in selecting  $K$  elements from the cost matrix  $\mathbf{A}$  such that every row or column has one and only one selected element. This can be realized by using the Hungarian algorithm [Kuh55].

After generating matrix  $A$  and selecting  $K$  elements, for each  $\lambda$ , we have maximized

$$\sum_{i=1}^K \sum_{j=1}^K \sum_{n=1}^N [f_{i,j,n}(Q_{i,j,n}(\lambda)) - \lambda Q_{i,j,n}(\lambda)] = R_{\text{sum}}(\lambda) - \lambda q_{\text{sum}}(\lambda), \quad (7.21)$$

where

$$q_{\text{sum}}(\lambda) \triangleq |\mathbf{q}(\lambda)|_1 = \sum_{i=1}^K \sum_{j=1}^K \sum_{n=1}^N Q_{i,j,n}(\lambda), \quad (7.22)$$

and

$$R_{\text{sum}}(\lambda) = \sum_{i=1}^K \sum_{j=1}^K \sum_{n=1}^N f_{i,j,n}(Q_{i,j,n}(\lambda)). \quad (7.23)$$

The values of  $R_{\text{sum}}(\lambda)$  and  $q_{\text{sum}}(\lambda)$  have been obtained. As analyzed in [WV17], the obtained rate function w.r.t. transmit power at the relay

$$\tilde{R}_{\text{sum}}(q_{\text{sum}}) = R_{\text{sum}}(q_{\text{sum}}^{-1}(\lambda)) \quad (7.24)$$

is a concave function of  $q_{\text{sum}}$  (with discontinuity as discussed in [WV17]), and  $\tilde{R}_{\text{sum}}(q_{\text{sum}})$  is maximized for each obtained  $q_{\text{sum}}$ . Hence the obtained EE function is a quasi-concave function of  $q_{\text{sum}}$ :

$$\text{EE}(q_{\text{sum}}) = \frac{\tilde{R}_{\text{sum}}(q_{\text{sum}})}{\phi_S \sum_{i=1}^K p_i + \phi_R q_{\text{sum}} + P_C}. \quad (7.25)$$

One-dimension bisection method can find the maximum of  $\text{EE}(q_{\text{sum}})$  by checking  $\text{EE}'(q_{\text{sum}})$ . The details of the algorithm in Algorithm 7.2 are provided in Subsection C.

### 7.3.2 Optimize $\mathbf{p}$ , $\{\alpha_{i,j,n}\}$ for given $\mathbf{q}$

In each even numbered iteration,  $\mathbf{p}$  and  $\{\alpha_{i,j,n}\}$  are optimized for a given  $\mathbf{q}$ . It is exactly the same optimization as in the previous subsection; therefore

Table 7.1: Complexity comparison.

Operations	EEPA	RPA	EEA	EE	AEE	FP
SP	L	L	0	0	L	1
SA	L	L	L	0	L	L
PAI	L	L	L	L	L	L
PAd	L	0	L	L	L	L

we will omit the analysis and only give the necessary values to be used:

$$w'(i, j, n) = \frac{1}{2}w(n) \quad (7.26)$$

$$a'(i, j, n) = q_j |h_i|^2 |g_{j,n}|^2 \quad (7.27)$$

$$b'(i, j, n) = |h_i|^2 \sigma^2 \quad (7.28)$$

$$c'(i, j, n) = (q_j |g_{j,n}|^2 + \sigma^2) \sigma^2. \quad (7.29)$$

Algorithm 3 will show the details for this part.

### 7.3.3 Algorithm

In the algorithm, we first initialize the power at the base station by uniform allocation to the subcarriers. Then the algorithm operates iteratively until convergence. Given the power allocation at the base station, we jointly optimize the power allocation at the relay, the subcarrier allocation, and the SP. The power allocation at the base station, the subcarrier allocation, and SP will be optimized using the obtained power allocation at the relay. Therefore, Algorithm 7.1 operates in an alternating manner: the transmission time slot  $T_s$  changes between 1 and 2 alternatingly. Since the EE function is discontinuous quasi-concave at each iteration, EE is maximized by forcing the derivative to be zero. The EE value will converge since it increases at each iteration and it is upper bounded.

## 7.4 Complexity Comparison

In this section, various schemes of RA and SP are compared in terms of complexity. The EE performance of these schemes will be compared in the

---

**Algorithm 7.1:** An alternating method for EE maximization

---

- 1: Initialization: Assume  $\mathbf{p} = P_s/K \times [1, \dots, 1]^T$ ,  $l = 0$ ,  $\epsilon^{(0)} = 0$ ,  $\Delta\epsilon = 1$ ,  $T_s = 2$
  - 2: **while**  $\Delta\epsilon > \delta_\epsilon$  **do**
  - 3:   **if**  $T_s = 2$  **then**
  - 4:      $l = l + 1$ ; Go to Algorithm 2
  - 5:      $\Delta\epsilon = \frac{\epsilon^{(l)} - \epsilon^{(l-1)}}{\epsilon^{(l)}}$ ;  $T_s = 1$
  - 6:   **else**
  - 7:      $l = l + 1$ ; Go to Algorithm 3
  - 8:      $\Delta\epsilon = \frac{\epsilon^{(l)} - \epsilon^{(l-1)}}{\epsilon^{(l)}}$ ;  $T_s = 2$
  - 9:   **end if**
  - 10: **end while**
- 

---

**Algorithm 7.2:** Optimize  $\mathbf{q}$  for given  $\mathbf{p}$ 

---

- 1: For each  $(i, j, n)$ , calculate  $w(i, j, n)$ ,  $a(i, j, n)$ ,  $b(i, j, n)$ ,  $c(i, j, n)$  in the function  $f(x)$  using (7.17),(7.18),(7.19),(7.20)
  - 2:  $\lambda_{\max} = \max\{\frac{a(i,j,n)}{\ln 2 \cdot c(i,j,n)}\}$ ,  $\lambda_{\min} = 0$
  - 3: **while**  $\lambda_{\max} - \lambda_{\min} > \Delta\lambda$  **do**
  - 4:    $\lambda = \frac{\lambda_{\min} + \lambda_{\max}}{2}$
  - 5:   For each  $(i, j, n)$ , calculate  $Q(i, j, n) = x$  using (7.16) by substituting  $w(i, j, n)$ ,  $a(i, j, n)$ ,  $b(i, j, n)$ ,  $c(i, j, n)$  and  $\lambda$  into  $w$ ,  $a$ ,  $b$ ,  $c$  and  $d'(x)$ ; obtain  $f_{i,j,n}(Q(i, j, n))$ ; calculate  $\Omega(i, j, n)$  in (7.10)
  - 6:   For each  $(i, j)$ , calculate  $A(i, j)$
  - 7:   Find SP in  $A$  using Hungarian algorithm
  - 8:   Calculate  $q_{\text{sum}}(\lambda)$  and  $R_{\text{sum}}(\lambda)$
  - 9:   **if**  $\lambda(\phi_S|\mathbf{p}|_1 + \phi_R q_{\text{sum}}(\lambda) + P_C) - \phi_R R_{\text{sum}}(\lambda) > 0$  and  $q_{\text{sum}}(\lambda) \leq P_r$  **then**
  - 10:      $\lambda_{\max} = \lambda$
  - 11:   **else**
  - 12:      $\lambda_{\min} = \lambda$
  - 13:   **end if**
  - 14: **end while**
  - 15: Output  $\mathbf{q}^* = \mathbf{q}(\lambda)$
-

---

**Algorithm 7.3:** Optimize  $\mathbf{p}$  for given  $\mathbf{q}$ 


---

- 1: For each  $(i, j, n)$ , calculate  $w'(i, j, n)$ ,  $a'(i, j, n)$ ,  $b'(i, j, n)$ ,  $c'(i, j, n)$  in the function  $f(x)$  using (7.26),(7.27),(7.28),(7.29)
  - 2:  $\lambda_{\max} = \max\left\{\frac{a(i,j,n)}{\ln 2 \cdot c(i,j,n)}\right\}$ ,  $\lambda_{\min} = 0$
  - 3:  $w(i, j, n) = w'(i, j, n)$ ;  $a(i, j, n) = a'(i, j, n)$ ;  $b(i, j, n) = b'(i, j, n)$ ;  $c(i, j, n) = c'(i, j, n)$
  - 4: Implement line 3 to line 15 in Algorithm 2 until  $\mathbf{q}^*$  is found
  - 5:  $\mathbf{p}^* = \mathbf{q}^*$
- 

section dealing with numerical results. In Table 7.1, the complexity of the proposed algorithm is compared with other algorithms which are explicitly described as follows.

- EEPA: the proposed method;
- RPA: rate maximization with both SP and allocation;
- EEA: EE maximization with only subcarrier allocation;
- EE: EE maximization without SP nor allocation;
- AEE (benchmark 1): the proposed method but using approximated rate function as in [LMB14];
- FP (benchmark 2): a fixed pairing after per-hop decreasing gain ordering of the subcarriers.

In Table 7.1,  $L$  is the number of iterations, which is mostly from 3 to 6 depending on system parameters such as SNR, power constraint, and constant circuit power. SP denotes SP, SA denotes subcarrier allocation, PAI denotes power allocation, and PAd denotes power adaptation. Please note that power allocation is implemented in all schemes since the focus of this chapter is to study the advantage of SP and allocation. Power adaptation means the total power changes with the instantaneous CSI for EE maximization, instead of keeping the same as for rate maximization. We take it into account in the table because power adaptation involves more manipulation for finding  $\lambda$  in Algorithms 7.2 and 7.3 to make the derivative of EE expression to be

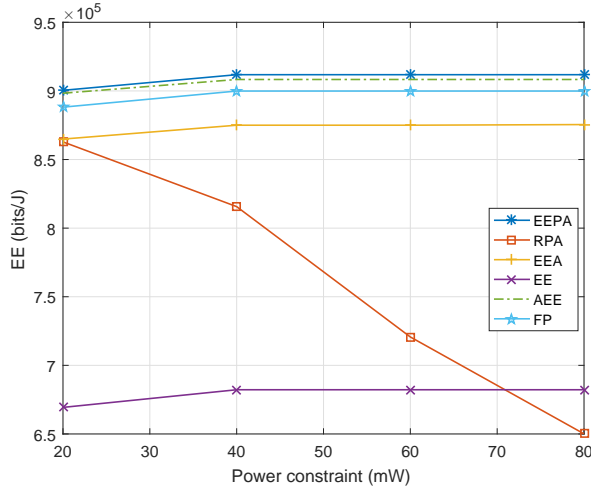


Figure 7.1: EE performances versus power constraints.  $d_1 = d_2 = 10\text{m}$ .

zero [LCL<sup>+</sup>07, WV17]. In practical applications, a tradeoff can be considered by referring to Table 7.1 and the numerical results in the next section.

## 7.5 Numerical results

In this section we show the numerical results. The parameters are set as follows:  $K = 16$ ,  $N = 4$ ,  $P_C = 150\text{mW}$ , and the bandwidth for each subcarrier is  $B = 10\text{KHz}$ ,  $\phi_S = \phi_R = 2.5$ ,  $w_1 = w_2 = w_3 = w_4 = 1$ ,  $\delta_\epsilon = 0.01$ ,  $\Delta\lambda = \lambda_{\max}/2^{20}$  for each  $\lambda_{\max}$ . The channels are assumed to be Rayleigh distributed and have an average channel gain  $G_0 d_i^{-n}$  where the pass loss exponent  $n = 4$ ,  $G_0 = -(G_1 M_l) = -70\text{dB}$  in which  $G_1 = 30\text{dB}$  is the gain factor at  $d = 1\text{m}$ .  $M_l = 40\text{dB}$  is the link margin compensating the hardware process variations and other noise and interference, the noise power  $\sigma^2 = BN_0 N_f$  where  $N_0 = -170\text{dBm/Hz}$  is the noise power spectral density and  $N_f = 10\text{dB}$  is the noise figure [CGB05].  $d_1$  is the distance between the base station and the relay and  $d_2$  is the distance between the relay and the users. The results are averaged over 10000 channel realizations.

In all figures, the proposed algorithm is compared with other algorithms listed in Section IV.

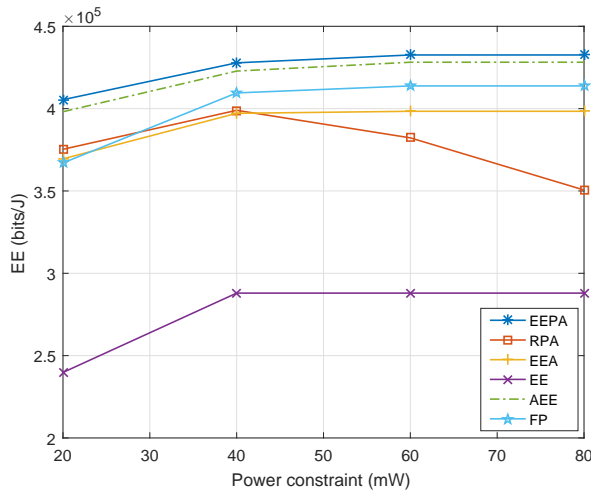


Figure 7.2: EE performances versus power constraints.  $d_1 = d_2 = 15\text{m}$ .

In all figures, we plot the EE performances versus power constraints for various RA strategies. Without loss of generality, we assume  $P_s = P_r$ . From Fig. 7.1 to Fig. 7.4, we set  $d_1 = d_2 = 10, 15, 25, 50\text{m}$  respectively. Therefore these figures correspond to the scenarios from high SNR to low SNR. We observe that EEPA always has the best performance. The EE of RPA even decreases at large power constraint because full available power is always used for rate maximization. AEE has a small gap with EEPA at high SNR but has a huge gap at low SNR. FP also has a small gap with EEPA at high SNR but has a huge gap at low SNR which is consistent with the conclusion in [HW07] that FP is optimal when the power is equally allocated to all subcarriers. In addition, an interesting finding is that the SP needs to be implemented only once to have almost the same performance as with multiple pairing operations. From the mathematical point of view, this is because the dominating entries of the matrix in the Hungarian algorithm always increase with almost the same gain at each iteration.

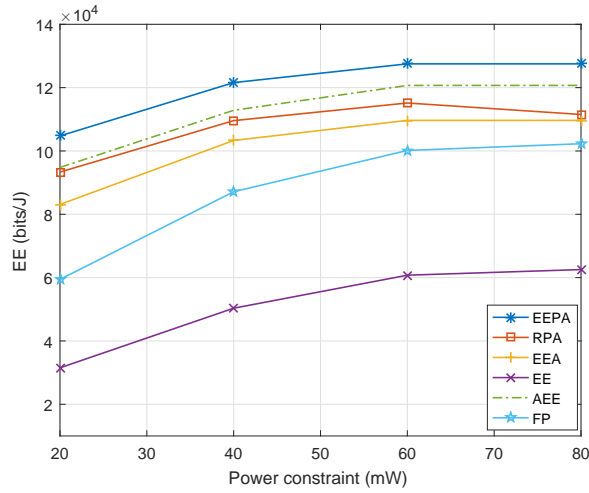


Figure 7.3: EE performances versus power constraints.  $d_1 = d_2 = 25\text{m}$ .

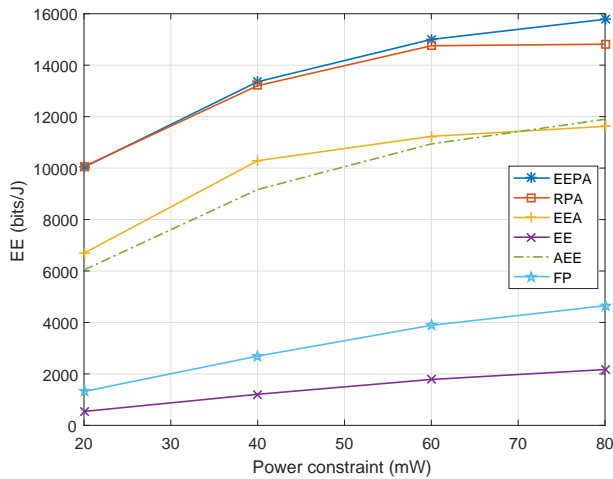


Figure 7.4: EE performances versus power constraints.  $d_1 = d_2 = 50\text{m}$ .

## 7.6 Conclusion

We have solved the EE maximization problem in relay-assisted OFDMA downlink channels using an alternating optimization approach. The RA and

SP are jointly optimized at each iteration under the power constraints of the source and the relay respectively. The method based on the approximated rate value and the one pairing subcarriers at identical positions after sorting, perform similarly to our proposed algorithm at high SNR, but they perform worse than ours at low SNR.



# Chapter 8

## Conclusions and perspectives for future works

In this chapter, we summarize the contributions of this thesis and provide some idea about future work.

### 8.1 Summary of contributions

In this thesis, we have studied EE maximized RA problems in various wireless communication systems.

In Chapter 2, some basic preliminaries and mathematical backgrounds were provided.

In Chapter 3, we studied the energy efficient design of precoders for point-to-point MIMO-OFDM systems. While most contributions focus on a constant circuit power, we showed that for the total power made of a constant term plus another one that is increasing and convex with the transmission rate, the consumed energy per bit is a quasi-convex function of the total transmission rate. Therefore, the problem of minimizing the consumed energy per bit, instead of maximizing its inverse, can be reformulated as a convex fractional program and solved by means of a simple bisection algorithm. The effects of various system parameters on the optimal value of the objective function have been analyzed, which provided a deeper insight for the system design.

In Chapter 4, we took into consideration an aspect often overlooked which is the nonlinearity associated with the HPA. Therefore, the optimal design of MIMO precoders has been studied for OFDM systems in the presence of nonlinear distortions due to the HPA. In traditional approaches, the designer lets the IBO of the HPA be large enough to neglect the unavoidable nonlinear effects of the amplifier. However, this hypothesis will severely hinder the efficiency of the HPA and, consequently, the global energy efficiency of the link. On the other hand, making full use of the available power gives rise to unbearable nonlinear effects with consequent strong rate degradations. We took advantage of the Bussgang theorem to unveil the impact of the nonlinear distortion noise on the optimal precoding and to derive a power allocation algorithm that achieves the optimal tradeoff between HPA efficiency and rate degradation. We also provided a sufficient condition for the concavity of the information rate objective function in this nonlinear scenario, which may help future research on concavity with similar considerations. Finally, numerical results showed that the proposed algorithm adapting IBO to the instantaneous CSI outperforms conventional fixed-IBO precoding strategies.

In Chapter 5, we studied the subcarrier allocation and precoder design problem for downlink MIMO-OFDMA systems to maximize the EE of the system. The time-sharing method was used to allocate each subcarrier to one user. We found that there exist gaps along the direction of total transmit power when the user selection switches for each subcarrier, which leads to a discontinuous EE function, for which quasi-concavity has to be checked. We first showed that the sufficient conditions obtained for the subcarrier allocation approach are the optimal ones among all possibilities with the same transmit power. Then we showed that the proposed subcarrier allocation results in a discontinuous and quasi-concave EE function. These findings are quite fundamental and are essential to the convergence of the related algorithms and the global optimality of the solution. An upper bound of the EE function was given when the solution cannot be found by the proposed sufficient conditions. Finally, we proposed an algorithm to find the maximal EE and its performance is illustrated by means of numerical results.

In Chapter 6, we considered MIMO-relay channels with relay selection and individual power constraints for each node. We implemented Dinkelbach's method for the whole system to iteratively select the relays, which

used fewer iterations than calculating the EE for each relay. Closed-form expressions of the precoding matrix at the source and the beamforming matrix at the selected relay are obtained thanks to the concavity of the objective function. We also gave the mathematical property of monotonicity which guarantees that the values of Lagrangian multipliers can always be found. Finally, the numerical results illustrated the performance gain of multiple relay.

In Chapter 7, we studied the EE maximization problem in AF relay-assisted downlink channels with OFDMA. The power allocation was optimized together with subcarrier allocation (SA) and subcarrier pairing (SP) at the relay. An alternating optimization approach was adopted to solve the problem. Numerical results showed that the proposed algorithm outperforms other benchmark schemes in terms of EE. Especially, implementing SP outperforms the predetermined fixed SP and the random SP.

## 8.2 Future work

In this section, some new directions are provided to extend the scope of this thesis.

- In Chapter 3, the impact of number of active antennas on EE were given by numerical results. In the future, analytical investigation could be carried out.
- In Chapter 4, the condition for the Hessian matrix to be negative semidefinite was given by a bound that is not quite tight. In the future, a tighter bound would be a more substantial contribution.
- In Chapter 5, each subcarrier was allocated to a unique user, therefore there exists no cochannel interference (CCI). In the future, the precoder design considering CCI would be more interesting.
- In Chapter 6, and in Chapter 7, relay-assisted networks often involve a great number of transmission nodes, making the assumption of perfect CSI at the base station too optimistic. In the future, robust design considering imperfect CSI would lead to more relevance.



# Chapter 9

## Bibliography

- [ASG13] P. Assimakopoulos, R. Santamaria, and N. J. Gomes, “EVM and SER performance of OFDM signals with different IFFT sizes under nonlinear distortion,” *Proc. IEEE ICC’ 09*, pp. 848-852, 9-13 Jun. 2013.
  
- [BAH<sup>+</sup>15] E. Bedeer, A. Alorainy, Md. J. Hossain, O. Amin and M. Alouini, “Fairness-Aware Energy-Efficient Resource Allocation for AF Co-Operative OFDMA Networks,” *IEEE Journal on Selected Areas in Communications*, vol. 33, no. 12, pp. 2478-2493, Dec. 2015.
  
- [BL11] E. V. Belmega, and S. Lasaulce, “Energy-efficient precoding for multiple-antenna terminals,” *IEEE Trans. Sig. Process.*, vol. 59, no. 1, pp. 329-340, Jan. 2011.
  
- [BV04] S. Boyd and L. Vandenberghe, “Convex Optimization,” *Cambridge University Press*, 2004.
  
- [BV12] T. E. Bogale and L. Vandendorpe, “Robust Sum MSE Optimization for Downlink Multiuser MIMO Systems With Arbitrary Power Constraint: Generalized Duality Approach,” *IEEE Trans. Signal Process.*, vol. 60, no. 4, pp. 1862-1875, Apr. 2012.

- [CFH14] Y. Chen, X. Fang and B. Huang, "Energy-Efficient Relay Selection and Resource Allocation in Nonregenerative Relay OFDMA Systems," *IEEE Trans. Vehicular Tech.*, vo. 63, no. 8, 3689-3699, Oct. 2014.
- [CGB05] S. Cui, A. Goldsmith, and A. Bahai, "Energy-Constrained Modulation Optimization," *IEEE Trans. Wireless Commun.*, vol. 4, no. 5, pp. 2349-2360, Sep. 2005.
- [CYH13] K. T. K. Cheung, S. Yang, and L. Hanzo, "Achieving maximum energy-efficiency in multi-relay OFDMA cellular networks: A fractional programming approach," *IEEE Trans. on Commun.*, vol. 61, no. 7, pp. 2746-2757, Jul. 2013.
- [CYH14] K. T. K. Cheung, S. Yang, and L. Hanzo, "Spectral and energy spectral efficiency optimization of joint transmit and receive beamforming based multi-relay MIMO-OFDMA cellular networks," *IEEE Trans. Wireless Commun.*, vol. 13, no. 11, pp. 6147-6165, Nov. 2014.
- [DTV00] D. Dardari, V. Tralli, and A. Vaccari, "A theoretical characterization of nonlinear distortion effects in OFDM systems," *IEEE Trans. Commun.*, vol. 48, pp. 1755-1764, Oct. 2000.
- [ED12] E. Eraslan and B. Daneshrad, "Practical energy efficient link adaptation for MIMO-OFDM systems," *Proc. IEEE WCNC*, pp. 480-485, Apr. 1-4, 2012.
- [FMF12] C. A. R. Fernandes, J. C. M. Mota, and G. Favier, "Analysis and power diversity-based cancellation of nonlinear distortions in OFDM systems," *IEEE Trans. Signal Process.*, vol. 60, pp. 3520-3531, no. 7, July, 2012.
- [GDM13] J. Guerreiro, R. Dinis and P. Montezuma, "Optimum and Sub-Optimum Receivers for OFDM Signals with Strong Nonlinear Distortion Effects," *IEEE Trans. Commun.*, vol. 61, pp. 3830-3840, 2013.

- [GDM15] J. Guerreiro, R. Dinis, and P. Montezuma, "On the optimum multicarrier performance with memoryless nonlinearities," *IEEE Trans. Commun.*, vol. 63, no. 2, Feb. 2015.
- [HCCZ13] S. Huang, H. Chen, J. Cai, and F. Zhao, "Energy efficiency and spectral efficiency tradeoff in amplify-and-forward relay networks," *IEEE Trans. Veh. Tech.*, vol. 62, no. 9, pp. 4366-4378, Nov. 2013.
- [HHJY13] S. He, Y. Huang, S. Jin, and L. Yang, "Coordinated beamforming for energy efficient transmission in multicell multiuser systems," *IEEE Trans. Commun.*, vol. 61, no. 12, pp. 4961-4971, Dec. 2013.
- [HW07] I. Hammerstrom and A. Wittneben, "Power Allocation Schemes for Amplify-and-Forward MIMO-OFDM Relay Links," *IEEE Trans. Wireless Commun.*, vol. 6, no. 8, pp. 2798-2802, Aug. 2007.
- [ICJF12] C. Isheden, Z. Chong, E. Jorswieck, and G. Fettweis, "Framework for link-level energy efficiency optimization with informed transmitter," *IEEE Trans. Wireless Commun.*, vol. 11, no. 8, pp. 2946-2957, Aug. 2012.
- [IF10] C. Isheden and G. P. Fettweis, "Energy-efficient multi-carrier link adaptation with sum rate-dependent circuit power," *Proc. IEEE GlobeCom' 10*, pp. 1-6, Miami, FL, Dec. 2010.
- [KD10] H. S. Kim and B. Daneshrad, "Energy-constrained link adaptation for MIMO OFDM wireless communication systems," *IEEE Trans. Wireless Commun.*, vol. 9, no. 9, pp. 2820-2832, Sept. 2010.
- [Kim97] J. Kim, "Iterated grid search algorithm on unimodal criteria," Ph.D.dissertation, Dept. Statist., Virginia Polytechnic Inst. State Univ., Blacksburg, VA, 1997.
- [KT01] A. Knutson and T. Tao, "Honeycombs and Sums of Hermitian Matrices," *Notices Amer. Amth. Soc.*, 48 (2001) 175-186.

- [Kuh55] H.W. Kuhn, "The Hungarian method for the assignment problem," *Naval Res. Logistic Quart.*, vol. 2, pp. 83-97, 1955.
- [KWT13] I. Ku, C.-X. Wang, and J. S. Thompson, "Spectral-Energy Efficiency Trade-Off in Relay-Aided Cellular Networks," *IEEE Trans. Wireless Commun.*, vol. 12, no. 10, pp. 4970-4982, Oct. 2013.
- [LC98] X. Li and L. J. Cimini, "Effects of clipping and filtering on the performance of OFDM," *IEEE Commun. Letter*, vol. 2, no. 5, May 1998.
- [LCL<sup>+</sup>07] E. Lo, P. Chan, V. Lau, R. Cheng, K. Letaief, R. Murch, and W. Mow, "Adaptive resource allocation and capacity comparison of downlink multiuser MIMO-MC-CDMA and MIMO-OFDMA," *IEEE Trans. Wireless Commun.*, vol. 6, no. 3, pp. 1083-1093, Mar. 2007.
- [LMB14] R. A. Loodaricheh, S. Mallick and V. K. Bhargava, "Energy-Efficient Resource Allocation for OFDMA Cellular Networks With User Cooperation and QoS Provisioning," *IEEE Trans. Wireless Commun.*, vol. 13, no. 11, 6132-6146, Nov. 2014.
- [LO15] Y. Lei and M. O'Droma, "A novel decomposition analysis of nonlinear distortion in OFDM transmitter systems," *IEEE Trans. Signal Process.*, vol. 63, no. 19, Oct. 2015.
- [LTY15] Y. Li, Y. Tian, and C. Yang, "Energy-Efficient Coordinated Beamforming Under Minimal Data Rate Constraint of Each User", *IEEE Trans. Veh. Tech.*, vol. 64, no. 6, pp. 2387-2397, Jun. 2015.
- [LXX<sup>+</sup>11] G. Li, Z. Xu, C. Xiong, C. Yang, S. Zhang, Y. Chen, and S. Xu, "Energy-efficient wireless communications: tutorial, survey, and open issues," *IEEE Wireless Commun. Mag.*, vol. 18, no. 6, pp. 28-35, Dec. 2011.

- [MB16] P. Mertikopoulos and E.V. Belmega, "Learning to Be Green: Robust Energy Efficiency Maximization in Dynamic MIMO-OFDM Systems", *IEEE J. Areas Commun.*, Vol. 34, no. 4, pp. 743-757, Apr. 2016.
- [MHL10] G. Miao, N. Himayat, and G. Y. Li, "Energy-efficient link adaptation in frequency-selective channels," *IEEE Trans. Commun.*, vol. 58, no. 2, pp. 545-554, Feb. 2010.
- [OHI13] O. Onireti, F. Heliot, and M. Imran, "On the energy efficiency-spectral efficiency trade-off of distributed MIMO systems," *IEEE Trans. Commun.*, vol. 61, no. 9, pp. 3741-3753, Sept. 2013.
- [PBS15] G. S. Peron, G. Brante, and R. D. Souza, "Energy-Efficient Distributed Power Allocation With Multiple Relays and Antenna Selection," *IEEE Trans. Commun.* vol. 63, no. 12, Dec. 2015.
- [PD10] R. S. Prabhu and B. Daneshrad, "An energy-efficient water-filling algorithm for OFDM systems," *Proc. IEEE ICC*, pp. 1-5, May 23-27, 2010.
- [QA12] J. Qi, and S. Aissa, "On the power amplifier nonlinearity in MIMO transmit beamforming systems," *IEEE Trans. Commun.*, vol. 60, no. 3, Mar. 2012.
- [SA09] M. Senst and G. Ascheid, "Optimal Output Back-Off in OFDM Systems with Nonlinear Power Amplifiers," *Proc. IEEE ICC'09*, pp. 1-6, Dresden, Germany, Jun. 2009.
- [SH14] A. H. Sakr and E. Hossain, "Energy-Efficient Downlink Transmission in Two-Tier Network MIMO OFDMA Networks," *Proc. IEEE ICC* pp. 3652-3657, Jun. 10-14, 2014.
- [SNN<sup>+</sup>16] Z. Song, Q. Ni, and K. Navaie, S. Hou, S. Wu and X. Sun, "On the Spectral-Energy Efficiency and Rate Fairness Tradeoff in Relay-Aided Cooperative OFDMA Systems," *IEEE Trans. Wireless Commun.*, vol. 15, no. 9, 6342-6355, Sept. 2016.

- [SST13] M. Sabbaghian, A. I. Sulyman, and V. Tarokh, "Analysis of the impact of nonlinearity on the capacity of communication channels," *IEEE Trans. Info. Theory.*, vol. 59, no. 11, Nov. 2013.
- [STT<sup>+</sup>02] H. Sampath, S. Talwar, J. Tellado, V. Erceg, and A. Paulraj, "A fourth-generation MIMO-OFDM broadband wireless system: design, performance, and field trial results," *IEEE Commun. Mag.*, vol. 40, no. 9, pp. 143-149, Sep. 2002.
- [SMC06] K. Seong, M. Mohseni, and J. Cioffi, "Optimal resource allocation for OFDMA downlink systems," *Proc. IEEE Int. Symp. Inf. Theory (ISIT)*, pp. 1394-1398, Jul. 9-14, 2006.
- [Tel99] I.E. Telatar, "Capacity of multi-antenna Gaussian channels," *Europ. Trans. Telecommun.*, vol. 10, pp. 585-596, Nov.-Dec. 1999.
- [TSA<sup>+</sup>15] J. Tang, D. K. C. So, E. Alsusa, K. Hamdi, and A. Shojaeifard, "On the Energy Efficiency-Spectral Efficiency Trade-Off in MIMO-OFDMA Broadcast Channels," *IEEE Trans. Veh. Tech.*, Aug. 2015.
- [VTFH16] Q. D. Vu, L. N. Tran, R. Farrell and E. K. Hong, "Energy-Efficient Zero-Forcing Precoding Design for Small-Cell Networks," *IEEE Trans. Commun.*, vol. 64, no. 2, pp. 790-804, Feb. 2016.
- [WCLM99] C. Y. Wong, R. Cheng, K. Letaief, and R. Murch, "Multiuser OFDM with adaptive subcarrier, bit, and power allocation," *IEEE J. Select. Areas Commun.*, vol. 17, no. 10, pp. 1747-1758, Oct. 1999.
- [WGLV13] T. Wang, F. Glineur, J. Louveaux and L. Vandendorpe, "Weighted Sum Rate Maximization for Downlink OFDMA with Subcarrier-pair based Opportunistic DF Relaying," *IEEE Trans. Sig. Process.*, vol. 61, no. 10, pp. 2512-2524, May. 2013.

- [XLL15] C. Xiong, L. Lu and G. Y. Li, "Energy-Efficient OFDMA-Based Two-Way Relay," *IEEE Trans. Commun.*, vol. 63, no. 9, 3157-3169, Sept. 2015.
- [WSV15] Z. Wang, I. Stupia and L. Vandendorpe, "Energy Efficient Precoder Design for MIMO-OFDM with Rate-dependent Circuit Power," *Proc. IEEE ICC*, pp. 1897-1902, Jun. 8-12, 2015.
- [WSV16] Z. Wang, I. Stupia and L. Vandendorpe, "Optimal Precoder Design for MIMO-OFDM: Understanding the Role of Power Amplifiers and Nonlinear Distortion Noise," *IEEE International Conference on Communications (ICC)*, 23-27, May, 2016.
- [WV13] T. Wang and L. Vandendorpe, "On the optimum energy efficiency for flat-fading channels with rate-dependent circuit power," *IEEE trans. Commun.*, vol. 61, no. 12, pp. 4910-4921, Dec. 2013.
- [WV16a] Z. Wang and L. Vandendorpe, "Energy Efficient Resource Allocation in MIMO-OFDMA Downlink Systems," *Proc. IEEE SPAWC*, Jul. 3-6, 2016.
- [WV16b] Z. Wang and L. Vandendorpe, "Energy efficient power allocation and relay selection in MIMO relay channels," *IEEE International Symposium on Personal, Indoor and Mobile Radio Communications (PIMRC)*, 4-7, Sept, 2016.
- [WV17] Z. Wang and L. Vandendorpe, "Subcarrier Allocation and Precoder Design for Energy Efficient MIMO-OFDMA Downlink Systems," *IEEE Trans. Commun.*, vol. 65, no. 1, pp. 136-146, Jan. 2017.
- [XLZ<sup>+</sup>11] C. Xiong, G. Li, S. Zhang, Y. Chen, and S. Xu, "Energy and spectral efficiency tradeoff in downlink OFDMA networks," *IEEE Trans. Wireless Commun.*, vol. 10, no. 11, pp. 3874-3886, Nov. 2011.

- [XLZ<sup>+</sup>12] C. Xiong, G. Li, S. Zhang, Y. Chen, and S. Xu, "Energy-efficient resource allocation in OFDMA networks," *IEEE Trans. Commun.*, vol. 60, no. 12, pp. 3767-3778, Dec. 2012.
- [XQ13] J. Xu and L. Qiu, "Energy efficiency optimization for MIMO broadcast channels," *IEEE Trans. Wireless Commun.*, vol. 12, no. 2, pp. 690-701, Feb. 2013.
- [XTL15] X. Xiao, X. Tao, and J. Lu, "Energy-Efficient Resource Allocation in LTE-Based MIMO-OFDMA Systems With User Rate Constraints," *IEEE Trans. Veh. Tech.*, vol. 64, no. 1, pp. 185-197, Jan. 2015.
- [XYL<sup>+</sup>13] Z. Xu, C. Yang, G. Y. Li, S. Zhang, Y. Chen, and S. Xu, "Energy-efficient configuration of spatial and frequency resources in MIMO-OFDMA systems," *IEEE Trans. Commun.*, vol. 61, no. 2, pp. 564-575, Feb. 2013.
- [YBC14] L. Yan, B. Bai, and W. Chen, "On Energy Efficiency Maximization in Downlink MIMO Systems Exploiting Multiuser Diversity," *IEEE Commun. Letters*, Vol. 18, No. 12, pp. 2161-2164, Dec. 2014.
- [ZBCH14] X. Zhou, B. Bai, W. Chen, and Y. Han, "On energy efficiency maximization of AF MIMO relay systems with antenna selection," *GlobalSIP 2014 (Invited Paper)*.
- [ZBJ11] A. Zappone, S. Buzzi, and E. Jorswieck, "Energy-Efficient power control and receiver design in relay-assisted DS/CDMA wireless networks via game theory," *IEEE Commun. Letters*, vol. 15, no. 7, pp. 701-703, July 2011.
- [ZCJ14a] A. Zappone, P. Cao, and E. Jorswieck, "Energy efficiency optimization in relay-assisted MIMO systems with perfect and statistical CSI," *IEEE Trans. on Signal Process.*, vol. 62, no. 2, pp. 443-457, Jan. 2014.
- [ZCJ14b] A. Zappone, P. Cao, and Eduard A. Jorswieck, "Low-complexity energy efficiency optimization with statistical CSI

- in two-hop MIMO systems,” *IEEE Signal Process. Lett.*, vol. 21, Nov. 2014.
- [ZCJB13] A. Zappone, Z. Chong, E. Jorswieck, and S. Buzzi, “Energy-aware competitive power control in relay-assisted interference wireless networks,” *IEEE Trans. on Wireless Commun.*, vol. 12, no. 4, pp. 1860-1871, April 2013.
- [ZF05] P. Zillmann and G. P. Fettweis, “On the Capacity of Multicarrier Transmission over Nonlinear Channels,” *Vehicular Technology Conference*, Stockholm, 29 May-1 June, 2005.
- [Zha05] X. Zhan, “Extremal eigenvalues of real symmetric matrices with entries in an interval,” *SIAM. J. Matrix Anal. Appl.*, vol. 27, pp. 851-860, 2005.
- [ZJB14] A. Zappone, E. A. Jorswieck, and S. Buzzi, “Energy efficiency and interference neutralization in two-hop MIMO interference channels,” *IEEE Trans. Signal Process.*, vol. 62, Oct. 2014.
- [Zyr07] J. Zyren, “Overview of the 3gpp long term evolution physical layer,” online available, Jul. 2007.